Combination of CAR and TCR technologies to increase efficacy of adoptive cell therapy

Inaugural-Dissertation

to obtain the academic degree
Doctor rerum naturalium (Dr. rer. nat.)

submitted to the Department of Biology, Chemistry, Pharmacy
of Freie Universität Berlin

by

KARIN ANNA MARIA TEPPERT

2024

1st reviewer:	Prof. Dr. med. Annette Künkele-Langer
2nd reviewer:	Prof. Dr. med. Andreas Diefenbach
Date of defense:	November 18, 2024

ACKNOWLEDGMENT

First, I would like to express my sincere gratitude to Prof. Dr. med. Annette Künkele-Langer for taking on the role as my academic supervisor. Annette, thank you very much for your exceptional scientific guidance, support, and expertise throughout the entire time. Your encouragement and constructive critique have been instrumental in shaping the direction of this doctoral thesis. Despite the geographical distance, we were able to connect and engage in thought-provoking discussions. I am truly grateful for your dedication and commitment, to not only my scientific work, but also my professional career. Thank you.

I am also deeply thankful to Prof. Dr. med. Andreas Diefenbach for supporting me as doctoral student in working on this research project. I would like to emphasize how much I appreciated your diverse perspectives, which triggered provocative discussions and significantly broadened the scope of the thesis.

A sincere and special thank you is conveyed to Dr. Dominik Lock. Nik, thank you for your consistent encouragement, your unwavering belief in me, your investment in my success, and thank you for the countless hours you have dedicated to providing me scientific and professional guidance. Together, this created an environment that supported my growth, curiosity, and passion for adoptive cell therapy. I am truly fortunate to have had you as supervisor and I will carry the lessons learned from you throughout my career.

I would also like to acknowledge the scientific advice of Dr. Pradyot Dash, Dr. Thomas Schaser and Dr. Mario Assenmacher. A special thank you is reserved for Isabella Ogusuku for her remarkable dedication in analyzing the RNA-seq data and for patiently sharing her knowledge and expertise with me. Moreover, I would like to thank all of my colleagues and friends at Miltenyi for the scientific and mental support, the exciting discussions and relaxing lunch breaks. *In vivo* and *ex vivo* data acquisition was kindly supported by Dr. Dominik Lock, Caroline Brandes, Isabella Ogusuku, Nora Winter, Nele Knelangen and Shima Ferdos. Thank you. In this regard, I am also very thankful for the mice that were fundamental in proving the significance of this scientific approach.

Finally, I would like to thank my family. Your love, understanding and belief in me have given me self-confidence, determination and security, paving the way to where I stand today and beyond.

DECLARATION OF INDEPENDENCE

Herewith I certify that I have prepared and written my thesis independently and that I have not used any sources and aids other than those indicated by me.

TABLE OF CONTENTS

LIST OF TABLES

LIST OF FIGURES

LIST OF ABBREVIATIONS

°C	Degree Celsius
7-AAD	7-aminoactinomycin D
Allo-HSCT	Allogenic hematopoietic stem cell transplantation
AML	Acute Myeloid Leukemia
APC	Allophycocyanin
CAR	Chimeric antigen receptor
CAR'TCR-T	T cell co-expressing CAR and transgenic TCR
CLL1	C-type lectin-like molecule 1
CD	Cluster of Differentiation
CDC42	Cell division cycle 42
CDR	Complementary determining regions
CM	Central memory
CO_2	Carbon dioxide
DEG	Differentially expressed genes
DMEM	Dulbecco's Modified Eagle Medium
DMSO	Dimethylsulfoxid
DNA	Deoxyribonucleic acid
E. *coli*	Escherichia coli
EDTA	Ethylenediaminetetraacetic acid
EM	Effector memory
EMRA	effector memory cells re-expressing CD45RA
FCS	Fetal calf serum
FFLuc	Firefly luciferase
FITC	Fluorescein isothiocyanate
FSC	Forward scatter
GFP	Green fluorescent protein
GM-CSF	granulocyte macrophage colony-stimulating factor
GO	Gene ontology
GvHD	Graft-versus-host disease
HLA	Human Leukocyte Antigen
i.p.	Intraperitoneal
i.v.	Intravenous
ICOS	Inducible T-cell costimulator
IFN	Interferon
IL	Interleukin
IS	Immunological synapse
ITAM	Immunoreceptor tyrosine-based activation motifs
LAG-3	Lymphocyte-activation gene 3
LCK	Lymphocyte-specific PTK
LNGFR	Low-affinity nerve growth factor receptor
LP	Leukapheresis
LVV	Lentiviral vector
MEM	Minimum Essential Mediums
MFI	Mean fluorescence intensity
MHC	Major histocompatibility complex
MOI	Multiplicity of infection

NPM1	Nucleophosmin 1
NSG	NOD scid gamma
PBMC	Peripheral blood mononuclear cell
PBS	Phosphate-buffered saline
PCR	polymerase chain reaction
PD-1	Programmed cell death protein 1
PE	Phycoerythrin
PEI	Polyethylenimine
PI	Propidium Iodide
PTK	Protein tyrosine kinases
RAC1	RAC family small GTPase 1
RHO-GTPases	Ras homologue
RNA-seq	Ribonucleic acid sequencing
rpm	Revolutions per minute
RPMI	Roswell Park Memorial Institute
scFv	Single-chain variable fragment
SCM	memory stem cells
SLP-76	SH2 domain-containing leukocyte phosphoprotein of 76 kDa
SMAC	Supramolecular activation clusters
SOC	Super optimal broth with catabolite repression
SSC	Sideward scatter
TCR	T cell receptor
TIL	Tumor infiltrating lymphocyte
TIM-3	T cell immunoglobulin and mucin domain-containing protein 3
TME	Tumor microenvironment
TNF	Tumor necrosis factor
UTD	Untransduced
WT	Wild type
ZAP-70	Zeta-chain-associated protein kinase-70
SD	Standard deviation
SEM	Standard error of mean

ABSTRACT

Adoptive chimeric antigen receptor (CAR)-T cell therapies have led to tremendous clinical success, especially in treatment of hematological malignancies. However, optimizations are still required to tackle remaining challenges such as antigen escape, on-target off-tumor toxicity, limited availability of tumor-specific antigens as well as insufficient T cell persistence and tumor infiltration. A significant level of expectation is currently placed in transgenic T cell receptors (TCRs), which feature a highly sensitive, naturally evolved signaling machinery and cover a broader range of targets. This work aimed at combining both technologies, CAR and transgenic TCR, to increase the anti-tumor response, to facilitate dual-targeting, to minimize the risk for antigen escape and to potentially achieve synergistic effects.

As proof of concept, initial experiments were focused on the combination of the clinically well-established second-generation CD20-CAR and the previously published transgenic dNPM1-TCR. CAR'TCR-T cells, co-expressing CD20-CAR and dNPM1-TCR, revealed increased anti-tumor activity upon dual stimulation, not only upon short-term co-culture but also upon long-term repetitive *in vitro* stimulation. Accordingly, CAR'TCR-T cells displayed a unique transcriptomic signature, indicating increased T cell activation and proximal signaling. In-depth characterization of CAR'TCR-T cell functionality also included the analysis of alternative costimulatory domains in the CAR designs, displaying no significant difference between 4-1BB- and CD28-costimulated CAR'TCR-T cells. Moreover, it was addressed whether co-expression of CD20-CAR promotes functional recovery of the MHC class I-restricted dNPM1-TCR in $CD4^+$ T cells. Finally, dual-specificity and enhanced anti-tumor activity of CAR'TCR-T cells were verified *in vitro* and *in vivo* for a clinically relevant AML setting by co-expressing dNPM1-TCR and CD33-CAR. Especially the treatment with Triple-T cells, meaning a cellular composition of CAR'TCR-T, CAR-T and TCR-T, led to promising results *in vivo*, demonstrating increased anti-tumor cytotoxicity compared to a mixture of CAR-T and TCR-T cells.

In summary, this work supports the approach of co-expressing a CAR and a transgenic TCR to achieve dual-specificity and enhanced T cell anti-tumor activity. The superior performance of Triple-T highlights the therapeutic benefit of CAR'TCR-T cells and the potential clinical applicability through co-transduction with two different lentiviral vectors.

ZUSAMMENFASSUNG

Sehr vielversprechende klinische Erfolge wurden durch die Behandlung mit genetisch-modifizierten T-Zellen vor allem im Hinblick auf hämatologische Neoplasien erzielt. Nichtdestotrotz, sind weitere Optimierungen der adoptiven T-Zell Therapie unabdingbar, um Herausforderungen wie Antigenverlust, *„On-Target/Off-Tumor"*-Effekte, die begrenzte Antigenauswahl, sowie die unzureichende T-Zell-Persistenz und -Tumorinfiltration zu bewältigen. Neben den Chimären Antigen Rezeptoren (CAR) erhalten die transgenen T-Zell Rezeptoren (TCR) vor allem im Hinblick auf solide Tumore besondere Aufmerksamkeit. Diese zeigen laut ersten klinischen Studien mehrere vielversprechende Charakteristika, wie zum Beispiel hohe Sensitivität, effiziente Tumorinfiltration und das breitere Spektrum an Zielproteinen. Die Grundidee der Arbeit war es CAR und TCR Technologien zu kombinieren, um die therapeutische Wirksamkeit zu erhöhen und auch im Fall von breiter Tumorheterogenität aufrecht zu erhalten.

Erste Experimente basierten auf der Co-Expression eines klinisch getesteten CD20-CAR und eines transgenen dNPM1-TCR. Gleichzeitige Stimulation von CAR und TCR in den sogenannten CAR'TCR-T Zellen führte zu erhöhter Tumorzelllyse – nicht nur nach kurz-zeitiger Co-Kultur, sondern auch nach langanhaltender, repetitiver Stimulation *in vitro*. Auch das einzigartige Transkriptomprofil von CAR'TCR-T Zellen deutete auf verstärkte Aktivierung und Signalübertragung hin. Alternative co-stimulatorische Domänen (4-1BB oder CD28) im CAR hatten keinen Einfluss auf CAR'TCR-T Zell Funktionalität. Es wurde außerdem untersucht, ob die Co-Expression des CD20-CARs, die Funktionalität des MHC-I-spezifischen dNPM1-TCRs in $CD4^+$ T-Zellen ermöglicht. Abschließend wurde das Modell mit einer klinisch-relevanten Kombination aus dNPM1-TCR und CD33-CAR im Rahmen von *in vitro* und *in vivo* Experimenten bestätigt. Sehr vielversprechende *in vivo* Ergebnisse wurden mit Triple-T Zellen erzielt, welches das natürliche Produkt aus Co-Transduktion darstellt und aus CAR'TCR-T, CAR-T und TCR-T besteht.

Zusammenfassend zeigten CAR'TCR-T-Zellen nicht nur duale Spezifität, sondern auch verstärkte anti-Tumor Aktivität. Neben der klinischen Anwendbarkeit, verdeutlicht die *in vivo* zytotoxische Überlegenheit von „Triple-T" gegenüber der Zellkomposition aus CAR-T und TCR-T das therapeutische Potenzial von CAR'TCR-T Zellen.

1 INTRODUCTION

1.1 Cancer immunology

Cancer immunology revolves around the role of the immune system in recognizing transformed cells and preventing cancer development[1]. Malignant cancer cells are generally characterized by the hallmarks of cancer, first defined by Douglas Hanahan and Robert A. Weinberg[2,3]. Although further specified by now[4], the multistep process of tumor development is generally caused by an accumulation of several genetic abnormalities, enabling continuous clonal selection and tumor progression. The hallmark characteristics of malignant cells include for example uncontrolled proliferation, resistance to programmed cell death, immunosuppression, induction of angiogenesis, invasion of healthy tissue and metastasis[2].

The immune system is classically subdivided into a fast and first-line innate response and a delayed but antigen-specific, highly-potent adaptive immunity[5]. The anti-tumor immune response is also referred to as the immune cycle of cancer, a re-occurring series of events with the potential of self-stimulation[6]. It is generally initiated by cancer cell death and release of “non-self” tumor-derived antigens, which are for example recognized and processed by dendritic cells and subsequently presented to naïve T cells residing in the lymph nodes[7-9]. Innate immune cells are also required for sensing of transformed cells through mechanisms, independent of antigen release[10]. For instance, nucleic acid sensors in antigen presenting cells detect tumor-derived cytosolic DNA or extracellular RNA, which is abundantly present in cancer cells due to abnormal proliferation, genome instability and oxidative stress[11]. Such nucleic acid sensing triggers secretion of type I interferon and activation of dendritic cells, leading to initiation as well as amplification of the adaptive immune response[10,12]. As part of the innate immunity, natural killer cells recognize tumors through ligands, which are upregulated upon cell stress[13], DNA damage[14], or abnormal proliferation[15]. In general, natural killer cells express a variety of receptors and only become activated when the stimulatory receptor activation abrogates the signaling through inhibitory receptors[16]. Target cell lysis involves secretion of cytotoxic granules or induction of apoptosis through death receptor signaling[16]. The adaptive immune system comprises B lymphocytes, $CD4^+$ T helper and $CD8^+$ cytotoxic T cells. In general, T cells

recognize intracellularly processed peptides, presented on major histocompatibility complex (MHC) molecules[17,18]. In the absence of cross-presentation, the T cell receptor (TCR) in $CD8^+$ T cells binds to endogenous protein-derived peptides presented on MHC class I, whereas $CD4^+$ T cells are restricted to MHC class II, displaying endocytosed or phagocytosed exogenous antigens[19,20]. In contrast, cross-presentation describes the priming of naïve $CD8^+$ T cells via peptides presented on MHC class II of activated dendritic cells, which for example occurs in tumor-draining lymph nodes upon sensing of tumor-derived nucleic acids[12]. Upon T cell priming, activated effector T cells are recruited to the tumor site through chemokine-secreting, tumor-residing dendritic cells[21-23]. Recognition of cancer cells through the antigen-specific TCR induces a cytolytic response and cancer cell death, which represents the last stage in the immune cycle of cancer[7,21]. The subsequent release of new cancer-derived antigens then causes re-initiation of the cancer-immune cycle, which can be summarized as follows: (1) Antigen processing and presentation by antigen presenting cells; (2) T cell priming and activation in lymph nodes; (3) Trafficking of cytotoxic T lymphocytes to the tumor; (4) T cell infiltration; (5) Recognition and killing of cancer cells[6].

The concept of immune surveillance, describing the detection and elimination of neoplastic cells (or pathogens) by the immune system, was first postulated by Frank Macfarlane Burnet[24,25]. Its indispensable role in protection against cancer is for example further supported by the observations that drug-induced immune suppression increases the risk for cancer development, or spontaneous tumor regression was observed in autoimmune patients[26-28]. In view of this, the question that arises is how do cancers develop despite such strong defense mechanisms? The answer is a process referred to as immunoediting, which includes several mechanisms of how tumor cells escape and hide from the immune system[29]. Several evasion mechanisms have been described, such as for example direct T cell impairment through downregulation of costimulatory receptors, disrupted tumor recognition through loss of MHC, and the development of an immunosuppressive tumor microenvironment (TME), inhibiting T cell infiltration and effector function[7]. Besides hiding from the immune system, tumors also actively recruit immune cells with immunosuppressive function. For instance, regulatory T cells naturally lead to immunosuppression and T cell anergy, thereby maintaining homeostasis and preventing excessive immune responses[30]. In tumors, those characteristics cause inhibition of tumor-

specific cytotoxic T cells and impaired anti-tumor immunity. Similar immunosuppressive and consequently pro-tumor effects were also described for innate immune cells such as tumor-associated macrophages and myeloid-derived suppressor[31]. Thus, a wide variety of therapeutic concepts, known under the term cancer immunotherapy, aim at amplifying and strengthening the immune response to overcome immunoediting.

1.2 Cancer immunotherapy

In contrast to more traditional cancer therapies such as surgery, chemo- or radiation-therapy, immunotherapy is not based on eliminating cancer cells from the outside, but instead, by recruiting and cooperating the internal natural defense system. The roots for this were already set more than 100 years ago by William Coley, who is often referred to as "Father of Immunotherapy"[32]. He successfully used heat-inactivated bacteria to stimulate the immune system and thereby achieved tumor regression in more than 1,000 cancer patients[32,33]. Nowadays, cancer immunotherapy is designed to achieve tumor-specific immunity and includes checkpoint inhibition, cancer vaccines and adoptive cell-based therapy[34]. Checkpoint molecules such as programmed cell death receptor 1 (PD-1) or cytotoxic T lymphocyte antigen 4, prevent T cell hyperactivation through negative regulation and help to maintain a well-balanced immune homeostasis. In cancer treatment, antibody-based blockade of such co-inhibitory receptors is successfully applied to prevent T cell exhaustion and tumor tolerance[35-37]. Antibodies do not only serve as checkpoint inhibitors, but especially T cell-engaging multivalent antibodies are applied to actively redirect effector T cells to the tumor[38-40], which generally also supports the idea behind cell-based immunotherapy. In 1989, Gideon Gross, Tova Waks and Zelig Eshhar published their pioneering work on gene-engineered T cells armed with the prototype of a chimeric antigen receptor (CAR), consisting of an extracellular antibody-derived tumor recognition domain fused to intracellular TCR α and β chains[41]. In this manner, they achieved MHC-independent T cell activation, resulting in cytokine secretion and antigen-specific target cell lysis[41]. During the last 30 years, multiple modifications in design and optimizations in manufacturing led to clinical approval of six different CARs for treatment of multiple myeloma and various B-cell malignancies[42]. However, successful elimination of solid tumors continues to pose a challenge[43]. Currently, more than 1,300 clinical CAR-T cell trials are registered, however, only one-third targeting solid tumors and less than 10% in phase

II or III[43]. TCR-T immunotherapy represents the pMHC-directed counterpart, comprising tumor infiltrating lymphocytes (TILs) and engineered T cells expressing a transgenic TCR. Beginning of the 1980s, Rosenberg and colleagues were first to describe the isolation, *in vitro* expansion and re-injection of TILs in combination with Interleukin-2 (IL-2) for adoptive treatment of cancer[44,45]. Since then, TILs were shown to be effective against several solid tumors, which was attributed to the high tumor specificity and the wide diversity in TCR repertoire[46]. However, challenges that are encountered are the identification and isolation of TILs, the insufficient persistence and tumor infiltration as well as the major prerequisite of exhibiting an adequate amount of effector T cells in the tumor[46,47]. Transgenic TCRs are currently regarded as promising alternative to target highly tumor-specific, intracellular antigens of solid tumors[48]. Characteristics such as high antigen sensitivity and physiological signaling are considered to support the anti-tumor response and T cell persistence[48]. Despite encouraging clinical results, a major difficulty are side effects for example through on-target off-tumor interaction with tumor associated antigens expressed on healthy tissues (NCT00509288[49], NCT00923806[50]). Furthermore, severe toxicities were observed due to off-target cross-reactivity, particularly in case of affinity-enhanced TCRs (NCT01273181[51], NCT01350401[52], NCT01352286[52]).

1.2.1 CAR versus TCR: Structure

Adoptive T-cell-based therapies are generally classified into TILs and gene-modified T cells expressing either a CAR or a transgenic TCR[53]. This chapter will focus on the differences in structure, immunological synapse (IS) formation, intracellular signal amplification and thereof resulting characteristics of CAR and TCR.

TCRs are subdivided into αβTCRs and γδTCRs, which are heterodimers assembled by alpha and beta or gamma and delta TCR chains, respectively[54]. Due to MHC-independency, specificity for pathogen-derived phosphoantigens and expression of natural killer cell receptors, γδTCR-T cells are often referred to as “unconventional” T-cell population[55,56]. The rapid response to stressors and the natural cytotoxicity against various types of transformed cells[57-59] underlines the potential of γδTCR-T cells in cancer therapy. Furthermore, first studies have already shown promising results with γδTCR-T cells expressing a CAR, also as donor-derived, off-the-shelf therapy[60-62].

The variable part of αβTCRs (in the following referred to as TCR) resembles the variable light chain of antibodies, also consisting of three hypervariable complementary determining regions (CDRs), which directly interact with the peptide-MHC complex and are flanked by a conformation-stabilizing framework[63]. In humans, MHC class I and II are classified according to the human leukocyte antigen (HLA) loci: HLA-A/-B/-C and HLA-DR/-DQ/-DM/-DP, respectively[64]. Ligand recognition via the TCR is not only restricted to the HLA locus, but also the serologically-defined antigen family and the respective allele number[65,66]. For instance, the allele HLA-A*02:01 designates the first protein within the HLA-A2 allele group. In comparison, CARs classically engage surface antigens on tumor cells through MHC-independent, antibody-derived single-chain variable fragment (scFvs)[41]. Similar to TCR variable chains, antibody specificity is also dictated through loop-forming CDRs, which on the contrary, show larger structural variety[67], shorter CDR3 loops[68], and fewer negatively charged amino acids in CDR1 and CDR2[69]. Since the design of CARs is rather flexible, some studies were also focused on developing pMHC-directed, so-called TCR-like CARs, which adds intracellular proteins (e.g. neoantigens) to the target repertoire[70-73].

TCR signaling generally requires association with the co-receptor (CD4 or CD8) and the endogenous CD3 chains, more precisely, the CD3εδ, CD3εγ and CD3ζζ dimers[74,75]. Upon TCR stimulation, immunoreceptor tyrosine-based activation motifs (ITAMs) within the CD3 chains become phosphorylated, which facilitate signal amplification[76]. The TCR-CD3-complex contains in total ten ITAMs, including one per CD3ε, δ, and γ subunit and three in each CD3ζ chain. CARs, on the other hand, typically contain the intracellular part of a CD3ζ chain and are consequently independent of the endogenous CD3 complex. The reduced number to three ITAMs was identified as contributing factor to the up to 100-fold lower CAR sensitivity, which sheds light on why an increased amount of stimulated CAR molecules is required for full T cell activation[76-78]. Therefore, several groups focused on developing novel constructs containing an HLA-independent antibody-derived scFv and intracellularly, a more physiological, TCR-adapted architecture[79-81]. This led to the understanding that the higher TCR sensitivity and the more powerful proximal signaling are not only based on the higher ITAM number, but also on the assembly with adhesion molecules such as CD2 and lymphocyte function-associated antigen 1[77,82,83].

As illustrated in Figure 1, CAR design was continuously modified and evolved throughout five generations: The first CAR only consisted of an extracellular antigen-binding domain and a transmembrane part, linked to a CD3ζ signaling region[84]. Despite initial cytotoxic activity, this CAR architecture demonstrated limited persistence and was consequently further optimized. With the knowledge that TCR engagement (signal 1) needs to be complemented by stimulation through costimulatory receptors (signal 2) and cytokines (signal 3) for complete effector function, second-generation CARs additionally contained CD28-, 4-1BB- or ICOS-derived costimulatory domains[85,86]. This format ensured serial killing capability, increased proliferation and represents the proven standard up until now[87-89]. Third-generation CARs are equipped with two different costimulatory domains, whereas fourth- and fifth-generation CARs engender all of the previously mentioned 3 signals by co-expression of pro-inflammatory cytokines or cytokine receptor domains, respectively[87,90]. For instance, CAR-activation-induced expression of IL-12 was shown to boost anti-tumor cytotoxicity and supported the innate immune response[91,92]. Similarly, increased proliferation and superior *in vivo* efficacy in treatment of solid tumors was observed with CARs encoding the cytokine receptor IL-2Rβ[93].

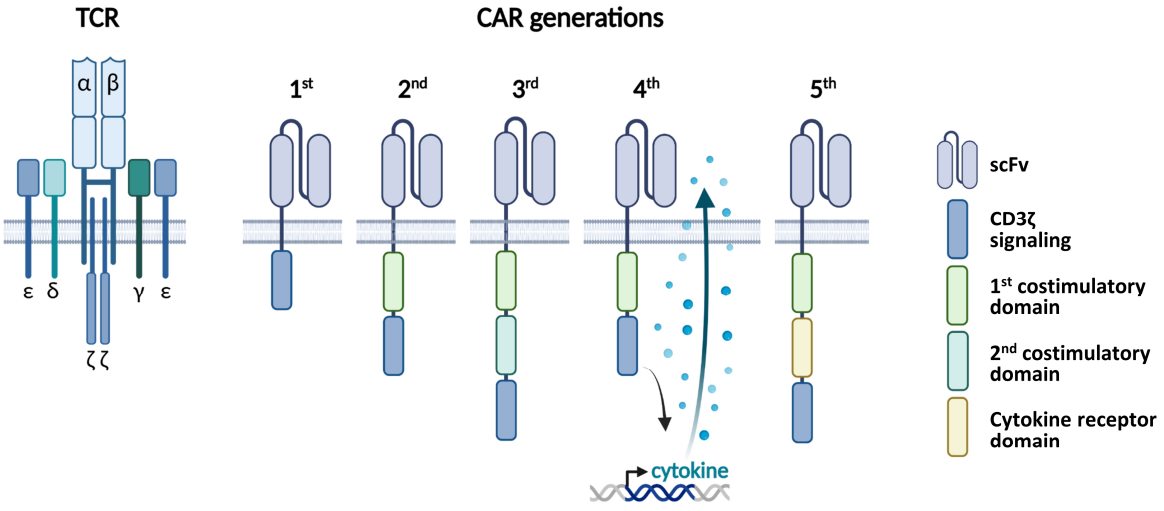

Figure 1: Structure of TCR and five different generations of CAR. The α- and β- chain of the TCR form a heterodimer and assemble with the CD3 complex consisting of CD3ε (2x), CD3δ, CD3γ and CD3ζ (2x). CARs contain an extracellular antigen-specific scFv, a hinge and transmembrane region, and depending on the generation, different intracellular domains. Adapted from Umut, Ö. *et al.* "CAR T cell therapy in solid tumors: a short review". Magazine of European Medical Oncology (2021)[94]. Illustration created with BioRender.com.

1.2.2 CAR versus TCR: Signaling

Upon pMHC-TCR-interaction, first step in signaling initiation is the recruitment of protein tyrosine kinases (PTK) for phosphorylation of ITAMs, which are located in the cytoplasmic tails of the CD3 chains[95,80]. Upon interaction with MHC, the CD8 co-receptor-bound lymphocyte-specific PTK (LCK) is brought into close proximity to the TCR-CD3-complex and phosphorylates tyrosine residues in ITAMs[96]. This leads to recruitment and phosphorylation of zeta-chain-associated protein kinase-70 (ZAP-70)[97], which triggers formation of the proximal signalosomes consisting of multiple additional proteins, as for instance phosphorylated Linker for activation of T cells or SH2 domain-containing leukocyte phosphoprotein of 76 kDa (SLP-76)[98,99]. This scaffold represents the basis for various distal signaling cascades, finally resulting in T cell activation, cytokine secretion, proliferation and differentiation[100]. For instance, phospholipase Cγ1 plays an essential role in signal transduction by hydrolyzing phosphatidylinositol bisphosphate into the two secondary messengers diacylglycerol and inositol triphosphate[101]. The latter binds to ion channels and induces Ca^{2+} influx into the cytoplasm, which induces expression of various effector genes (e.g. IL-2 or Interferon γ (IFN-γ)) through dephosphorylation and activation of nuclear factor of activated T cells[102-104]. Diacylglycerol, on the other hand, triggers the nuclear factor κB pathway, which regulates inflammation, proliferation and full T cell activation[105]. Generally speaking, CARs are designed to mimic the activation pattern of the native TCR, ultimately triggering antigen-specific effector function. Although CARs bind their target antigens with higher affinity, sensitivity was shown to be up to 100-fold lower than in TCRs[78,106]. This might present an explanation for the need of CAR clustering to achieve full CAR-T cell activation, and accordingly, a larger number of target antigens[79,107-109]. Interestingly, CARs are able to initiate downstream signaling independent of LAT phosphorylation, without any influence on the SLP-76 levels or recruitment of other adaptor molecules for IS formation[110]. It was hypothesized that compared to TCRs, this shortcut in CAR signaling eventually enables faster Ca^{2+} influx, granule recruitment and killing[110,111].

Striking differences were found in the IS of CAR and TCR, which is illustrated in Figure 2. Classically, interaction of TCR and pMHC induces formation of three highly-organized supramolecular activation clusters (SMACs): the central cSMAC, the peripheral pSMAC and the distal dSMAC[112]. TCR and LCK are categorized into the cSMAC, triggering the initial

activation[113]. Adhesion molecules such as Lymphocyte function-associated antigen 1 account for the stabilizing pSMAC, whereas actin accumulation in the dSMAC leads to the typical bull's-eye appearance[114]. In contrast, CARs form a rather disorganized and diffused IS consisting of multiple dispersed LCK microclusters, no stabilizing adhesion ring and a significantly smaller actin ring[111,115]. This unordered structure allows for faster CAR signaling, cytotoxic granule delivery, target cell lysis and eventually also earlier IS dissolution and migration of CAR-T cells to the next target cell[111]. The cytoskeleton reorganization during IS formation is dependent on RHO-GTPases, which consequently support recruitment of signaling molecules, receptor clustering in lipid rafts and T cell polarization towards the receptor-antigen complex[116,117].

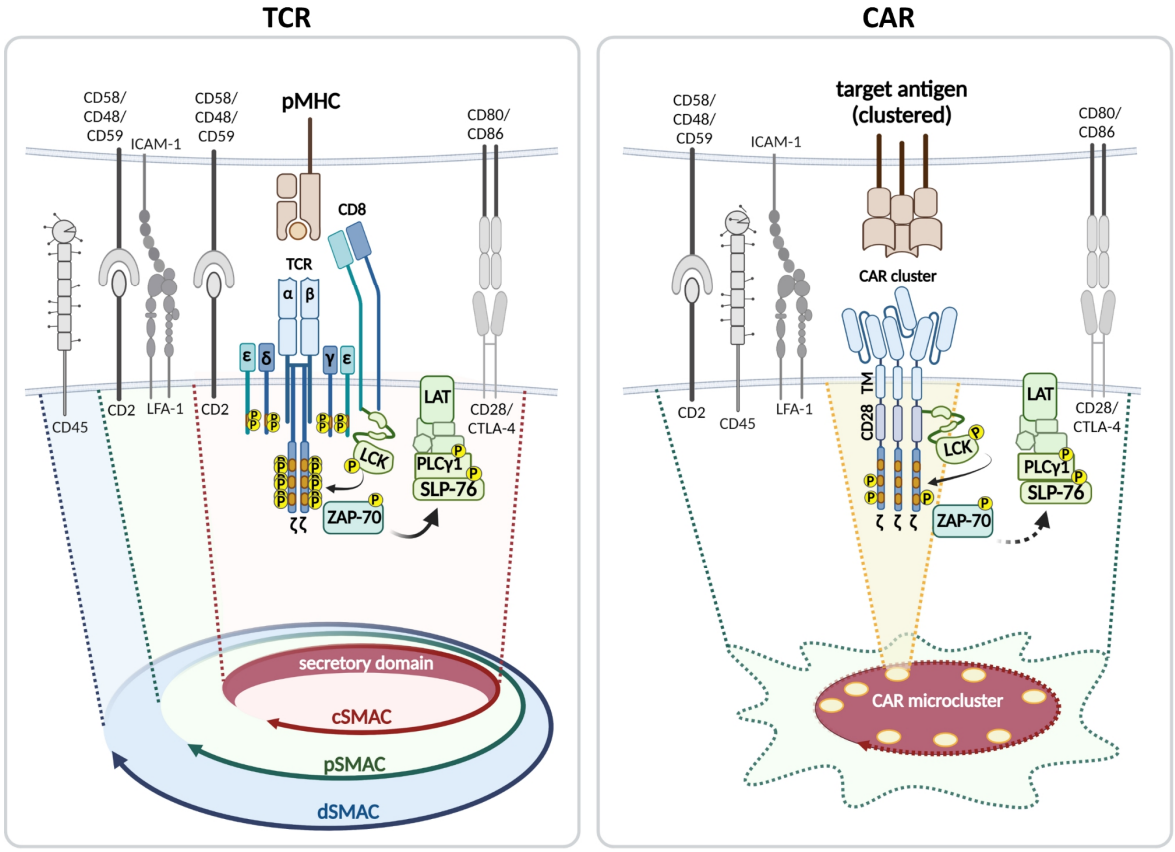

Figure 2: Differences and similarities in IS formation of TCR and CAR. TCR activation typically leads to formation of three highly-organized clusters: cSMAC, pSMAC and dSMAC. In contrast, the IS of CARs is diffused and disorganized, consisting of dispersed LCK microclusters, no adhesion ring and a smaller actin cluster. Adapted from Teppert, K. and Wang, X. *et al.* "Joining Forces for Cancer Treatment: From TCR versus CAR to TCR and CAR". International Journal of Molecular Sciences (2022)[118] and Meng, X. *et al.* "Engineering Cytoplasmic Signaling of CD28ζ CARs for Improved Therapeutic Functions". Frontiers in Immunology (2020)[119]. Illustration created with BioRender.com.

1.2.3 Combination of CAR and native TCR

With the goal to strengthen the efficacy of adoptive T cell therapies, several studies were focused on combination of CAR and TCR. Particularly promising results were obtained through concomitant stimulation of the native TCR. The role of the endogenous TCR in CAR-T cells was already investigated more than ten years ago[120]. To be more precise, it was proposed that CARs containing a CD3ζ transmembrane domain are able to interact with the native TCR and thereby potentiate T cell activation. Accordingly, another study demonstrated reduced *in vivo* CAR-T cell persistence after knock-out of the endogenous TCR[121]. This was explained by the lack of simultaneous TCR stimulation and physiological activation of the CAR-T cells through the xenogeneic mouse tissue. In line with this, actively engaging the native TCR in virus-specific T cells *in vitro* led to prolonged CAR-T cell functionality and proliferation[122]. Cliona M. Rooney and colleagues successfully continued the work on virus-specific CAR-T cells, paving the way "from bench to bedside" (NCT00085930[123], NCT00840853[124,125]). CD19-28ζ-CAR-T cells showed stronger native TCR-dependent proliferation, only in patients with detectable virus load[124]. Another observed benefit was the strongly minimized TCR repertoire due to the virus specificity, which was stated to decrease the risk for graft-versus-host disease (GvHD), even allowing for treatment of HLA-mismatched patients. Expanding on this concept, vaccination was implemented to actively stimulate the virus-specific TCR in CAR-T cells: The power of this approach was underlined by the fact that *in vitro* stimulation with viral peptide-presenting dendritic cells induced partial recovery of exhausted and dysfunctional third-generation 28-OX40ζ-CAR-T cells[126]. Especially as repetitive T cell stimulation was linked to impaired responsiveness and effector function, it represents a remarkable finding that additional signaling via the endogenous TCR did not further promote CAR-T cell exhaustion[118].

Several aspects need to be taken into account to understand the impact of native TCR-signaling on CAR-T cell functionality. First, all of the above-mentioned studies were based on TCR engagement in CAR-T cells containing a CD28 costimulatory domain and were verified for various targets and different CAR generations[124,126,127]. Interestingly, a side-by-side comparison showed that simultaneous engagement of CAR and native TCR led to enhanced activation, but also faster exhaustion and programmed cell death in virus-specific CAR-T cells with 4-1BB as costimulatory domain instead of CD28[127]. This finding is rather

counterintuitive, since CARs equipped with a 4-1BB costimulatory domain are generally known to support persistence, while CD28 was associated with stronger cytotoxicity but also faster exhaustion[128-130]. Second, the type of stimulus might influence the experimental outcome and the effect of TCR engagement on CAR-T cell functionality. Whereas vaccination-induced native TCR signaling was generally linked to enhanced CAR-T cell functionality and persistence[122,124,126,127], the opposite was observed in two different syngeneic mouse models. It has been shown that dual stimulation caused $CD8^+$ T cell exhaustion, reduced persistence and impaired tumor elimination[131]. This contradictory outcome was clarified by the different type of TCR stimulation, specifically referring to the activation through ubiquitously expressed endogenous antigens, potentially resulting in more repetitive stimulation and excessive activation[132]. Not only attenuated virus- and peptide-based vaccines but also oncolytic viruses were used to stimulate the native TCR in $CD8^+$ CAR-T cells[132]. *In vivo* injection of T cells, pre-loaded with vesicular stomatitis virus or reovirus, demonstrated improved migration, tumor infiltration, prolonged anti-tumor activity, and most importantly, led to a diversification of the endogenous anti-tumor TCR repertoire through epitope spreading[132]. The latter is triggered through tumor cell lysis as part of the recurring cancer-immune cycle, finally stimulating not only the T cell-mediated but also the humoral immunity via B cell activation[133,134]. Epitope spreading is generally thought to enhance clinical success of adoptive T cell therapy and might of course be constricted by prior lymphodepletion[133]. Finally, the T cell differentiation state was considered to influence the outcome of native TCR stimulation in CAR-T cells: viral infection was shown to only be beneficial in virus-specific CAR-T cells with central memory phenotype[124,125], which are commonly known for higher proliferative capacity and persistency than more differentiated effector memory T cells[135-137]. However, a strict categorization is not possible and the nature of TCR stimulation might again play an important role, especially as even terminally differentiated CAR-T cells were effectively re-activated through peptide-based vaccination using dendritic cells[126].

1.2.4 Combination of CAR and transgenic TCR

Major aim of simultaneously activating CAR and native TCR was to boost the anti-tumor response and effector T cell survival. Studies on co-expression of a CAR and a transgenic TCR are very limited and rather based on the idea of achieving dual-stimulation[138,139], which

can also be facilitated through combination of two CARs, tandem CARs equipped with two different scFvs or a mixture of T cells expressing various CARs[140-142]. However, as postulated by Carl June, the probability for simultaneous loss of MHC and target antigen is anticipated to be very low, meaning that the risk for tumor escape might be minimized with T cells co-expressing CAR and transgenic TCR[143].

Ugur Uslu and colleagues were first to functionally co-express a CAR and a transgenic TCR in $CD8^+$ T cells[139]. Compared to CAR-T or TCR-T cells, the so-called TETARs (T cell expressing two additional receptors) demonstrated equivalent anti-tumor activity. Interestingly, dual stimulation of TETARs resulted in boosted anti-tumor activity, which was not achieved with pooled CAR-T and TCR-T cells. A few years later, the work was continued with exactly the same CSPG4-CAR and gp100-targeting TCR, but the findings were not reproducible and simultaneous engagement led to impaired cytotoxicity[138]. Such differences could be explained by variations in the *in vitro* co-culture conditions or by the change from transient electroporation-based to lentiviral TCR delivery[118]. Together, the studies verified functionality of CAR and TCR in TETARs and more in-depth analysis is required to understand the potential range of application.

Besides this, other studies focused on costimulating transgenic TCRs through co-expression of truncated CARs. Increased transgenic TCR-dependent proliferation and repetitive tumor cell lysis was observed *in vitro* and *in vivo* upon co-expression of a BBζ-CAR missing the extracellular antigen-binding domain[144]. Similar TCR-supporting effects were observed upon co-expression of CD3ζ-truncated CARs, so-called chimeric costimulatory receptors: only CD28-costimulated chimeric costimulatory receptors (particularly containing CD28-OX40) supported expansion and serial killing capacity by the transgenic TCR, whereas 4-1BB-equipped chimeric costimulatory receptors led to apoptosis during *in vitro* co-culture experiments[127].

To sum this up, the positive effect of concomitant engagement of CAR and TCR was shown in various studies, however, further in-depth studies, particularly evaluating the *in vivo* efficacy and persistence of T cells co-expressing CAR and transgenic TCR, are required for clinical implementation[118].

1.3 Acute myeloid leukemia

Acute myeloid leukemia (AML) has its origin in the bone marrow, where differentiation of myeloid stem cells to white blood cells is impaired due to genetic mutations, causing clonal accumulation of immature myeloid progenitors[145,146]. For AML classification into genomic subgroups, special focus is placed on somatic driver mutations, which occur in more than 95% of patients[147]. Nucleophosmin 1 (NPM1) was shown to be the most frequently mutated gene in AML (27%), followed by chromatin and/or RNA-splicing genes (18%) and the commonly known tumor suppressor gene TP53 (13%)[147,148]. Despite AML with genetic abnormalities, there are five more groups categorized by the World Health Organization (2016 revision): AML with myelodysplasia-related changes, chemo-/radiotherapy-related myeloid neoplasm, myeloid sarcoma, myeloid proliferations related to Down syndrome and finally a non-specified group without prognostic significance[149]. Although therapeutic options for AML are slowly expanding, the prognosis remains poor with a five-year survival of approximately half of the patients under 60 years-old[146,150].

1.3.1 AML therapy

Current AML treatment consists of induction chemotherapy with either cytotoxic (cytarabine/anthracycline) or hypomethylating agents, optionally combined with immunotherapy targeting for example CD33 or FMS-like tyrosine kinase 3 (FLT3)[146]. In order to prevent disease recurrence after remission, the treatment is continued with consolidation therapy, meaning a second round of chemotherapy or allogenic hematopoietic stem cell transplantation (allo-HSCT)[146]. Allo-HSCT represents a double-edged sword: The graft-versus-leukemia effect facilitates extremely potent elimination of AML cells, especially in patients with high risk for relapse[151]. However, the non-AML-specific effect of allo-HSCT treatment is linked to high risk for GvHD and transplant-related mortality[151]. Considering the success of adoptive cell therapy in treatment of B cell-derived malignancies, a lot of effort is currently also put into identifying and testing suitable targets for treatment of AML[150].

1.3.2 CAR and TCR for treatment of AML

Immunotherapy for treatment of AML was first described in 1965 by Georg Mathé, who reported complete hematologic elimination through bone marrow transplantation, or

more precisely, through allo-HSCT-induced graft-versus-leukemia[152]. Nowadays, CAR- or TCR-T cell therapies are tested in order to facilitate a more specific anti-leukemic response with minimized toxicity against non-malignant tissue[150]. However, the extremely low mutational burden in AML compared to other cancers, presents a major challenge for identification of tumor-specific targets[150,153]. CD33, CD123 and C-type lectin-like molecule 1 (CLL1) are the most commonly targeted tumor-associated antigens in CAR-T cell therapy for AML[150]. Despite high expression on leukemic blasts, all of those targets are also found on healthy cells[154]. For instance, CD33 belongs to the sialic acid-binding immunoglobulin-like lectin family and is also expressed on normal myeloid progenitor cells, hepatic Kupffer cells and even immune cells such as monocytes and macrophages[155,156]. In line with this, severe myelosuppression or sinusoidal obstruction syndrome have been reported as potential off-target side effects[157-159]. Hence, TCR-T cells targeting particularly neoantigens represent a possible solution by increasing tumor-cell specificity through targeting of mutated intracellular proteins[154]. The previously mentioned driver mutation in NPM1 is for instance seen as optimal target for AML[160]: Van der Lee and colleagues identified an HLA-A2*02:01-restricted TCR specific for the epitope CLAVEEVSL, and demonstrated *in vitro* and *in vivo* cytotoxicity against primary AML blasts[161]. So far, however, only tumor-associated antigens such as Wilm's tumor-1 were targeted in clinical trials, already showing first promising results (NCT02550535[162])[154].

In order to minimize the risk for antigen escape and to overcome the large clonal heterogeneity in AML, various combinatorial approaches for dual-targeting are currently tested in clinical trials: CD123/CLL1-CAR-T cells (NCT03631576), CD123/CD33-CAR-T cells (NCT04156256) or CD33/CLL1-CAR-T cells (NCT05016063), which already led to first encouraging results in patients with relapsed or refractory AML[150,163,164].

Finally, therapeutic efficiency is impaired through immunoediting mechanisms such as downregulation of MHC molecules, secretion of immunosuppressive factors, overexpression of inhibitory receptors and mobilization of healthy, non-malignant cells to the AML niche[165]. Thus, a possible solution might be to combine adoptive cell therapy with checkpoint inhibitors, which was already successfully demonstrated in pre-clinical CD123-CAR-T cell studies with blockade of the inhibitory receptors such as PD-1 or T cell immunoglobulin and mucin domain-containing protein 3 (TIM-3)[154,155]. Other

combinatorial strategies are for instance focused on directly targeting immunosuppressive tumor-resident immune and stromal cells[166] or disrupting stem cell homing and thereby the interaction between leukemic blasts and the TME (NCT00512252[167])[154,165].

In summary, despite the risk for relapse or even therapy-associated mortality, HSCT still represents the preferred second-line treatment option for AML[150]. However, encouraging results of CAR- and TCR-T cell clinical trials are emerging, pushing forward the implementation of targeted immunotherapies in AML[154]. Further optimizations are required to overcome challenges such as on-target off-tumor toxicities, the broad tumor heterogeneity, the risk for immune escape and the immunosuppressive TME in AML[165].

1.4 Objective of the work

T cell-based therapies have led to encouraging treatment responses in several clinical trials, however, optimizations are indispensable as therapeutic success is often limited by tumor escape, lack of suitable target antigens or side effects such as on-target-off-tumor toxicity. Therefore, novel therapeutic approaches are required, which allow for enhanced therapeutic potency and tumor cell restriction.

Primary goal of this work was to assess, in which way CAR and TCR technologies can be combined, so that they can act as a counterbalance to each other's limitations while fully exploiting their respective strengths and benefits. As postulated by Carl June, the likelihood of simultaneous downregulation of MHC and CAR-target antigen is expected to be very low[143], suggesting that either one, CAR or transgenic TCR, would still allow for tumor recognition by dual-specific T cells. Current research on the combination of CAR and transgenic TCR in the same T cell is limited. However, several groups have shown that stimulation of the endogenous TCR (e.g. in virus-specific T cells) has beneficial effects on CAR T cell expansion, persistence and anti-tumor activity[124,127,134], even being capable of functionally recovering terminally differentiated and exhausted CAR T cells[126]. Therefore, it was hypothesized that the stimulation of a transgenic TCR in CAR-T cells might have a similarly advantageous outcome, while simultaneously facilitating dual-specificity.

The most important scientific question addressed in this work is whether it is advantageous to combine a CAR and a transgenic TCR in the same T cell (referred to as CAR'TCR-T). How does dual stimulation affect T cell effector function? Is there reciprocal inhibition? Are CAR'TCR-T cells beneficial in case of tumor heterogeneity?

For proof of concept, first experiments were focused on the combination of the clinically well-established second-generation CD20-CAR[84,168,169] and the previously published transgenic dNPM1-TCR[161]. This combination allowed for in-depth characterization of CAR- and TCR-functionality in CAR'TCR-T cells, the impact of costimulatory domains in the CAR context and the functionality in $CD8^+$ versus $CD4^+$ T cells. In order to verify the findings with a clinically relevant setting, dNPM1-TCR was co-expressed in combination with CD33-CAR and tested in an AML setting *in vitro* and *in vivo*.

2. MATERIAL

2.1 General material

Table 1: Consumables.

Item	Supplier
T75/ T175 cell culture flask	Corning (New York, USA)
10 cm culture dish	Sarstedt (Nümbrecht, GER)
CellSTACK® Culture Chambers (CF5)	Corning (New York, USA)
Filter unit 0.45 µm	Merck Millipore (Burlington, USA)
Nalgene™ Rapid-Flow™ Sterile Disposable Bottle Top Filter, 0.45 µm, 45 mm	Thermo Fisher Scientific (Waltham, USA)
24-/ 48-/ 96-well flat-bottom plate	Corning (New York, USA)
96-well U-bottom plate	Corning (New York, USA)
Deep well plate, 96 square well, U-bottom	VWR International (Darmstadt, GER)
MACS separation column (LS, LD)	Miltenyi Biotec (Bergisch Gladbach, GER)
Tubing set TS520	Miltenyi Biotec (Bergisch Gladbach, GER)
Transfer bag 600 ml	Miltenyi Biotec (Bergisch Gladbach, GER)
Cryo vials, 1.5 ml	Thermo Fisher Scientific (Waltham, USA)
CryoMACS® Freezing Bag 500	Miltenyi Biotec (Bergisch Gladbach, GER)
Syringe 5 ml, 50 ml	Becton Dickinson (New Jersey, USA)
Insulin syringe BD Micro Fine 0,5 ml U-100	Mercateo (Leipzig, GER)
BD tuberculin syringes G27	Thermo Fisher Scientific (Waltham, USA)
gentleMACS™ C Tubes	Miltenyi Biotec (Bergisch Gladbach, GER)
MACSPlex filter plate	Miltenyi Biotec (Bergisch Gladbach, GER)
Luer/Spike interconnector	Miltenyi Biotec (Bergisch Gladbach, GER)
SurPhob Gelloader 200 µl, 0.57 mm, sterile	Biozym (Hessisch Oldendorf, GER)
MACSQuant® Tyto® Cartridge	Miltenyi Biotec (Bergisch Gladbach, GER)
MACSQuant® Tyto® Running Buffer	Miltenyi Biotec (Bergisch Gladbach, GER)
Pre-separation filter, 70 µm	Miltenyi Biotec (Bergisch Gladbach, GER)
Eppendorf Safe-Lock tubes (0.5, 1.5, 2 ml)	Eppendorf (Hamburg, GER)

Table 2: Instruments/ laboratory devices.

Instrument	Model	Supplier
Thermomixer	Eppendorf ThermoMixer® C	Eppendorf (Hamburg, GER)
Incubator	Brutschrank IN75 ISF1-X HERACELL 240i	Memmert (Schwabach, GER) Adolf Kühner (Birsfelden, CH) Thermo Fisher Scientific (Waltham, USA)
Centrifuge	Centrifuge 5424 R Multifuge X3R	Eppendorf (Hamburg, GER) Haraeus Instruments (Hanau, GER)
Photometer	NanoDrop ND-1000	Thermo Fisher Scientific (Waltham, USA)
Cultivation device	CliniMACS Prodigy™	Miltenyi Biotec (Bergisch Gladbach, GER)
Flow Cytometer	MACSQuant® Analyzer 10 MACSQuant® Analyzer X	Miltenyi Biotec (Bergisch Gladbach, GER) Miltenyi Biotec (Bergisch Gladbach, GER)
Cell sorter	MACSQuant ® Tyto ®	Miltenyi Biotec (Bergisch Gladbach, GER)
Freezing container	Mr. Frosty™	Thermo Fisher Scientific (Waltham, USA)
Water bath	SW22 Shaking water bath	JULABO (Seelbach, GER)
Live cell imaging	Incucyte® S3 System	Sartorius (Göttingen, GER)
Imaging System *in vivo*	IVIS Lumina III imaging system	Perkin Elmer (Waltham, USA)
Tissue dissociator	gentleMACS™ Octo Dissociator	Miltenyi Biotec (Bergisch Gladbach, GER)
Microscope	Leica DM IL LED	Leica Microsystems (Wetzlar, GER)
Surgical Scalpel	-	Aesculap AG (Tuttlingen, GER)
Cell counter	Sysmex XP-300	Sysmex Deutschland, (Norderstedt, GER)
Cell culture hood	Hera Safe KS	Thermo Fisher Scientific (Waltham, USA)

Table 3: Kits.

Kit	Application	Supplier
NucleoSpin Plasmid (NoLid) Mini kit	DNA isolation	Macherey-Nagel (Düren, GER)
NucleoBond Xtra Maxi EF, Maxi kit (endotoxin-free plasmid DNA)	DNA isolation	Macherey-Nagel (Düren, GER)
$CD8^+$ T cell Isolation Kit, human	T cell isolation	Miltenyi Biotec (Bergisch Gladbach, GER)

$CD4^+$ T cell Isolation Kit, human	T cell isolation	Miltenyi Biotec (Bergisch Gladbach, GER)
Pan T cell Isolation Kit, human	T cell isolation	Miltenyi Biotec (Bergisch Gladbach, GER)
MACSelect™ LNGFR system	T cell enrichment	Miltenyi Biotec (Bergisch Gladbach, GER)
MACSPlex Cytokine 12 Kit, human	Cytokine multiplex assay	Miltenyi Biotec (Bergisch Gladbach, GER)
Inside Stain Kit	Fixation	Miltenyi Biotec (Bergisch Gladbach, GER)

2.2 Molecular Biology

Table 4: Media and supplements.

Medium/supplement	Composition	Supplier
LB medium solid	5 g/l Veggie Yeast Extract	Merck (Darmstadt, GER)
	10 g/l Veggie Peptone	Merck (Darmstadt, GER)
	5 g/l NaCl	Roth (Karlsruhe, GER)
	dissolved in ddH_2O and sterilized through autoclaving	
LB medium liquid	5 g/l Veggie Yeast Extract	Merck (Darmstadt, GER)
	10 g/l Veggie Peptone	Merck (Darmstadt, GER)
	10 g/l NaCl	Roth (Karlsruhe, GER)
	15 g/l LB Agar	Roth (Karlsruhe, GER)
	dissolved in ddH_2O and sterilized through autoclaving	
SOC medium	Super optimal broth with catabolite repression medium	NewEngland Biolabs (Ipswich, USA)
Kanamycin 50 mg/ml	used 1:1000	Sigma-Aldrich (St. Louis, USA)

Table 5: Plasmids.

Plasmid	Description	Source
pCMVdR8.74	CMV promotor, gag, pol, rev, RRE	Addgene (Watertown, USA)
pMDG	CMV promotor, VSV-G	Addgene (Watertown, USA)
p1293	CMV promoter, rev	Miltenyi Biotec (Bergisch Gladbach, GER)
p1294	CMV promoter, gag, pol, PRE	Miltenyi Biotec (Bergisch Gladbach, GER)

p1292	CMV promoter, VSV-G	Miltenyi Biotec (Bergisch Gladbach, GER)
MB_TV_LPC_CD20_eGFP	PGK promotor, 5'LTR, 3' sinLTR, CD20, P2A-eGFP	Miltenyi Biotec (Bergisch Gladbach, GER)
MB_TV_LPC_020_044	PGK promotor, 5'LTR, 3' sinLTR, Leu16-scFv, hCD8hinge, CD8-TM, 4-1BB costim., CD3ζ, P2A-LNGFR	Miltenyi Biotec (Bergisch Gladbach, GER)
MB_TV_LPC_020_047	PGK promotor, 5'LTR, 3' sinLTR, Leu16-scFv, hCD8hinge, CD8-TM, CD28 costim., CD3ζ, P2A-LNGFR	Miltenyi Biotec (Bergisch Gladbach, GER)
pLV_dNPM1-TCR	EF1α promotor, 5'LTR, 3' sinLTR, dNPM1-TCR β-chain, T2A, dNPM1-TCR α-chain	Miltenyi Biotec (Bergisch Gladbach, GER)
pLV_CD33-CAR	EF1α promotor, 5'LTR, 3' sinLTR, My96-scFv, hCD8hinge, CD8-TM, 4-BB costim., CD3ζ, P2A, LNGFR	Miltenyi Biotec (Bergisch Gladbach, GER)

Abbreviations: CMV: Cytomegalovirus; gag: group specific antigen; pol: polymerase; RRE: rev response element, VSV: vesicular stromatitis virus; LTR: long terminal repeat; PGK phosphoglycerate kinase, EF1α: elongation factor-1 alpha; scFV: single-chain variable fragment; TM: transmembrane

2.3 Cell culture media, supplements and reagents

All cell culture media and supplements were stored according to manufacturer's instructions and handled under sterile conditions.

Table 6: Media and supplements.

Medium/ Supplement	Medium/ Supplier/ Composition
Oci-AML medium	αMEM (PAN-Biotech, Aidenbach, GER) + 20% FCS
Raji/ Sup-T1 medium	RPMI 1640 w/o L-glutamine (Biowest Nuaillé, France) + 10% FCS + 2mM L-glutamine

HEK293T medium	DMEM high glucose w/ L-glutamine w/ sodium pyruvate (Biowest Nuaillé, France) + 10% FCS
T cell medium	TexMACS GMP medium (Miltenyi Biotec, Bergisch Gladbach, GER) + 12.5 ng/ml IL-7 + 12.5 ng/ml IL-15 + 3% human AB-serum
Fetal Calf Serum, FCS-Maximus	Catus Biotech (Tutzing, GER)
Human AB serum	Capricorn Scientific, Ebsdorfergrund, GER
L-glutamine, 200 mM	Lonza (Basel, CH)
T cell TransAct™, human	Miltenyi Biotec (Bergisch Gladbach, GER)
MACS® GMP T cell TransAct™	Miltenyi Biotec (Bergisch Gladbach, GER)
MACS® Recombinant human IL-7	Miltenyi Biotec (Bergisch Gladbach, GER)
MACS® Recombinant human IL-15	Miltenyi Biotec (Bergisch Gladbach, GER)
Freezing medium cell lines	10% DMSO 90% FCS
Freezing medium primary T cells	40% TexMACS GMP medium 10% DMSO 50% AB Serum

Table 7: Buffers and reagents.

Buffer/Reagents	**Supplier**
Dimethyl sulfoxide (DMSO)	Sigma-Aldrich (St. Louis, USA)
MACS® BSA Stock Solution	Miltenyi Biotec (Bergisch Gladbach, GER)
ClinicMACS® PBS/EDTA Buffer	Miltenyi Biotec (Bergisch Gladbach, GER)
MACSQuant bleach solution	Miltenyi Biotec (Bergisch Gladbach, GER)
MACSQuant storage solution	Miltenyi Biotec (Bergisch Gladbach, GER)
MACSQuant washing solution	Miltenyi Biotec (Bergisch Gladbach, GER)
MACSQuant running buffer	Miltenyi Biotec (Bergisch Gladbach, GER)
Pancoll	Pan-Biotech (Aidenbach, GER)
Gibco™ PBS, pH 7.2	Thermo Fisher Scientific (Waltham, USA)
Accutase® Cell Detachment Solution	BioLegend (SanDiego, USA)
Polyethylenimine, MW 25000 (PEI)	Polyscience (Warrington, USA)
Sodium butyrate	Sigma-Aldrich (St. Louis, USA)
CliniMACS® Formulation Solution	Miltenyi Biotec (Bergisch Gladbach, GER)
Red blood cell lysis buffer	Miltenyi Biotec (Bergisch Gladbach, GER)

D-Luciferin, Potassium Salt	GoldBio (St. Louis, USA)
Isoflurane	Zoetis (New Jersey, USA)
MACS® Quant calibration beads	Miltenyi Biotec (Bergisch Gladbach, GER)
CliniMACS CD8 Reagent	Miltenyi Biotec (Bergisch Gladbach, GER)
CellTrace™ Violet	Thermo Fisher Scientific
Anti-APC MicroBeads	Miltenyi Biotec (Bergisch Gladbach, GER)
Anti-PE MicroBeads, UltraPure	Miltenyi Biotec (Bergisch Gladbach, GER)

Table 8: Cell lines.

Name	Application	Source
Oci-AML2 cl. 20 (GFP^+)	Target cell line *in vitro*	Leiden University
Oci-AML3 cl. 22 (GFP^+)	Target cell line *in vitro*	Leiden University
Oci-AML3 m. 10 ($tdTomato^+/FFluc^+$)	Target cell line *in vivo*	Leiden University
Oci-AML3^{CD33ko} (GFP^+)	Target cell line *in vitro*	Oci-AML3 cl. 22 modified by Miltenyi Biotec
Raji^{WT} ($GFP^+/FFluc^+$)	Target cell line *in vitro*	ATCC CCL-86 modified by Miltenyi Biotec
Raji^{CD20ko} ($GFP^+/FFluc^+$)	Target cell line *in vitro*	ATCC CCL-86 modified by Miltenyi Biotec
HEK293T	Lentiviral vector production	ATCC CRL-3216
Sup-T1	Lentiviral vector titration	ATCC CRL-1942

2.4 Conjugated antibodies

All antibody conjugates were obtained from Miltenyi Biotec (Bergisch Gladbach, GER) and applied in a dilution of 1:50 for flow cytometric analysis and sorting.

Table 9: Antibodies and staining reagents.

Specificity	Conjugate	Clone
dNPM1-HLA-A*02 Tetramer	PE	-
CD33-CAR detection reagent	Alexa Fluor® 647	-
CD271 (LNGFR)	APC/ PE	REA844
CD8	VioBlue®/ FITC/ APC-Vio® 770	REA734
CD4	VioBlue®/ VioGreen™/ APC	REA623

CD95	PE-Vio770®	REA738
CD45RO	APC/ APC-Vio 770®	REA611
CD62L	PE-Vio® 770/ PE	REA615
CD223 (LAG-3)	APC/ APC-Vio® 770	REA351
CD366 (TIM-3)	PE-Vio® 770	REA636
CD45	VioBlue®	REA747
CD3	FITC	REA613
CD16	PE	REA423
CD56	PE	REA196
CD20	PE-Vio® 770	REA780
CD14	APC	REA599
CD137 (4-1BB)	PE	REA765
CD25	APC-Vio® 770	REA570
CD15	APC	VIMC6
CD33	APC	REA775
Ter-119 (anti-mouse)	PerCP-Vio® 700	REA847
7-AAD Staining Solution	-	-
Propidium Iodide Solution (PI)	-	-

2.5 Software

Table 10: Software.

Software	Supplier
Flowlogic 8.4	Inivai Technologies (Mentone Victoria, AUS)
MACSQuantify™ 2.13.0	Miltenyi Biotec (Bergisch Gladbach, GER)
Geneious Prime 2023.0.1	Biomatters (Boston, USA)
GraphPad Prism 8.2.1	GraphPad Software (Boston, USA)
Living Image® 4.5.2	Perkin Elmer (Waltham, USA)

3. METHODS

3.1 Molecular biology methods

3.1.1. Transformation of competent E. *coli*

Transformation of NEB 5-alpha competent E. *coli* DH5α (New England Biolabs, Ipswich, US) was performed by thawing the E. *coli* on ice for 10 mins and subsequently adding ≤ 1 µg DNA. Cells were carefully mixed by flicking the vial 4-5 times and then placed on ice for half an hour. After heat shock for exactly 30 seconds at 42°C the vial was immediately placed on ice for 5 mins. For outgrowth and efficient recovery of the cells, 950 µl SOC media was added to the tube and incubated at 37°C for 45 mins while vigorously shaking the tube at 250 rpm. The cells were centrifuged at 8000 × g for 1 min and after discarding the supernatant, 20-50 µl were transferred on pre-warmed selection plates supplemented with 50 µg/µl Kanamycin. After incubation at 37°C for 16 hours, a single transformed bacteria colony was transferred to 3 ml of LB medium containing 50 µg/µl Kanamycin. The culture was incubated overnight at 37°C and 280 rpm for plasmid amplification.

3.1.2. Amplification and isolation of plasmid DNA

DNA isolation was performed using NucleoSpin Plasmid Mini kit (Macherey-Nagel, Düren, GER) according to manufacturer's instructions. Subsequently, maxi preparation was performed using NucleoBond Xtra Maxi EF kit (Macherey-Nagel, Düren, GER) according to manufacturer's instructions. DNA concentrations were determined using NanoDrop ND-1000 spectro-photometer, based on the typical absorption maximum of 260 nm. Finally, Sanger sequencing was performed by GATC using appropriate sequencing primers and results were analyzed via Geneious Prime.

3.2 Cell culture methods

3.2.1 Cell cultures

All cell lines were cultured at 37°C and 5% CO_2 in appropriate media (Table 6, chapter 2.3). The cell concentrations were maintained according to suppliers recommendations by splitting the cultures two to three times a week. Adherent HEK293T cells were detached by

removing the culture medium, washing the cells with PBS and incubating 2.5 ml of Accutase for 5 min at 37°C. Next, 7.5 ml fresh media was added and the desired volume was transferred to a new culture flask.

3.2.2 Cryopreservation and thawing of cell lines and primary T cells

Cell lines and primary T cells were frozen in respective freezing medium as depicted in (Table 6, chapter 2.3). In both cases, the cell suspension was centrifuged at 300 × g for 5 min, resuspended in freezing medium. Cell lines and primary cells were frozen at a final concentration of 1×10^7 cells/ml and 5×10^7 cells/ml per cryo vial, respectively. Cryo vials were immediately placed in a pre-cooled Mr. Frosty™ and after 24 hours at -80°C, frozen cells were transferred to storage in liquid nitrogen.

Thawing of cells was performed by placing the vials in water bath at 37°C. Next, the cell suspension was immediately transferred into 10 ml fresh medium and centrifuged for 10 min at 300 × g. The cell pellet was resuspended in fresh medium and taken into culture.

3.2.3 Cryopreservation and thawing of leukapheresis

The leukapheresis (LP) was obtained from a healthy donor (Biomex, Heidelberg, GER) and used for large-scale manufacturing of engineered T cells using the CliniMACS Prodigy™. After transferring the LP into a 600 ml transfer bag, CliniMACS® Formulation Solution was added to a final volume of 600 ml. Next, the transfer bag was sterilely connected to a second transfer bag and centrifuged at 200 × g for 15 min. After this washing step, the plasma was carefully removed via a plasma extractor and cells were diluted in 100 ml pre-cooled CliniMACS® Formulation Solution. A sample of 100 µl was analyzed via flow cytometry to determine cellular composition and cell count. Finally, 2×10^9 total white blood cells in a final volume of 66 ml were transferred into a CryoMACS® Freezing Bag 500. Next, 34 ml of pre-cooled Cryo Supplement 3x was added, a sterile syringe was used to remove remaining air and the bag was closed. After using Consarctic BV-40 (Westerngrund, GER) for gentle freezing of the LP, cells were transferred to storage in liquid nitrogen.

After thawing the LP in water bath at 37°C, the cell suspension was immediately transferred into 600 ml transfer bag containing 180 ml TexMACS™ medium. Automated $CD8^+$ T cell isolation, transduction and cultivation was performed using the CliniMACS Prodigy™.

3.2.4 Isolation and cultivation of primary human T cells

For all *in vitro* experiments, T cells were isolated from 1-2 days old buffy coats of healthy donors after informed consent (University hospital Hagen or Dortmund). First, 25 ml of anticoagulated blood sample were diluted with 10 ml of CliniMACS® PBS/EDTA buffer supplemented with 0.5 % MACS® BSA (PEB). A new 50 ml falcon containing 15 ml Pancoll was prepared and the diluted blood sample was carefully layered on top of the Pancoll by tilting the falcon by at least 45 degree. Density gradient centrifugation was performed at 445 × g for 35 min (acceleration: 3, deceleration: 3). PBMC were carefully transferred into a new falcon, PEB was added to a final volume of 50 ml. After centrifugation for 15 min at 300 × g, supernatant was discarded and washing step was repeated with 200 × g for 10 min.

3.2.5 Cell surface marker staining and flow cytometry analysis

Up to 1×10^6 cells were transferred in a 96-well U-bottom plate and centrifuged at 300 × g for 5 min. After resuspending the cell pellet with 200 µl PEB and centrifuging at 300 × g for 5 min, 50 µl of the antibody mixture (diluted in PEB according to manufacturer's instructions) was added to the cells. All antibody stainings were performed in the dark at 4°C for 10 min. Tetramer staining was performed at room temperature, also in the dark for 10 min. Tetramer staining was always performed as first step and separated from the subsequent antibody staining. Viability staining was either performed through addition of 7-AAD to the antibody mixture or via PI staining right before analysis. Finally, 150 µl PEB were added and cells were washed twice by centrifuging for 5 min at 300 × g and resuspending the cell pellet in 100 µl - 200 µl PEB.

Analysis was performed at MACSQuant® Analyzer 10 or MACSQuant® X, which was prior calibrated using MACSQuant® calibration beads. Data analysis was performed using Flowlogic 8.4. Generally, the gating strategy was always performed according Figure 4 and consisted of first debris exclusion (FSC/SSC), next gating of singlets (SSC-H/SSC-A), and finally gating of viable cells (7-AAD$^-$ or PI$^-$). Subsequent gates were set based on fluorescent minus one (FMO) controls or negative controls.

3.3 Gene engineering

3.3.1 Lentiviral vector production

Three days prior to transient transfection, 4.5×10^6 or 5×10^7 HEK293T cells were seeded in a T175 flask or for large-scale production in a five chamber Corning® CellSTACK®, respectively. At day of transfection, confluence of HEK293T was between 70% - 90%.

Depending on the transfer plasmid, a different plasmid system was used. Plasmids listed in Table 5 beginning with "pLV" or "MB_TV_LPC" were used in the 4-plasmid or 3-plasmid system (Table 11), respectively.

Table 11: Transfection with 4-plasmid and 3-plasmid system.

4-plasmid system	µg of total/ 100%	3-plasmid system	µg of total/ 100%
p1292 (VSV-G)	17.4%	pMDG	10%
p1294 (gag/pol)	26%	pCMVdR8.74	37%
p1293 (rev)	13%	-	-
pLV_*transgene*	43%	MB_TV_LPC_*transgene*	51%

A fresh aliquot of PEI was thawed, vortexed for at least 1 min and added to the appropriate volume of DMEM without supplements (Table 12). Next, DNA solution was prepared by adding DMEM to the prepared plasmid mixture, as described in Table 11. Both solutions were vortexed for at least 1 min. Afterwards, the PEI solution was added to the DNA solution and the resulting transfection mix was again vortexed for not less than 1 min. After incubation at room temperature for 20 min, the medium was completely removed from the cell culture flasks and replaced by dropwise adding the transfection mix.

Table 12: DNA and PEI solution for transient transfection.

DNA solution	T175	5CF	PEI solution	T175	5CF
1. DNA [µg]	35.1	634.8	**1. DMEM [µl]**	3360	60500
2. DMEM [µl]	3464.9	62368.2	**2. PEI [µl]**	140	2500
Total volume [µl]	*3500*	*63000*	***Total volume [µl]***	*3500*	*63000*

FCS was added to the cell culture flasks as described in Table 13 after 4 - 6 hours of incubation at 37°C. The following day, 520 µl/ T175 flask or 10 ml/ 5CT of sodium butyrate were added in order to enhances the viral titer through histone deacetylase inhibition[170].

Table 13: Volume of FCS.

DNA solution	T175	5CF
FCS [ml]	2.5	50
Total volume [ml]	*26*	*500*

After 48 hours, the supernatant containing lentiviral vectors (LVs) was harvested, centrifuged at 300 × g to remove residual cells and filtered through a 0.45 µm filter. Optionally, new medium was added to the cells for a second harvest after in total 72 hours. Centrifugation at 4700 × g and 4°C for 24 hours was performed to achieve concentration of the vector particles. After discarding the supernatant, the LVs were resuspended in pre-cooled TexMACS™ medium (100- to 200-fold concentration), incubated 10 min at 4°C and resuspended by pipetting ~ 60 times up and down. Finally, the LVs were aliquoted and stored at -80°C.

3.3.2 Lentiviral vector titration

SupT1 cells were transduced with a serial dilution of lentiviral vectors in order to determine the titer. 2 × 10^5 SupT1 cells were seeded in a 96-well U-bottom plate in 100 µl RPMI 1640 supplemented with 2mM L-glutamine. Next, a serial dilution with the LVs was prepared and added to the cells by mixing gently (total lentiviral vector volume per well: 3 µl, 1 µl, 0.1 µl, 0.01 µl, 0 µl). After incubation for 4 - 6 hours at 37°C, 90 µl/ well of pre-warmed complete RPMI 1640 media supplemented with 2mM L-glutamine and 10% FCS was added to the plate. The transduction efficiency was analyzed 4 days later by flow cytometry and the titer (TU/ ml) calculated based on following equation:

$$Titer\ \left[\frac{TU}{ml}\right] = \left(\frac{cell\ number}{well} \times \left(\frac{transduction\ efficiency\ [\%]}{100}\right)\right) \times \frac{LVV\ [ml]}{well}$$

3.3.3 Generation of CD20-expressing Oci-AML2 and Oci-AML3 cells

1 × 10^6 Oci-AML2 (cl. 20) or Oci-AML3 (cl. 22) cells were seeded in a 48-well plate in αMEM medium (without supplements) and transduced with different volumes of LV encoding recombinant CD20 protein (Table 5). After 4 - 6 hours, 200 µl FCS was added per well (≙ 20% FCS). Transduction efficiency was analyzed after 5 days. Next, single cell clones were produced by seeding seeded ~ 0.3 cells per well in a flat-bottom 96-well plate. The

generated cell clones were expanded and mean fluorescent intensities (MFIs) were compared to Raji^{WT} cells as displayed in Figure 3.

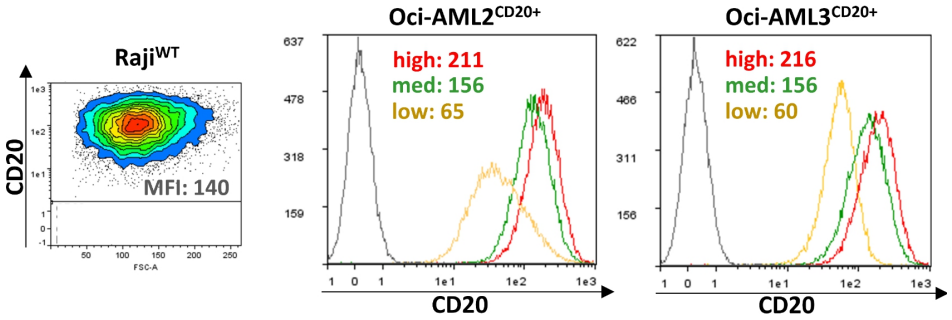

Figure 3: Cell line engineering of CD20-expressing Oci-AML cell clones for studying dual stimulation in cis. Raji^{WT} cells were used as control cell line and Oci-AML2^{CD20+} and Oci-AML3^{CD20+} cell clones displaying a CD20 MFI of 156 (green histogram) were used *for in vitro* functionality testing.

The expanded CD20^{+} Oci-AML cell clones were frozen and stored in liquid nitrogen according to chapter 3.2.2.

3.3.4 Small-scale lentiviral transduction

T cells were isolated from PBMCs as described in chapter 3.2.4. T cells were seeded in a concentration of 1 × 10^6 cells per ml in a 24-well plate containing 2 ml per well. The TexMACS^{TM} medium was supplemented with 12.5 ng/ml IL-7 and IL-15 and TransAct^{TM} diluted 1:100. The following day, LVs were added to the cells and carefully resuspended. On day 3, the supernatant containing TransAct^{TM} and potentially residual LVs was removed and new TexMACS^{TM} medium was supplemented with 12.5 ng/ml IL-7 and IL-15 was added. Transduction efficiency was measured on day 6 using flow cytometry analysis.

3.3.5 Large-scale automated manufacturing of engineered T cells

Manufacturing of gene-engineered T cells for the *in vivo* study was performed using the GMP-compliant, fully-closed and automated CliniMACS Prodigy^{TM} platform-based TCT process (version 8.4). Priming of the applied TS520 tubing set was performed using CliniMACS® PBS/EDTA supplemented with 0.5% human serum albumin. The LP was thawed as described in 3.2.3 and sterile connected to the previously primed tubing set. As displayed in Table 14, a different manufacturing protocol was used for the condition “sorted CAR’TCR-T cells”, meaning that after using the TCT 8-day process, the double-positive cells

were enriched and subsequently cultured for one more week. In parallel, the other conditions (TCR-T, CAR-T, Triple-T) were produced using the 12-day TCT process (Table 14). In both processes $CD8^+$ T cells were magnetically enriched on day 0 and the purity was subsequently determined by analyzing the cellular composition via flow cytometry. 7-10 × 10^7 $CD8^+$ T cells were prepared for activation via TransAct™. The following day, LV were diluted in TexMACS™ GMP medium in a total volume of 10 ml and sterile welded to the tubing set. LVs encoding CD33-CAR or dNPM1-TCR were applied at MOIs of 35 and 25, respectively. Co-transduction (in case of Triple-T) was achieved through mixing of the two lentiviral vectors CD33-LV and dNPM1-LV.

Table 14: Activity matrix 8-day and 12-day process.

8-day	Activity	Vol [ml]
-1	Medium preparation + tubing set installation	-
0	CD8 enrichment	-
1	Transduction	100
3	Culture wash	200
3	Activate shaker type 2	200
5	Media exchange	200 (±50)
6	Media exchange	200 (±130)
6	Activate shaker type 3	200
7	Media exchange	200 (±130)
8	End of culture	-

12-day	Activity	Vol [ml]
-1	Medium preparation + tubing set installation	-
0	CD8 enrichment	-
1	Transduction	100
3	Culture wash	200
3	Volume reduction	100
5	Feed	150 (+50)
5	Media exchange	150 (±50)
6	Feed	200 (+50)
6	Media exchange	200 (±130)
7	Media exchange	200 (±130)
8	Media exchange (2x/day)	200 (±130)
9	Media exchange	200 (±130)
10	Media exchange (2x/day)	200 (±130)
11	Media exchange	200 (±130)
12	End of culture	-

After harvest, cell numbers and transduction efficiency were determined via flow cytometric analysis. Accordingly, the various conditions were prepared for *in vivo* intravenous (i.v.) injection.

3.3.6 Sorting of gene-engineered T cells

For comparison reasons, all of the *in vitro* experiments were performed with previously sorted gene-engineered T cells. The cells were stained for CD8 and transgenic TCR and/or CAR expression according to staining protocol in 3.2.5. In order to ensure optimal detection in MACSQuant® Tyto®, containing a 405 nm, 488 nm and 638 nm laser, cells were stained with CD8-VioBlue®, CD33-CAR detection reagent conjugated to Alexa Fluor® 647 and dNPM1-TCR-specific Tetramer labeled with PE. Finally, 2 - 3 × 10^7 cells were resuspended in 10 ml of PBS-based MACSQuant® Tyto® running buffer. The sample was loaded through a 70 µm filter into a syringe, which was connected to the input chamber of a previously primed Tyto Cartridge HS. Using the plunger, the cells were then carefully transferred into the input chamber. Sorting was performed using the MACSQuant® Tyto® with software version cap 1.0. The gating strategy included determining noise threshold via backscatter signals, and TCR^+ and/or CAR^+ gene-engineered $CD8^+$ T cells. After completion of the sort, the cells were carefully collected from the positive output chamber using a capillary pipette tip and by washing several times. A sample was analyzed via flow cytometry to determine the total cell number and the sort efficiency. Finally, the cells were re-activated using TransAct™ (1:500) and cultured in a concentration of 1 × 10^6 cells for 5 - 7 days before assessing the functionality.

3.4 Functional analysis of engineered T cells

3.4.1 Flow cytometry-based co-culture assay

All flow cytometry-based co-culture assays were performed in 96-well U-bottom plate with 1 × 10^4 target cells and in TexMACS™ medium without supplements.

In order to distinguish between the lysis of two different cell lines, which were mixed together, one of the cell lines was stained with Violet CellTrace™. Selective analysis was hence possible through gating on GFP^+ and GFP^+/$VioBlue^{®+}$ cells as exemplarily shown in Figure 4, displaying the generally applied gating strategy. This was especially required for co-culture with trans stimulation, meaning CAR- and TCR-target on two different cell lines. CellTrace™ working concentration (5µM) was prepared by adding 20 µl of DMSO to the stock solution according to manufacturer's instruction. Staining was performed by resuspending 1 × 10^6 target cells in 1 ml of 0.1 nM and incubate for 5 min at 37°C. Next, 5

ml of complete αMEM medium supplemented with FCS was added to the cells and incubated for 5 min at 37°C. Finally, the cells were centrifuged at 300 × g for 5 min and resuspended in fresh TexMACS™ medium without supplements after completely removing the supernatant. A sample was analyzed via flow cytometry to determine staining efficiency and cell concentration.

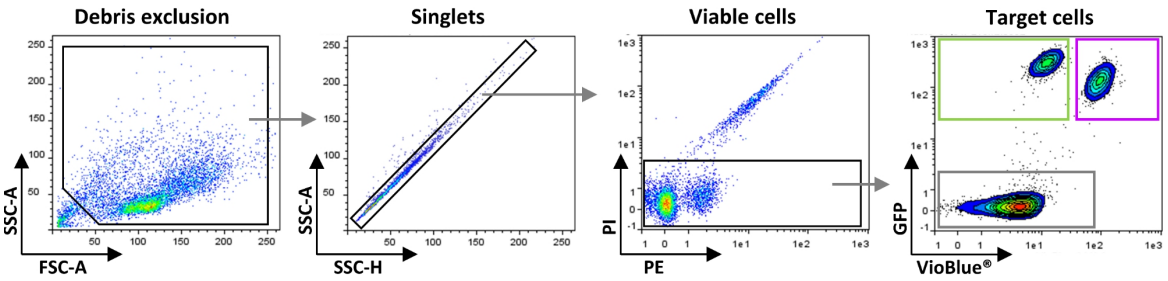

Figure 4: Gating strategy for analysis of the flow-cytometry-based killing assay. Gating strategy including debris and doublets exclusion via SSC-A/FSC-A and SSC-A/SSC-H, respectively. PI staining was applied for detection of viable cells. Finally mixed target cell lines were distinguished via GFP expression (FITC) and Violet CellTrace™ staining (VioBlue®).

Next, 100 µl of target cells was co-cultured with 100 µl of effector cells per well. Effector cells were transduced, cultured and optionally sorted as described in the previous chapters. In the case that effector cells were not enriched prior to co-culture, untransduced cells were spiked-in to normalize all conditions and donors to equivalent and comparable transduction efficiencies.

In general, every condition was tested in duplicates. Effector cell concentration was prepared to achieve an E:T ratio of either 2:1 or 1:1, as indicated in the figure legends of the respective experiments. Finally, the plate was centrifuged for 1 min at 100 × g to ensure close proximity of all cells. After 18 - 20 hours at 37°C and 5% CO_2, target cell count was determined via MACSQuant® 10 or MACSQuant® X by setting the analysis parameters on mix/ shake gentle, addition of PI (1:00) and measuring a fixed uptake volume of 50 µl for each well. Killing frequency in percent was then calculated by normalizing the target cell count upon treatment to the condition target cells only.

3.4.2 Live cell imaging-based co-culture assay

In parallel to analysis via flow cytometry, *in vitro* target cell lysis upon long-term co-culture was optionally also determined using cell imaging via Incucyte® S3 system. Cell

concentrations were applied according to 3.4.1. However, staining with Violet CellTrace™ was not performed, as only GFP^+ cells could be detected. This explains, why no differentiation between CAR- or TCR-target cells was possible regarding the trans setting. Due to microscope-based analysis, co-cultures were prepared in 96-well U-bottom plate, centrifuged for 1 min at 100 × g and then placed in the Incucyte® S3 system at 37°C. The acquisition time for the brightfield and the fluorescent imaging channel was set to 300 msec. Every 2 hours, GFP fluorescent intensity of 4 pictures per well was analyzed using standard scan type. Repetitive stimulation was achieved removing 100 µl of supernatant of the co-culture and subsequently adding 1×10^4 target cells in 100 µl of TexMACS™ medium. As previously, the plate was centrifuged for 1 min at 100 × g before continuing live cell imaging. Finally, the Incucyte® S3 system analysis software was used to develop a suitable mask, which is differentiation between GFP^+ target cells and GFP^- effector cells. The GFP signal was then quantified by analyzing the integrated intensity per well normalized to start of the measurement.

3.4.3 Cytokine release assay

Before measuring the target cell lysis upon *in vitro* co-culture experiments, 70 µl supernatant per well was collected from the plate and stored at -20°C. After thawing, duplicates were pooled and cytokine concentrations was analyzed in 50 µl per condition using MACSPlex Cytokine 12 Kit, human according to manufacturer's instructions.

3.4.4 Whole transcriptome analysis

Effector cell for bulk RNA-sequencing (RNA-seq) analysis were manufactured according to previous chapters by isolation of $CD8^+$ T cells from PBMC, transduction with LV-CD33-CAR and/or LV-dNPM1-TCR, sorting of transduced cells using MACSQuant® Tyto® and subsequent cultivation for 7 more days. 1×10^6 effector cells were co-cultured with 0.5×10^6 target cells in a total volume of 1.5 ml per 24-well plate well. After 18 hours at 37°C and 5% CO_2, depletion of target cells was performed to achieve high purity of effector cells: After centrifugation at 300 × g for 5 min, samples were washed with 5 ml PEB. The cells were incubated for 10 min at 4°C with CD4-PE and CD15-PE antibodies and washed with 5 ml PEB. Next, anti-PE MicroBeads were added according to manufacturer's instructions and incubated for 10 min at 4°C. The labeled target cells were then depleted via an LS column

and the untouched effector cell fraction was prepared for bulk RNA-seq by the NGS facility of Miltenyi Biotec. Data analysis was performed by Miltenyi Biotec Bioinformatics.

3.5 *In vivo* study

The *in vivo* study was approved by the local ethics committee (Landesamt für Natur, Umwelt und Verbraucherschutz Nordrhein-Westfalen). European (EU, Directive 2010/63/EU) and German guidelines for protection of laboratory animals, including the animal welfare act (TierSchG §§ 7-9) and the laboratory Animal Welfare Ordinance (TierSchVerV), were followed.

3.5.1 CAR'TCR-T efficacy study

Female immunodeficient NOD.Cg-Prkdc^{scid} IL2rg^{tm1Wjl}/SzJ (NSG) mice (Charles River Laboratories, Wilmington, USA) were kept in individually ventilated IVIC SMUC cages in groups of 4 - 5 animals with food and water provided ad libitum. The experiment was initiated 10 days after arrival of the mice to ensure slow adaptation to the housing conditions and the wellbeing of all animals was monitored daily.

1×10^6 Oci-AML3^{FFluc} m.10 cells diluted in 100 µl PBS were injected intravenously via the tail vain and engrafted for 4 days. The day after randomization, 5×10^6 gene-engineered T cells (normalized to total of 7.9×10^6 cells) diluted in 100 µl CliniMACS® Formulation Solution were injected intravenously. Tumor growth was monitored twice a week using the *in vivo* imaging system IVIS Lumina III. For this purpose, 100 µl D-Luciferin potassium salt dissolved in PBS (final concentration: 30 mg/ml) was injected intraperitoneally (i.p.) and IVIS measurement was performed after 6 min under anesthetization using 2.0 % (v/v) isoflurane (Zoetis, Zürich, CH).

3.5.2 *Ex vivo* analysis of spleen

Each step was performed on ice. Spleens were transferred into gentleMACS™ C Tubes prefilled with 5 ml RPMI 1640 medium and dissociated using the gentleMACS™ Octo Dissociator with program m_spleen_01_01. The spleen samples were filtered through a 70 µm MACS SmartStrainer and subsequently centrifuged at 300 × g for 5 min. After discarding

the supernatant, the pellet was resuspended in 200 µl PEB and transferred to a 96-well U-bottom plate for staining.

3.5.3 *Ex vivo* analysis of bone marrow

Femur and tibia were removed from the mice and residual tissue was removed completely. A hole was punched into a 0.5 ml tube placed in a larger 1.5 ml tube. Both ends at the epiphyses of femur and tibia were opened and the bones were placed in the 0.5 ml tube. After adding 100 µl PBS and centrifugation at 8000 rpm for 10 min at 4°C, the cell pellet was resuspended with 1 ml 1x RBC lysis buffer and incubated at room temperature for 5 min. Again, the cells were centrifuged at 300 × g for 5 min and resuspended in 200 µl PEB for staining in a 96-well U-bottom plate.

3.5.4 Flow cytometric analysis of spleen and bone marrow

Tissue samples were stained in a volume of 50 µl using a two-step staining protocol as described in Table 15.

Table 15: *Ex vivo* staining protocol.

Step	Staining reagent	Incubation
1	dNPM1-TCR-specific Tetramer	10 min, room temperature, dark
wash with 150 µl PEB/ well, centriguation at 300 × g for 5 min		
2.1. (phenotype)	7-AAD (1:10) CD8-FITC CD4-VioBlue® CD33-APC Ter-119-PerCP-Vio® 700 CD45RO-APC-Vio® 770 CD62L-PE-Vio® 770	10 min, 4°C, dark
2.2. (exhaustion)	7-AAD (1:10) CD8-FITC CD4-VioBlue® CD33-APC Ter-119-PerCP-Vio® 700 CD223- APC-Vio® 770 CD366-PE-Vio® 770	10 min, 4°C, dark
wash with 150 µl PEB/ well, centriguation at 300 × g for 5 min (twice)		
resuspending cell pellet in 200 µl PEB/ well and transfer to 96-well deep well plate		
addition of 200 µl InsideFix solution/ well		

Flow cytometric analysis was performed using MACSQuant® 10 with the following parameter settings: volume uptake: 350 µl, total volume: 400 µl, mix gentle, flow rate: medium. Bleach solution was applied after every 2 - 3 tissue samples.

3.6 Statistics

GraphPad Prism software 8.1.2. (GraphPad, USA) was used for statistical data analysis. The applied statistical method, number of biological replicates (donors) as well as number of independent experiments is mentioned in corresponding figure legends. Significance was defined by a ρ-value of ≤ 0.05 (*ρ ≤ 0.05, **ρ ≤ 0.01, ***ρ ≤ 0.001, ****ρ ≤ 0.0001, and ns = not significant).

4. RESULTS

4.1 Functionality of dNPM1-TCR

In order to evaluate the functionality of T cells simultaneously expressing a transgenic TCR and a CAR, a decisive prerequisite was to understand the characteristics of the two constructs by itself. First aim was to confirm that the reported 4bp TCTG insertion in Exon 12 of chromosome 5q35, which causes a frame shift and encodes for the neoantigen CLAVEEVSL[161], can be found in the Oci-AML3 target cell line. To this end, genomic DNA was isolated from two target cell lines Oci-AML2 (wtNPM1) and Oci-AML3 (dNPM1) and NPM1 PCR fragments were analyzed by Sanger sequencing (Figure 5). As expected, Oci-AML2-derived DNA displayed the wtNPM1 sequence, while the dNPM1-specific 4bp TCTG insertion was found in DNA isolated from Oci-AML3.

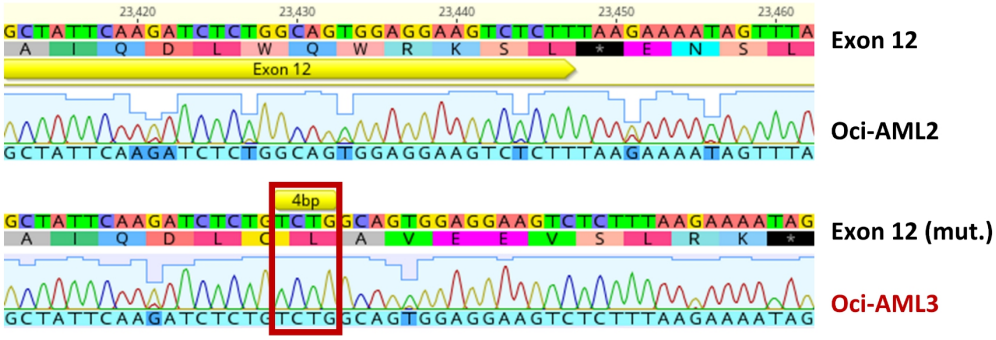

Figure 5: Genomic characterization of Oci-AML2 and Oci-AML3 target cells. DNA isolated from Oci-AML2 and Oci-AML3 cell line was analyzed for dNPM1 mutation (4bp TCTG insertion in Exon 12 of chromosome 5q35) using Sanger sequencing.

Next, the aim was to verify functionality and specific lysis of Oci-AML3 cells via the dNPM1-TCR. Especially in light of the restriction to MHC class I HLA-A*02:01, a dependency on the interaction with the CD8 co-receptor was expected[161,171]. Therefore, it was crucial to compare the functionality of the dNPM1-TCR in $CD8^+$ versus $CD4^+$ T cells. As displayed in Figure 6 A, only $CD8^+$ T cells transduced with dNPM1-TCR specifically lysed dNPM1-expressing Oci-AML3 target cells. In contrast, significantly decreased cytotoxicity was observed upon co-culture with dNPM1-TCR^+ $CD4^+$ T cells, which displayed a level of target cell lysis comparable to $CD4^+$ or $CD8^+$ untransduced (UTD) T cells. Accordingly, activation-induced secretion of pro-inflammatory cytokines such as IFN-γ, TNF-α, GM-CSF and IL-2

were only detected upon co-culture of dNPM1-TCR$^+$ CD8$^+$ T cells with Oci-AML3 target cells (Figure 6 B).

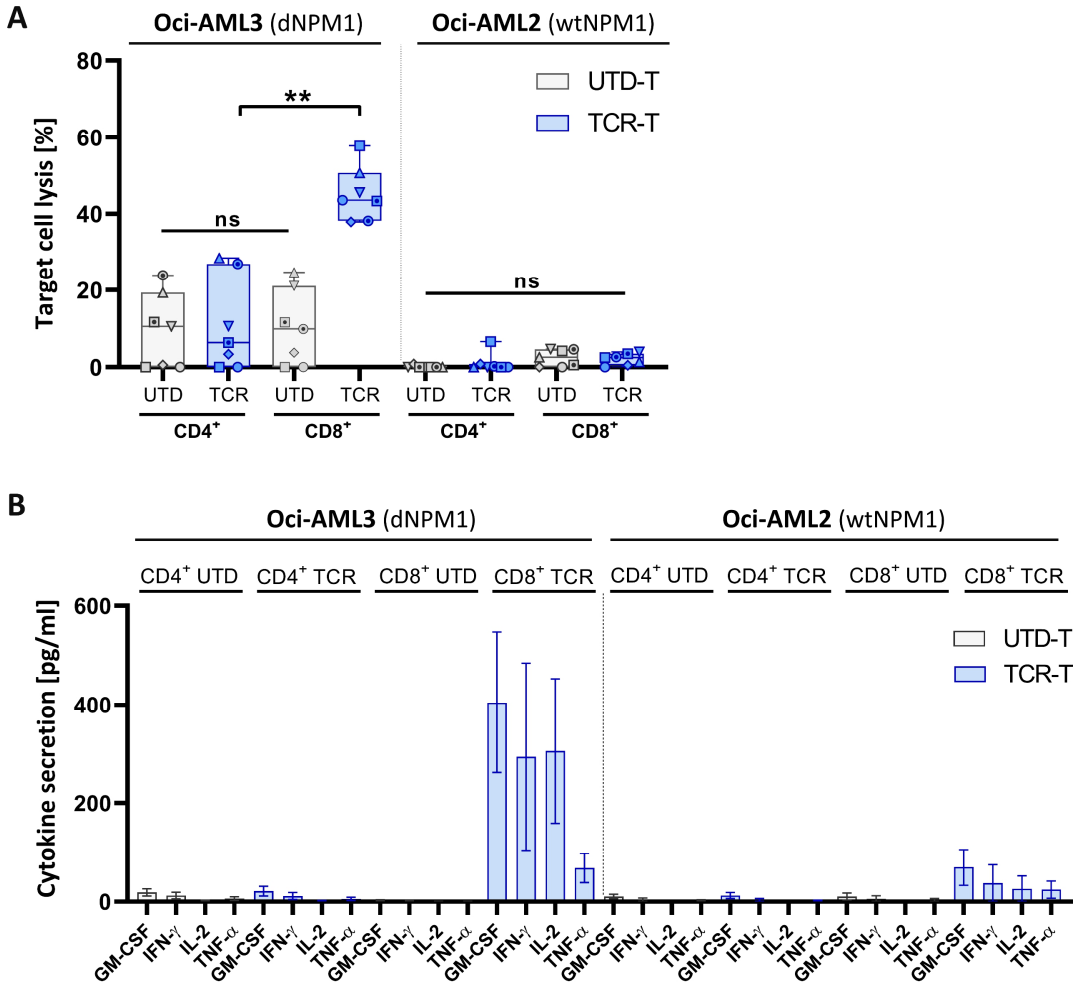

Figure 6: **Functionality of CD4$^+$ and CD8$^+$ T cells expressing dNPM1-TCR.** (A) Lysis of Oci-AML3 (dNPM1) or Oci-AML2 (wtNPM1) target cells upon 18 hours co-culture with either CD4$^+$ or CD8$^+$ UTD-T (untransduced) or dNPM1-TCR$^+$ T cells. Box and whiskers plot shows individual and median values of seven different donors from three independent experiments. The ρ-values were calculated using ordinary one-way analysis of variance with Tukey's correction for multiple comparison (ns = not significant, **ρ ≤ 0.01). (B) Cytokine secretion upon 18 hours co-culture of either CD4$^+$ or CD8$^+$ UTD-T (untransduced) or dNPM1-TCR T cells with Oci-AML3 or Oci-AML2. Shown are individual and mean values ±SEM of five different donors from two independent experiments.

4.2 Combination of dNPM1-TCR and CD20-CAR

4.2.1 Manufacturing of dNPM1-TCR$^+$/CD20-CAR$^+$ CAR'TCR-T cells

Based on the previous finding that the dNPM1-TCR is non-functional in CD4$^+$ T cells, the subsequent co-transduction experiments were performed with CD8$^+$ T cells only. For the initial proof of concept experiments, the dNPM1-TCR was combined with the clinically well-established second-generation Leu16-derived CD20-CAR with 4-1BB costimulatory domain. A polycistronic construct encoding for both CAR and TCR would reach a transfer vector size of almost 10 kbp and consequently the vector capacity limit. Therefore, manufacturing of dual-specific T cells was facilitated through co-transduction with two different LVs encoding either CD20-CAR or dNPM1-TCR. In this regard, it was crucial to ensure that the co-transduction does not influence the expression level of neither CAR nor TCR. As displayed in Figure 7 A, no significant difference in MFI was observed between dual-specific CAR'TCR-T cells and single-transduced CAR-T or TCR-T cells, suggesting equivalent expression levels despite co-transduction.

The overall transduction efficiency was relatively low, only achieving up to 10% of double-positive CAR$^+$/TCR$^+$ T cells (Figure 7 B). Therefore, cell sorting via dNPM1-TCR and/or dLNGFR as reporter gene co-expressed with the CAR, was performed to ensure high purity of transduced cells (> 80%) and comparability between all tested conditions for subsequent functionality experiments. Transduction levels are exemplarily displayed pre- and post-sorting in Figure 7 C.

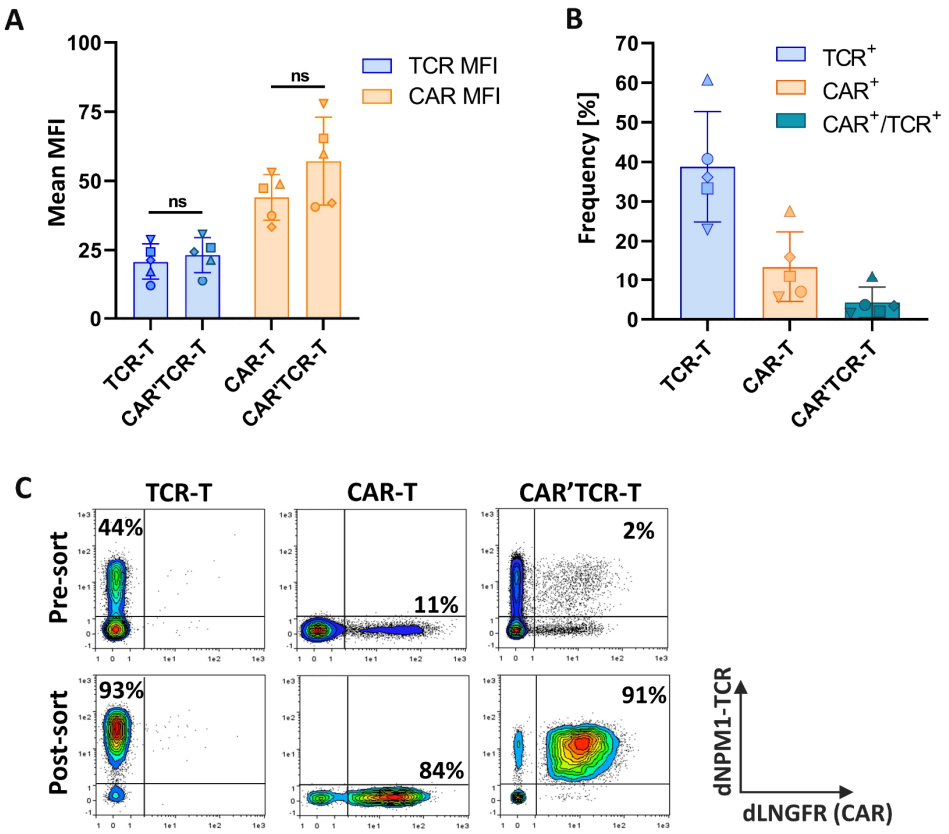

Figure 7: **Manufacturing of CD20-CAR- and dNPM1-TCR-co-expressing CAR'TCR-T cells.** (A) MFI and (B) transduction efficiency of dLNGFR (reporter gene co-expressed with CAR) and dNPM1-TCR in CAR-T, TCR-T or CAR'TCR-T cells on day 6 post-transduction. Shown are individual and mean values ±SD of five different donors from two independent experiments. The *p*-values were calculated using ordinary one-way analysis of variance with Tukey's correction for multiple comparison (ns, not significant). (C) Exemplary flow cytometry plots of one representative donor expressing TCR+, CAR+ or TCR+/CAR+ double-positive T cells pre- and post-sorting by staining with anti-dLNGFR antibody and dNPM1-TCR-specific pMHC tetramer.

4.2.2 Functionality of CD20-CAR$^+$/dNPM1-TCR$^+$ CAR'TCR-T cells

After ensuring that co-expression of CAR and TCR does not influence the respective expression levels, next goal was to assess the functionality of CAR'TCR-T cells. Functionality of the enriched CAR'TCR-T cells, co-expressing CD20-CAR and dNPM1-TCR, was assessed by analyzing the anti-tumor activity during co-culture experiments. The experimental set-up is illustrated in Figure 8. Different target cell mixtures were applied in order to achieve directed stimulation via TCR, CAR or both simultaneously. The trans setting, in which the CAR- and TCR- targets are expressed on different cell lines, allowed for separated analysis of CAR and TCR functionality in CAR'TCR-T cells upon dual stimulation.

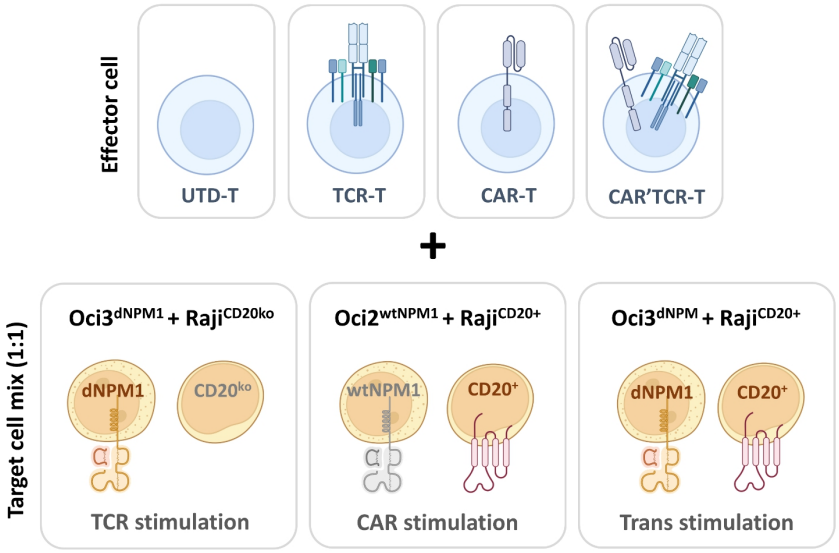

Figure 8: Illustration of experimental set-up for functionality analysis of CAR'TCR-T cells. Functional comparison of CAR'TCR-T cells with UTD-T, TCR-T and CAR-T. Co-culture assay was performed with different target cell mixtures to facilitate stimulation of various effector cell types via TCR, CAR or both in trans (dual stimulation through CAR- and TCR-target expression on different cell lines). In order to distinguish between CAR- or TCR-dependent target cell lysis after co-culture with effector cells, the GFP$^+$ CAR-target cell line was labeled with CellTrace^{TM} and target cell counts of the mixed cell lines were analyzed separately. Illustration created with BioRender.com.

First, it was important to ensure that the co-expression of CAR and transgenic TCR does not negatively influence the functionality of the two receptors. As displayed in Figure 9 A, no significant difference was observed between CAR'TCR-T cells and TCR-T cells upon stimulation of only TCR. Likewise, CAR-stimulation led to comparable anti-tumor response in CAR'TCR-T and CAR-T cells, suggesting that there was no reciprocal inhibition between CAR and TCR signaling in CAR'TCR-T cells. Strikingly, dual stimulation in trans led to significantly enhanced TCR-dependent cytotoxicity with CAR'TCR-T cells compared to TCR-T cells: co-expression and co-engagement of the CAR resulted in increase of the TCR-target cell lysis from 24% with TCR-T cells to 70% CAR'TCR-T cells. In contrast, CAR-target cell lysis was comparable between CAR'TCR-T cells and CAR-T cells upon trans stimulation, however, it needs to be pointed out that very high CAR-target cell lysis of around 75% was already achieved with CAR-T cells alone, suggesting that the cytotoxicity is already closer to saturation.

This TCR-dependent boost upon dual stimulation was not only observed regarding the target cell lysis but also in the IFN-γ secretion, which was more than twice as high for

CAR'TCR-T compared to TCR-T cells upon trans stimulation (Figure 9 B). Despite strong donor variability, it was also remarkable that the IFN-γ release by CAR'TCR-T cells only reached around half the level secreted by CAR-T cells. This decrease in cytokine secretion was independent of the stimulus, as it occurred not only upon trans stimulation but also in case of CAR-only stimulation.

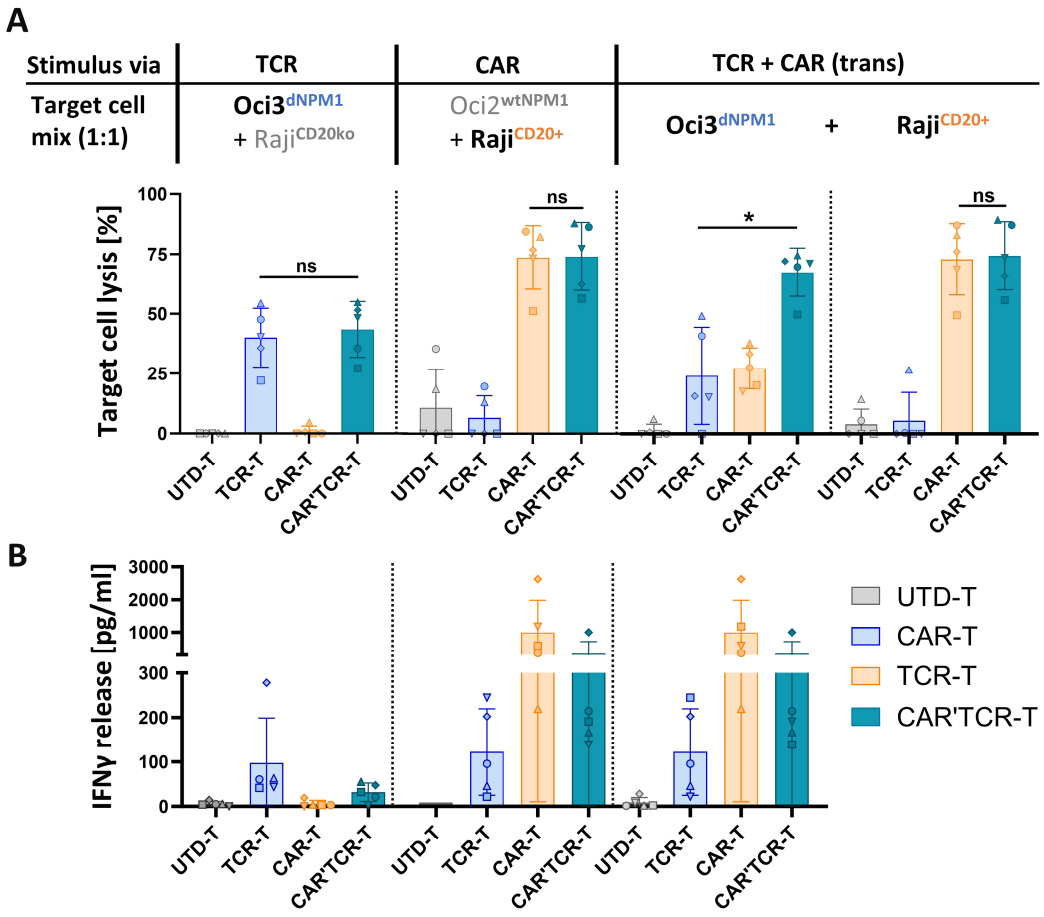

Figure 9: **Cytotoxicity of CD20-CAR- and dNPM1-TCR-co-expressing CAR'TCR-T cells.** (A) Target cell lysis of TCR-target- or CAR-target-expressing cells after 18 hours of dual stimulation in trans (1:1 mixture of two different target cell lines) with an E:T ratio of 2:1. Displayed are individual and mean values ±SD of five different donors from two independent experiments. The *p*-values were calculated using ordinary one-way analysis of variance with Tukey's correction for multiple comparison (ns, not significant; $*p \leq 0.05$). (B) IFN-γ concentration released to the supernatant after 18 hours of co-culture for co-culture conditions described in (A).

In summary, upon single stimulation, CAR'TCR-T cells led to similar CAR- or TCR-target cell lysis compared to CAR-T or TCR-T cells, respectively. IFN-γ release was twice as high in CAR-T cells compared to CAR'TCR-T cells, independent of the type of stimulation. Despite this,

dual stimulation in trans resulted in significantly enhanced TCR-target cell lysis with CAR'TCR-T cells, whereas CAR-target cell lysis was unaffected.

4.2.3 Influence of costimulatory domains in CAR'TCR-T cells

In order to study the influence of various costimulatory domains in the CAR context, a side-by-side comparison of CAR'TCR-T cells either expressing a second-generation 4-1BB- (BBζCAR'TCR) or CD28-costimulated (28ζCAR'TCR) CD20-CAR was performed. It is generally accepted that costimulation via CD28 induces a rapid but potentially more exhausting response, while 4-1BB is thought to support T cell persistence[128-130]. Therefore, it was hypothesized that differences in costimulation might also have an influence on CAR'TCR-T cell functionality.

Novel Oci-AML cell lines expressing CD20 receptor were generated (chapter 3.3.3), in order to test dual stimulation not only in trans but additionally also in cis (both CAR- and TCR-target expressed on same cell line). As in previous experiments with CAR'TCR-T cells, all of the effector cells were sorted before functional assays, in order to ensure high purity and comparability. As shown in Figure 10 A, no difference in cytotoxicity was observed between BBζCAR'TCR-T and 28ζCAR'TCR-T cells, neither upon trans nor upon cis stimulation. In contrast to previous findings, TCR-dependent cytotoxicity was not increased in dual-stimulated CAR'TCR-T cells compared to TCR-T cells. This might be explained by the overall higher target cell lysis of above 75% by TCR-T cells, which was already closer to saturation, potentially limiting the boosting potential.

While only minor differences were observed in the anti-tumor efficacy of CAR'TCR-T cells and CAR- or TCR-only T cells, staining of activation (CD137/CD25) and exhaustion markers (TIM-3/ LAG-3) upon co-culture led to interesting findings (Figure 10 B). All of the conditions (except unmodified T cells) showed a comparable expression of activation markers, ranging from approximately 10-20% of cells expressing CD137 and CD25. Equivalent results were obtained upon cis and trans stimulation. Strong differences in expression of the exhaustion markers TIM-3 and LAG-3 were observed, however, it needs to be kept in mind that this analysis was based on one, rather early time-point after only 20 hours of co-culture and might consequently be activation-dependent. BBζCAR'TCR-T and 28ζCAR'TCR-T cells displayed more than 3-fold lower exhaustion marker expression than BBζCAR-T and

28ζCAR-T, respectively. In general, a lower percentage of TIM-3$^+$/LAG-3$^+$ cells was detected in the CAR'TCR-T or CAR-T cells with CD28 instead of 4-1BB costimulatory domain. Contrary to the initial expectation, BBζCAR-T cells generally displayed higher activation and exhaustion marker expression than 28ζCAR-T cells.

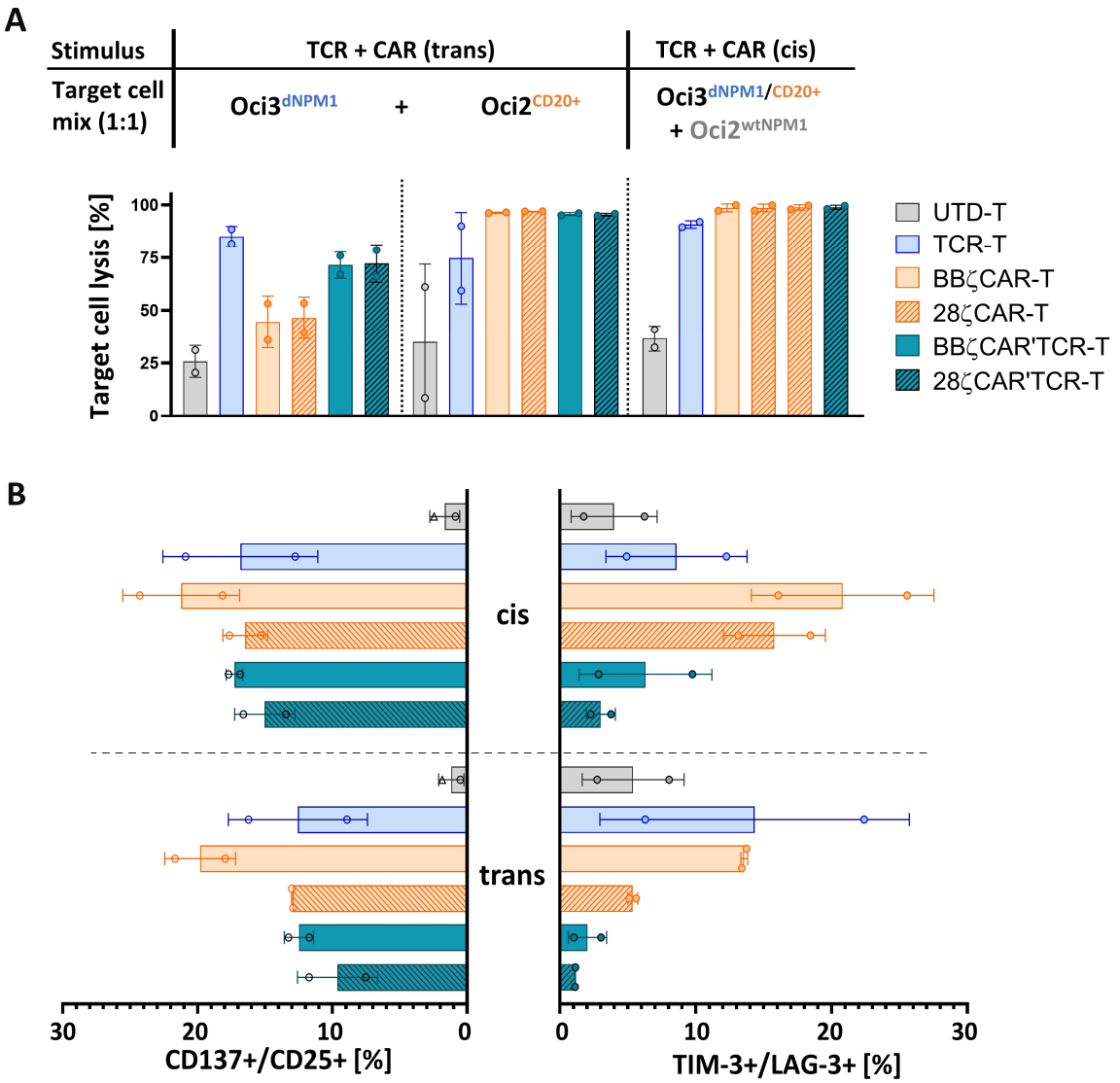

Figure 10: CAR'TCR-T cells expressing CARs with different co-stimulatory domains. (A) Target cell lysis upon 20 hours of dual stimulation in trans (1:1 mixture of Oci-AML3^{dNPM1} and Oci-AML2^{CD20+}) or in cis (1:1 mixture of Oci-AML3$^{dNPM1/CD20+}$ and Oci-AML2) with an E:T ratio of 2:1. The CD20-CAR either contained a 4-1BB or CD28 costimulatory domain (BBζ and 28ζ, respectively). (B) Expression of activation (CD137+/CD25+) and exhaustion (TIM-3+/LAG-3+) markers in the various effector cell conditions after 20 hours of co-culture. Displayed are individual and mean values ±SD of two different donors.

It was hypothesized that dual stimulation through simultaneous engagement of CAR and transgenic TCR might result in faster exhaustion of CAR'TCR-T cells. Therefore, it was crucial

to also assess the anti-tumor activity over the course of long-term co-culture experiments with repetitive stimulation. Target cells were repeatedly added for a total of three rounds, demonstrating the superiority of CAR'TCR-T cells upon cis and trans stimulation (Figure 11). The latter comprised a mixture of CAR- and TCR-target cells and was thus mimicking a heterogeneous tumor cell population. While CAR-T or TCR-T cells led to reduced target cell lysis or even outgrowth of the tumor cells after repeated stimulation, co-culture with CAR'TCR-T cells resulted in complete tumor clearance up to the last round. Again, both BBζCAR'TCR-T and 28ζCAR'TCR-T cells displayed comparable cytotoxicity. The results obtained upon cis stimulation, in which CAR- and TCR-target are expressed on the same target cell line, suggest that dual stimulation did not negatively influence the cytotoxic potential of CAR'TCR-T cells. On the contrary, CAR'TCR-T cells even showed slightly stronger anti-tumor activity after repetitive target cell encounter than CAR-T or TCR-T cells.

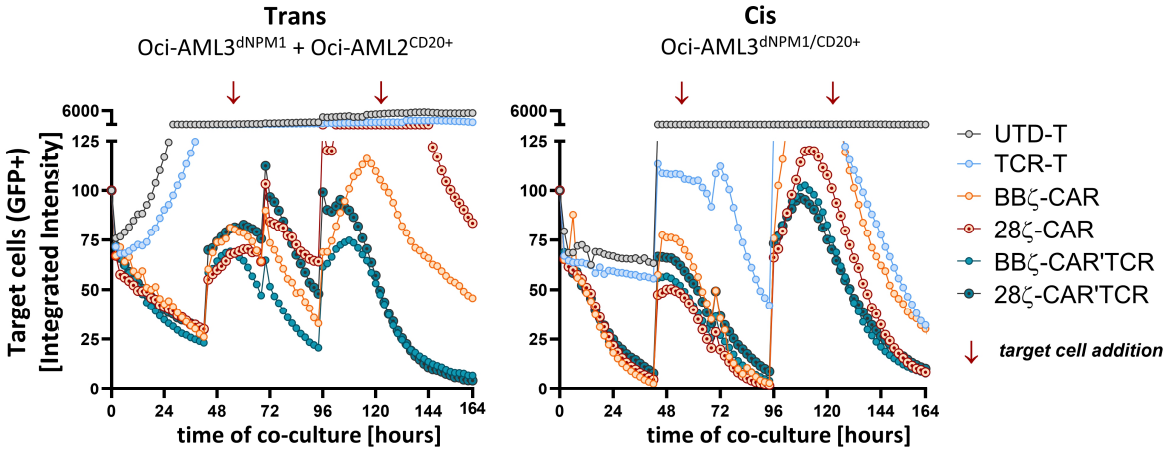

Figure 11: Repetitive co-culture of CAR'TCR-T cells expressing dNPM1-TCR and CD20-CARs with different costimulatory domains. Incucyte analysis showing cytotoxicity upon repeated target cell addition (indicated by red arrow). Stimulation (A) in trans (1:1 mixture of Oci-AML3^{dNPM1} and Oci-AML2^{CD20+}) or (B) in cis (1:1 mixture of Oci-AML3$^{dNPM1/CD20+}$ and Oci-AML2 with an E:T ratio of 2:1. The CD20-CAR either contained a 4-1BB or CD28 costimulatory domain (BBζ and 28ζ, respectively). Displayed are the mean values from two different donors.

Since the CD28 costimulatory domain was linked to faster exhaustion of CAR-T cells[128-130] and due to the finding that BBζCAR'TCR-T and 28ζCAR'TCR-T showed comparable cytotoxicity, subsequent experiments were performed with BBζCAR'TCR-T cells.

4.2.4 Combination of CAR and transgenic TCR in CD4+ T cells

Recent findings of Melenhorst and colleagues underlined the importance of CD4+ T cells in CAR-based adoptive cell therapy for achieving long-term remission[172]. Previous experiments have shown that the dNPM1-TCR is non-functional in CD4+ T cells (Figure 6). However, based on the boosted TCR-mediated killing observed in CD8+ CAR'TCR-T cells (Figure 9 A), it was hypothesized that the combination with a CAR might cause functional recovery in CD4+ T cells. For this purpose, a side-by-side comparison with CD4+ T cells expressing either CD20-CAR, dNPM1-TCR or both was performed. As expected, lysis of the TCR-target cell line Oci-AML3 was only achieved with CD8+ TCR-expressing T cells (~50%) and neither with CD4+ TCR-T nor with CD4+ CAR'TCR-T cells (Figure 12 A). However, upon dual stimulation in trans and in cis, CD4+ CAR'TCR-T cells induced TCR-target cell lysis comparable to the CD8+ counterpart (>75%). However, functional recovery of the dNPM1-TCR in CD4+ cells through co-engagement of the CD20-CAR cannot be assumed, since CD4+ CAR-T cells also caused approximately 75% lysis of TCR-target cells in the trans setting. This suggests CAR-dependent bystander effects though co-presence and killing of CAR-target cells.

After 18 hours of co-culture, the effector cells were analyzed for expression of activation (CD137+/CD25+) and exhaustion markers (TIM-3+/LAG-3+), which is displayed in Figure 12 B. Regardless of the type of stimulation, CD4+ CAR'TCR-T cells displayed higher activation marker and at the same time reduced exhaustion marker expression than CD4+ CAR-T cells. This was coherent with the results shown in Figure 10, also demonstrating reduced exhaustion marker expression with CAR'TCR-T cells. Again, exhaustion status needs to be interpreted carefully when looking at short-term co-culture experiments of 18 hours.

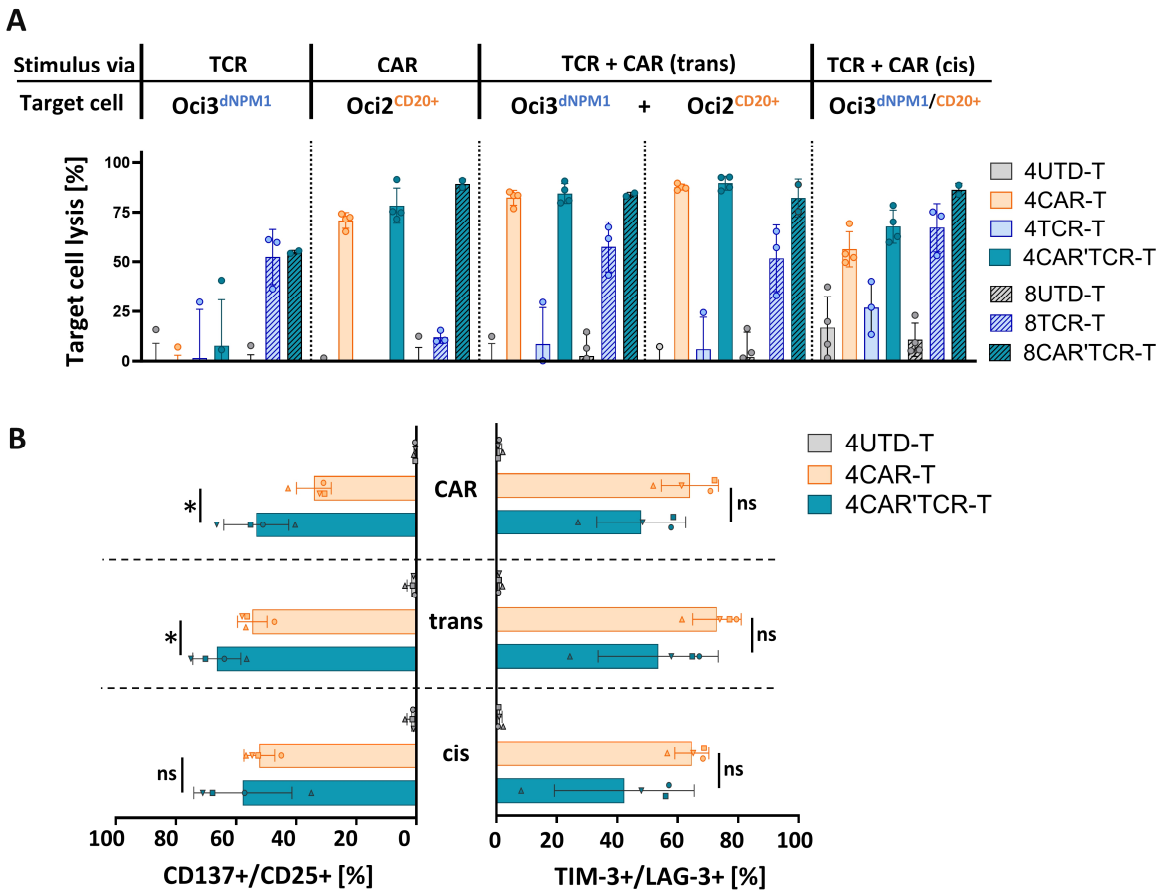

Figure 12: Combination of CD20-CAR and dNPM1-TCR in CD4⁺ T cells. Target cell lysis after 18 hours co-culture (E:T 2:1) with CD4⁺ UTD-T, CAR-T, TCR-T, CAR'TCR-T and CD8⁺ UTD-T, TCR-T and CAR'TCR-T. Stimuli tested: target cells only expressing TCR-target (Oci-AML3^{dNPM1}) or CAR-target (Oci-AML2^{CD20+}), a 1:1 mixture of TCR-target cells and CAR-target cells (trans stimulation), or target cells expressing both CAR- and TCR-target (cis stimulation). (B) Percentage of activation marker (CD137⁺/CD25⁺) and exhaustion marker (TIM-3⁺/LAG-3⁺) expressing CD4⁺ UTD-T, CAR-T and CAR'TCR-T cells upon 18 hours co-culture. Displayed are individual and mean values ±SD of four different donors. The *p*-values were calculated using ordinary one-way analysis of variance with Tukey's correction for multiple comparison (ns, not significant; *$p \leq 0.05$).

Besides studying the dNPM1-TCR functionality in CD4⁺ CAR'TCR-T cells, it was additionally fundamental to verify that the co-expression of a transgenic TCR is not negatively affecting CAR potency. As in previous experiments, repetitive co-culture experiments were performed to assess the long-term anti-tumor functionality of CD4⁺ CAR'TCR-T compared to CD4⁺ CAR-T cells. As displayed in Figure 13 A and B, target cell lysis in the third round of CAR-only and cis stimulation was not significantly different in CD4⁺ CAR'TCR-T compared to CD4⁺ CAR-T cells. Interestingly, co-expression of dNPM1-TCR led to significantly faster target cell killing in case of trans stimulation – not only indicating TCR functionality in CD4⁺

CAR'TCR-T cells, but also a beneficial effect of CD4⁺ CAR'TCR-T cells in case of antigen escape or tumor cell heterogeneity.

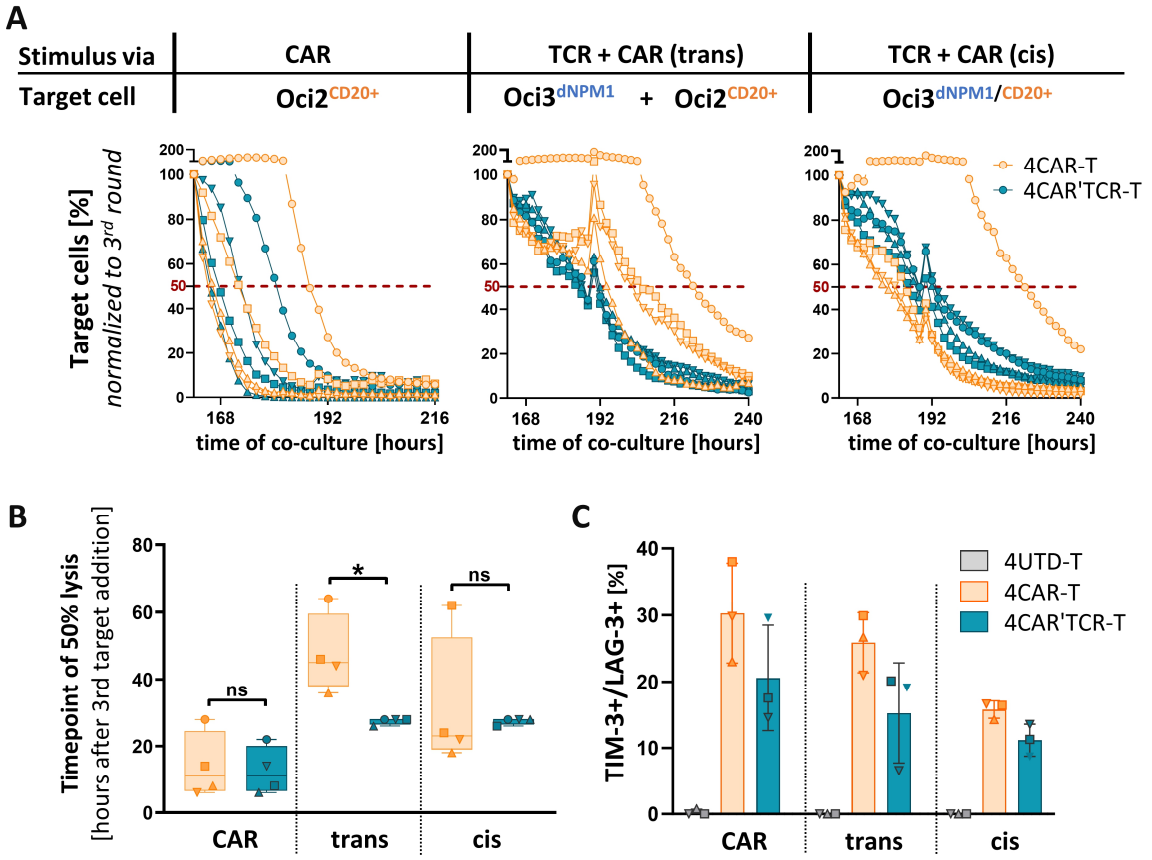

Figure 13: Repetitive stimulation of CD4⁺ CAR'TCR-T versus CD4⁺ CAR-T cells. (A) Killing efficacy of CD4⁺ CD20-CAR T cells and CD4⁺ CAR'TCR-T cells co-expressing CD20-CAR and dNPM1-TCR upon repetitive stimulation (E:T 2:1). Displayed is the target cell lysis normalized to the third round of target cell addition. The time point of 50% target cell lysis in round 3 (indicated by red line) is plotted in (B) comparing CAR-stimulus only, and dual stimulation in trans and in cis. Box and whiskers plot shows individual and median values. (C) Exhaustion marker expression (TIM-3+/LAG-3+) in UTD-T, CD4⁺ CAR T (4CAR) and CD4⁺ CAR'TCR-T cells (4CAR'TCR) after 240 hours of co-culture with three rounds of target cell addition in total. Displayed are individual and mean values ±SD of four different donors. The *p*-values were calculated using ordinary one-way analysis of variance with Tukey's correction for multiple comparison (ns, not significant; *$p \leq 0.05$).

With reference to the previously stated hypothesis that co-engagement of two receptors might increase the risk for faster exhaustion, the data again suggests that rather the opposite holds true. Upon 240 hours of co-culture with repetitive stimulation, CD4⁺ CAR'TCR-T cells displayed lower expression of the exhaustion markers TIM-3 and LAG-3 than CD4⁺ CAR-T cells (Figure 13 C), while additionally even demonstrating stronger cytotoxicity upon dual stimulation in trans.

4.3 Combination of dNPM1-TCR and CD33-CAR

4.3.1 Manufacturing of dNPM1-TCR$^+$/CD33-CAR$^+$ CAR'TCR-T cells

Previous CAR'TCR-T cell experiments were based on the combination of dNPM1-TCR and the clinically well-established CD20-CAR, which served as proof of concept and supported the approach of T cells co-expressing CAR and transgenic TCR. In order to establish a generic proof of concept, the findings were verified with an additional, clinically relevant combination of dNPM1-TCR and CD33-CAR. Since both dNPM1 and CD33 are found in AML, this novel combination might represent a clinically relevant therapeutic concept. As exemplarily displayed in Figure 14 A, all effector cell conditions were sorted via dNPM1-TCR and/or CD33-CAR to ensure high purity and comparability during *in vitro* co-culture experiments. As a result, all conditions displayed comparable expression levels of above 80% prior to killing assay (Figure 14 B). Moreover, all conditions showed comparable viability of above 80% with slightly lower frequency in CAR'TCR-T cells.

Again, it was important to verify that the MFI of CAR or TCR was not significantly different in CAR'TCR-T cells compared to CAR-T or TCR-T cells, respectively. As displayed in Figure 14 C, CAR or TCR MFI were comparable between CAR'TCR-T cells and CAR-T or TCR-T cells, respectively.

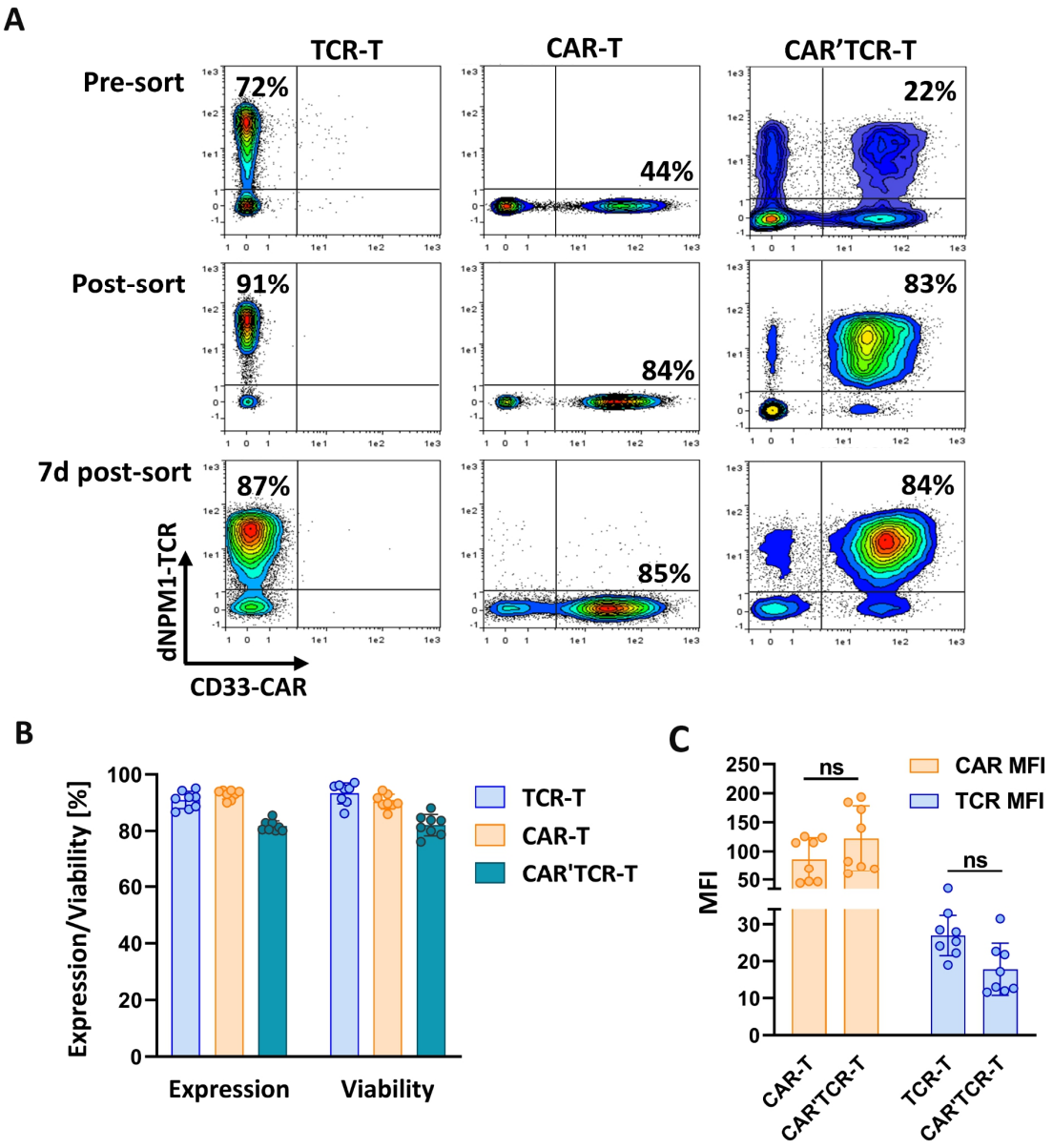

Figure 14: Generation of CAR'TCR-Ts co-expressing CD33-CAR and dNPM1-TCR[173]. (A) Dot plots of one representative donor displaying the expression level of CD33-CAR and or dNPM1-TCR pre- and post-sorting. (B) CAR and/or TCR expression level, viability in percent and (C) MFI measured the day before co-culture with target cells. Shown are individual and mean values ±SD of eight different donors from two independent experiments. The ρ-values were calculated using ordinary one-way analysis of variance with Tukey's correction for multiple comparison (ns, not significant; *ρ ≤ 0.05).

4.3.2 Functionality of dNPM1-TCR$^+$/CD33-CAR$^+$ CAR'TCR-T cells

Despite assessing the functionality of CAR'TCR-T cells co-expressing dNPM1-TCR and CD33-CAR, it was also important to test whether there is a benefit compared to the mixture of dNPM1-TCR-T cells and CD33-CAR-T cells (referred to as Double-T). Both approaches aim to minimize the risk for antigen escape through dual targeting. However, one hypothesis is that CAR'TCR-T cells show increased anti-tumor activity through simultaneous signaling via CAR and TCR. Co-transduction naturally results in generation of CAR'TCR-T cells and T cells, which either express CAR or TCR. Since sorting is hardly feasible for clinical application, an additional condition named Triple-T was included, which consisted of a mixture of CAR-T, TCR-T and CAR'TCR-T cells. The goal was to compare the functionality of CAR'TCR-T cells with, not only TCR-T and CAR-T cells, but also with Double-T cells (mixture of CAR-T and TCR-T) and Triple-T cells (mixture of CAR-T, TCR-T and CAR'TCR-T). In order to facilitate equal cell numbers of CAR$^+$ or TCR$^+$ T cells as well as consistent total cell numbers per condition, the experiment was set-up as illustrated in Figure 15. Consequently, the number of gene-modified T cells was twice as high in the Double-T than in the CAR'TCR-T or Triple-T condition, which is important for interpretation of the data.

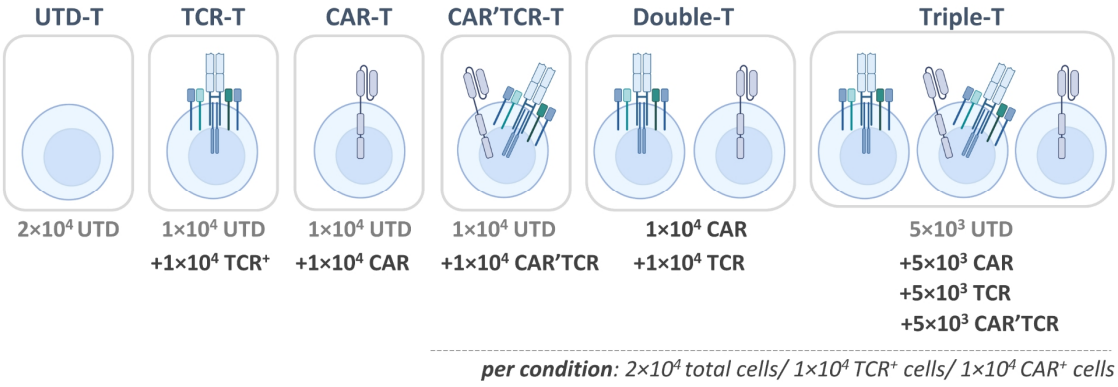

Figure 15: Experimental set-up for testing CAR'TCR-T cells co-expressing CD33-CAR and dNPM1-TCR. Illustrated experimental set-up for comparison of CAR'TCR-T cells (co-expression of CAR and TCR), Double-T cells (mixture of CAR-T and TCR-T cells) and Triple-T cells (CAR-T, TCR-T and CAR'TCR-T cells). Numbers of CAR$^+$ and TCR$^+$ T cells and total cell numbers per condition are indicated. Illustration created with BioRender.com.

According to previous findings, the cytotoxicity was not significantly increased with CAR'TCR-T cells compared to TCR-T or CAR-T cells upon 18 hours stimulation of only TCR or CAR, respectively (Figure 16 A). However, dual stimulation in trans led to significantly higher TCR-target cell lysis with CAR'TCR-T compared to TCR-T cells. Double-T and Triple-T cells induced comparably high cytotoxicity as CAR'TCR-T cells. Since CAR-target cell lysis upon trans stimulation was already at maximum with CAR-T cells, no boost in anti-tumor activity could be observed with dual-targeting conditions CAR'TCR-T, Double-T or Triple-T cells compared to CAR-T cells. This could be further evaluated using more challenging E:T ratios. Surprisingly, co-culture with CD33- and dNPM1-expressing Oci-AML3 cells (cis) resulted in enhanced target cell killing with CAR'TCR-T cells compared to not only TCR-T but also CAR-T cells. In this context, it needs to be highlighted that the level of CD33 expression is very low in Oci-AML3 cells compared to Oci-AML2 cells, which might have an influence on the CAR response upon cis ($CD33^{dim}$) and CAR-stimulation ($CD33^{high}$), respectively (Figure 16 B). This underscores the therapeutic potential of CAR'TCR-T cells especially in case of CD33 downregulation or the presence of leukemic blasts expressing lower levels of the target antigen.

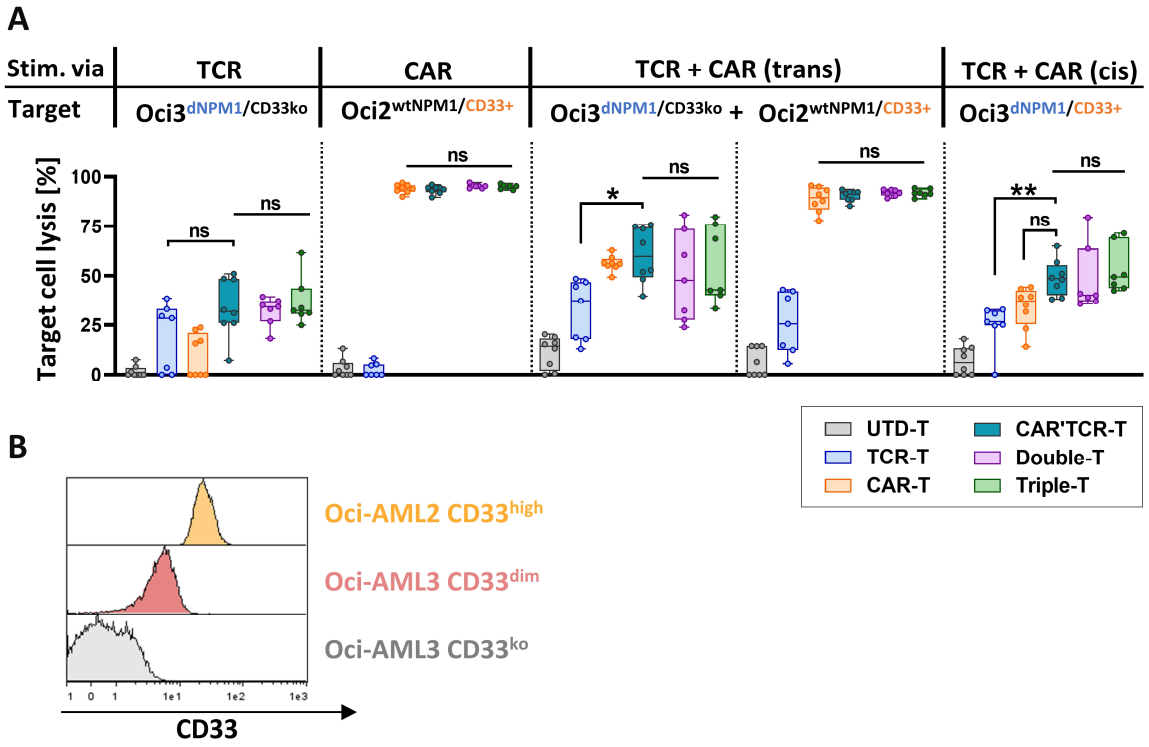

Figure 16: Functionality of CAR'TCR-Ts co-expressing CD33-CAR and dNPM1-TCR[173]. (A) Functionality of UTD-T, TCR-T, CAR-T, CAR'TCR-T, Double-T (1:1 mixture of TCR-T and CAR-T) and Triple-T (1:1:1 mixture of CAR'TCR-T, TCR-T, CAR-T) cells. Effector cell counts were normalized through addition of UTD-T. Displayed is the target cell lysis after 18 hours of co-culture with target cells only expressing TCR-target (Oci-AML3$^{dNPM1/CD33ko}$) or CAR-target (Oci-AML2^{CD33+}), a 1:1 mixture of TCR-target cells and CAR-target cells (trans stimulation), or target cells expressing both CAR- and TCR-target simultaneously (cis stimulation with Oci-AML3$^{dNPM1/CD33+}$). Box and whiskers plot shows individual and median values of eight different donors from two independent experiments. The ρ-values were calculated using ordinary one-way analysis of variance with Tukey's correction for multiple comparison (ns, not significant; *$\rho \leq 0.05$, **$\rho \leq 0.01$). (B) Surface expression level of CD33 in different cell lines used in killing assay.

Since CAR'TCR-T, Double-T and Triple-T cells led to comparable cytotoxicity upon 18 hours co-culture, it was hypothesized that differences in anti-tumor response might become visible upon repetitive, long-term co-culture. Similar to previous findings with combination of CD20-CAR and dNPM1-TCR, CAR'TCR-T cells co-expressing CD33-CAR and dNPM1-TCR outperformed TCR-T and CAR-T cells upon trans and also cis stimulation, facilitating strong anti-tumor response until the third round of target cell addition (Figure 17 A and B, respectively). Although the differences were only minor, Triple-T cells showed significantly higher anti-tumor activity than CAR'TCR-T cells upon trans stimulation, suggesting a beneficial effect with the mixture of CAR-T, TCR-T and CAR'TCR-T cells. However, no

significant difference between the three dual-targeting conditions (CAR'TCR-T, Double-T and Triple-T) was observed in the cis setting.

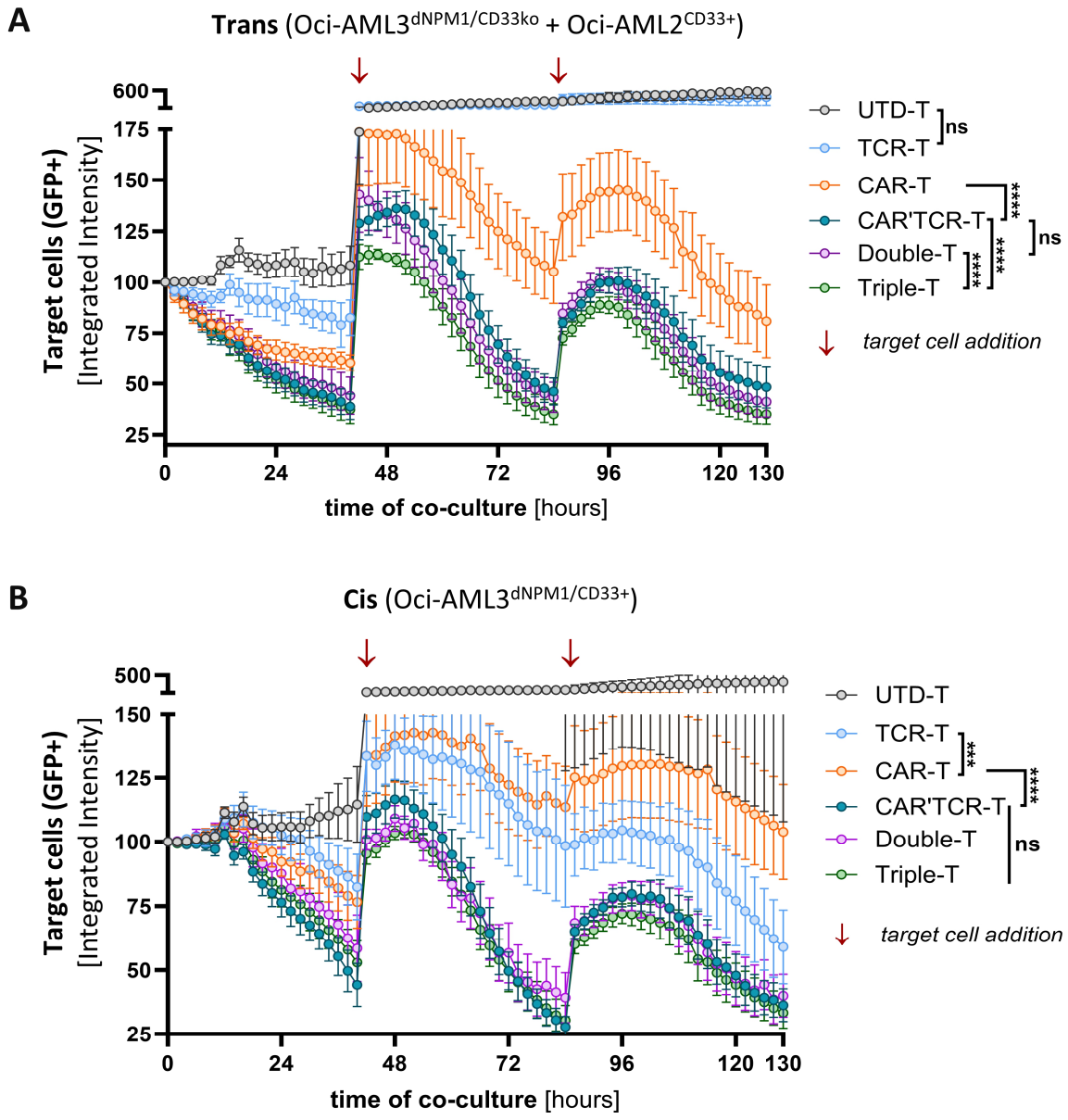

Figure 17: Efficacy of CAR'TCR-T cells co-expressing CD33-CAR and dNPM1-TCR upon repeated stimulation[173]. Incucyte analysis showing cytotoxicity upon repeated target cell addition (indicated by red arrow) for (A) *trans* and (B) *cis* stimulation with an E:T ratio of 1:1. Shown mean values ±SEM of eight different donors from two independent experiments. The *p*-values were calculated using Tukey's multiple comparison test and the mixed-effects model with Geisser-Greenhouse correction (two-way analysis of variance) (ns, not significant; *$p \leq 0.05$, **$p \leq 0.01$, ***$p \leq 0.001$, ****$p \leq 0.0001$).

After 130 hours of long-term co-culture with three rounds of target cell addition, the effector cells were collected to assess the level of exhaustion. The frequencies of TIM-3$^+$

LAG-3$^+$ double-positive cells are displayed in Figure 18. Neither trans nor cis stimulation caused significant differences in exhaustion marker expression between the various effector cell conditions. Although not significant, CAR'TCR-T cells demonstrated a trend towards increased exhaustion marker expression compared to TCR-T and Double-T.

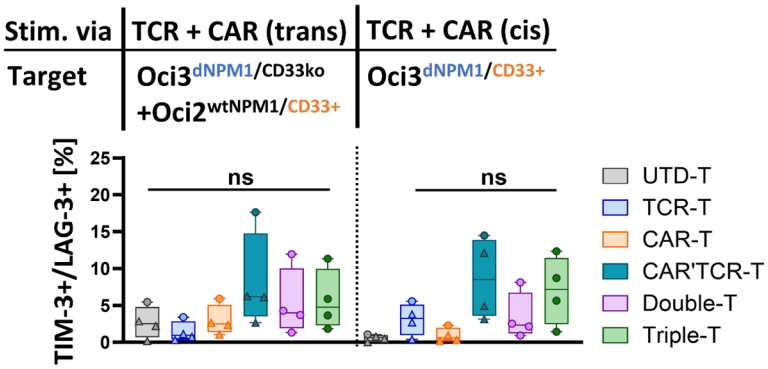

Figure 18: Exhaustion marker expression after long-term co-culture[173]. Frequencies of exhaustion marker TIM-3$^+$/LAG-3$^+$ T cells upon 130 hours long-term co-culture with repetitive dual stimulation in cis and in trans of UTD-T, TCR-T, CAR-T, CAR'TCR-T, Double-T and Triple-T cells. Box and whiskers plot shows individual and median values of four different donors. The *p*-values were calculated using Tukey's multiple comparison test and the mixed-effects model with Geisser-Greenhouse correction (two-way analysis of variance) (ns, not significant).

Additionally, the supernatant was collected 24 hours after first and third target cell addition in order to determine the level of cytokine secretion for the different co-culture conditions (Figure 19). Cytokine concentrations in response to target cell addition were comparable between first and third round. According to the level of target cell lysis, no significantly increased secretion of GM-CSF or IFN-γ by CAR'TCR-T cells was detected compared to TCR-T or CAR-T in case of TCR- or CAR-stimulation, respectively. Neither in the first nor in the last round of co-culture. Dual stimulation in trans, however, resulted in more than two times higher GM-CSF secretion by CAR'TCR-T cells compared to TCR-T or CAR-T. This finding was in line with the strongly enhanced target cell lysis with CAR'TCR-T cells upon simultaneous engagement of CAR and TCR (Figure 16). Overall, only weak cytokine secretion was detected by CAR-T cells, not only upon co-culture with CD33^{dim} Oci-AML3 but also with CD33^{high} Oci-AML2 cells. In the trans setting, Double-T cells produced the highest level of IFN-γ, 10-fold higher than CAR'TCR-T cells and more than two times higher than Triple-T cells. An explanation for this might be the fact that Double-T comprised twice as many engineered effector cells than the CAR'TCR-T condition. In the cis setting, however,

no significant difference was observed in IFN-γ release by CAR'TCR-T, Double-T or Triple-T cells.

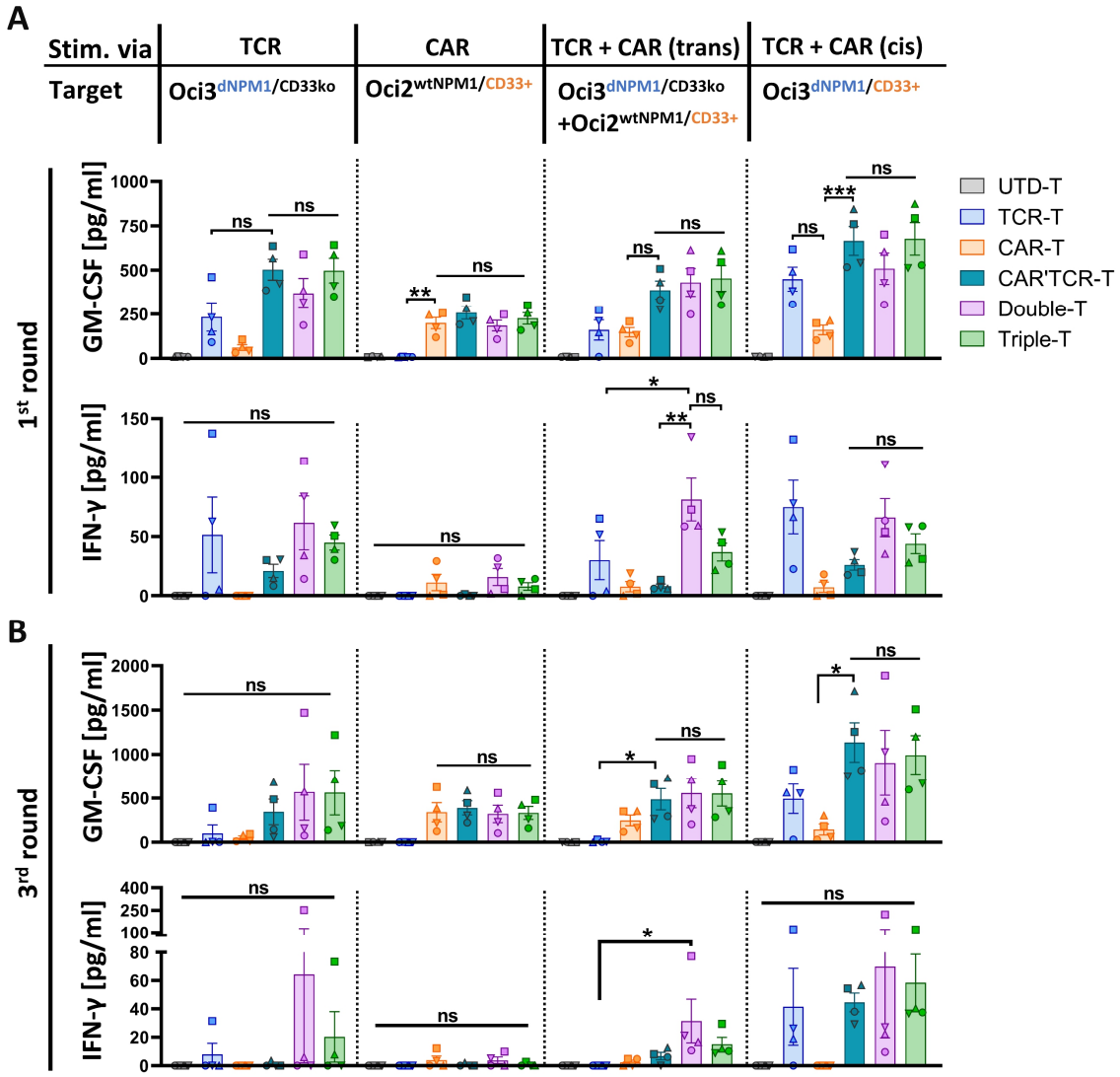

Figure 19: Cytokine secretion by CAR'TCR-Ts after repetitive stimulation. Secretion of GM-CSF and IFN-γ by UTD-T, TCR-T, CAR-T, CAR'TCR-T, Double-T (1:1 mixture of TCR-T and CAR-T) and Triple-T (1:1:1 mixture of CAR'TCR-T, TCR-T and CAR-T) cells upon co-culture with different target cells: target cells only expressing TCR-target (Oci-AML3$^{dNPM1/CD33ko}$) or CAR-target (Oci-AML2^{CD33+}), a 1:1 mixture of TCR-target cells and CAR-target cells (trans stimulation), or target cells expressing both CAR- and TCR-target (cis stimulation with Oci-AML3$^{dNPM1/CD33+}$). Cytokine release was determined 24 hours after (A) first and (B) third target cell addition. Shown are individual and mean values ±SEM of four different donors. The *p*-values were calculated using ordinary one-way analysis of variance with Tukey's correction for multiple comparison (ns, not significant; *$p \leq 0.05$, **$p \leq 0.01$, ***$p \leq 0.001$).

4.3.3 Whole transcriptome analysis of CAR'TCR-T cells

Bulk RNA-seq was performed with the goal to in-depth compare the transcriptomic profiles of CAR'TCR-T with CD33-CAR, dNPM1-TCR or UTD-T cells upon stimulation in cis. After sorting, the effector cells were re-activated and cultured for one more week. Upon 18 hours of co-culture, target cells were magnetically depleted to ensure high purity of effector cells for bulk RNA-seq analysis. Consistent with previous findings, CAR'TCR-T cells led to significantly higher target cell lysis than TCR-T or CAR-T cells (Figure 20 A). Hierarchical clustering of the 500 most variable genes yielded in distinct grouping of the various effector cell types, additionally suggesting that the transcriptomic profile of CAR'TCR-T cells is closer to CAR-T than TCR-T cells (Figure 20 B). For a systematic evaluation of the similarities between CAR'TCR-T cells and CAR-T or TCR-T differential gene expression analysis was used to first quantify the overlaps in the gene expression profile from the modified cells in reference to UTD-T, and second, to determine gene expression differences between CAR'TCR and CAR-T or TCR-T. Benchmarked to UTD-T, TCR-T cells showed the highest number of 9,790 differentially expressed genes (DEGs), followed by 7,542 DEGs in CAR'TCR-T cells and the lowest number of 2,331 DEGs in CAR-T cells. Consequently, CAR'TCR-T and TCR-T cells displayed the highest number of overlapping genes. Differential gene expression was also compared to CAR'TCR-T instead of UTD-T cells (Figure 20 D): TCR-T cells demonstrated more DEGs than CAR-T cells, again indicating a closer similarity between CAR'TCR-T cells and CAR-T cells. Log2 fold changes of CAR'TCR-T, CAR-T and TCR-T cells were determined for the 7,542 DEGs specifically found in CAR'TCR-T cells. Subsequent linear regression analysis displayed a stronger correlation in Log2 fold changes between CAR'TCR-T and CAR-T (71%) than CAR'TCR-T and TCR-T (61%) (Figure 20 E). To sum this up, the transcriptomic profile of CAR'TCR-T cells was observed to be more similar to CAR-T cells than TCR-T cells, suggesting that the CAR exerts more dominant signaling in CAR'TCR-T cells.

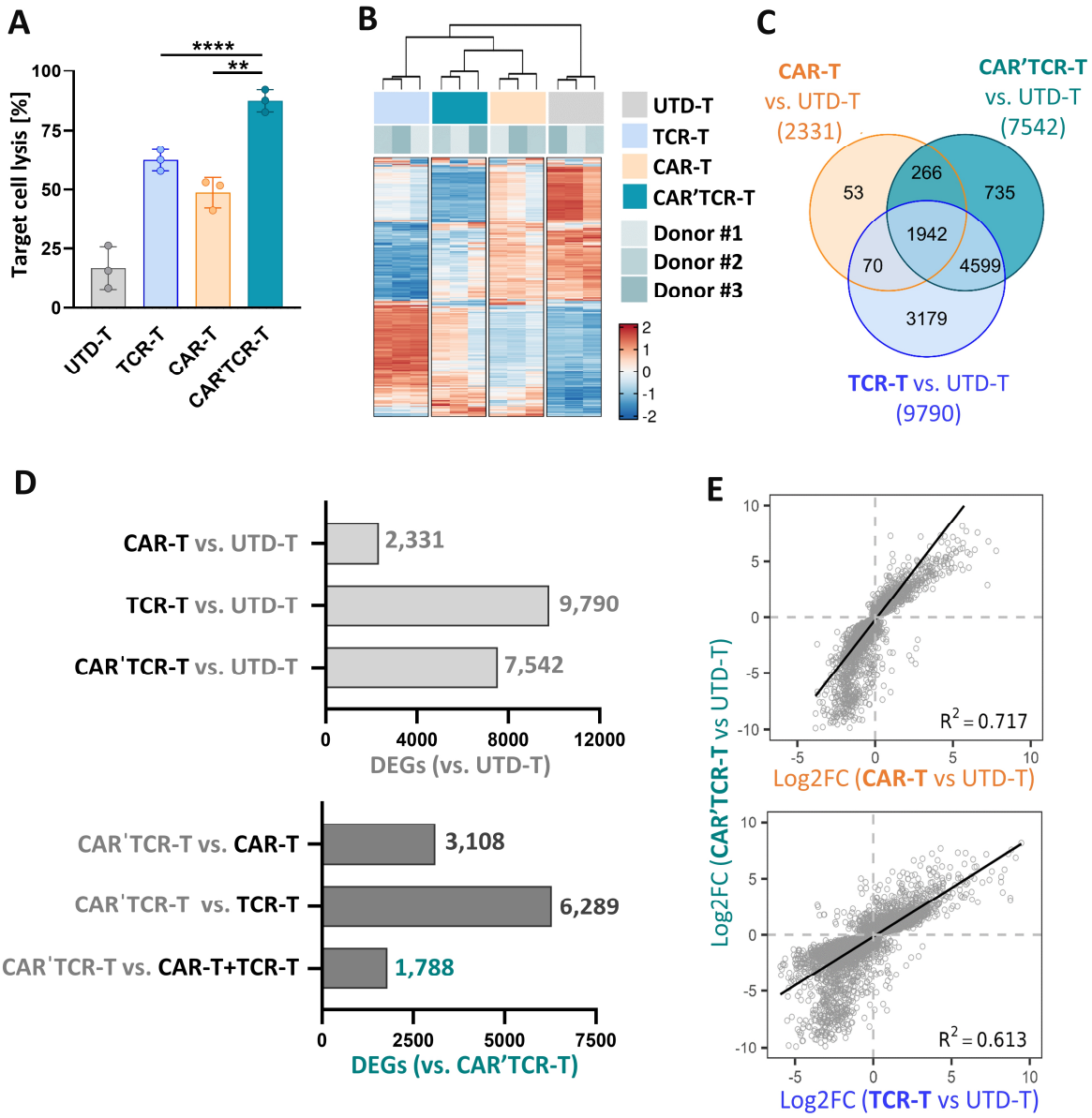

Figure 20: Similarities and differences in RNA-seq profiles of CAR'TCR-T and CAR-T or TCR-T cells[173]. (A) Cytotoxicity of UTD-T cells, TCR-T cells, CAR-T or CAR'TCR-T cells upon 18 hours of cis stimulation with Oci-AML3 cells at an E:T ratio of 2:1. Shown are individual and mean values ±SD of three different donors. The *ρ*-values were calculated using ordinary one-way analysis of variance with Tukey's correction for multiple comparison (ns = not significant, *$\rho \leq 0.05$, **$\rho \leq 0.01$, ***$\rho \leq 0.001$, ****$\rho \leq 0.0001$). (B) Heatmap displaying hierarchical clustering of 500 most variable genes for stimulated UTD-T, CAR-T, TCR-T and CAR'TCR-T. (C) Venn diagram showing total and overlapping number of differentially expressed genes (DEGs) in CAR-T, TCR-T or CAR'TCR-T compared to UTD-T cells. (D) Total DEGs resulting from comparison to UTD-T (upper graph) and to CAR'TCR-T (lower graph). (E) Log2 fold changes of the 7,542 DEGs from CAR'TCR-T versus UTD-T were compared to those of CAR-T or TCR-T versus UTD-T, displayed in upper and lower scatterplot, respectively. Linear regression was used to determine R^2.

Besides assessing the similarities, it was also crucial to determine the biological processes and pathways unique for CAR'TCR-T cells. Therefore, functional annotation was performed applying TopGO and Reactome databases[174-176]. TopGO gene ontology (GO) terms relating to regulation of catalytic activity as well as positive regulation of cell migration, T cell activation and GTPase activity were significantly enriched for the differentially upregulated genes in CAR'TCR-T cells (Figure 21 A). This was confirmed by analysis using Reactome database, which detected pathways primarily corresponding to the RHO GTPases, including RAC family small GTPase 1 (RAC1) and cell division cycle 42 (CDC42) GTPase cycles (Figure 21 B). Both, RAC1 and CDC42 are required for actin cytoskeletal reorganization, TCR clustering into lipid rafts, and consequently, T cell activation upon receptor engagement[116,177]. Besides supporting IS formation and signaling, RAC1 and CDC42 also play an important role in T cell polarization and migration[116]. The enhanced T cell activation and signaling in CAR'TCR-T cells was further confirmed through significant upregulation of DEGs corresponding to Reactome GO terms such as phosphorylation of CD3ζ chains, translocation of ZAP-70 to the IS and generation of second messenger molecules (Figure 21 B).

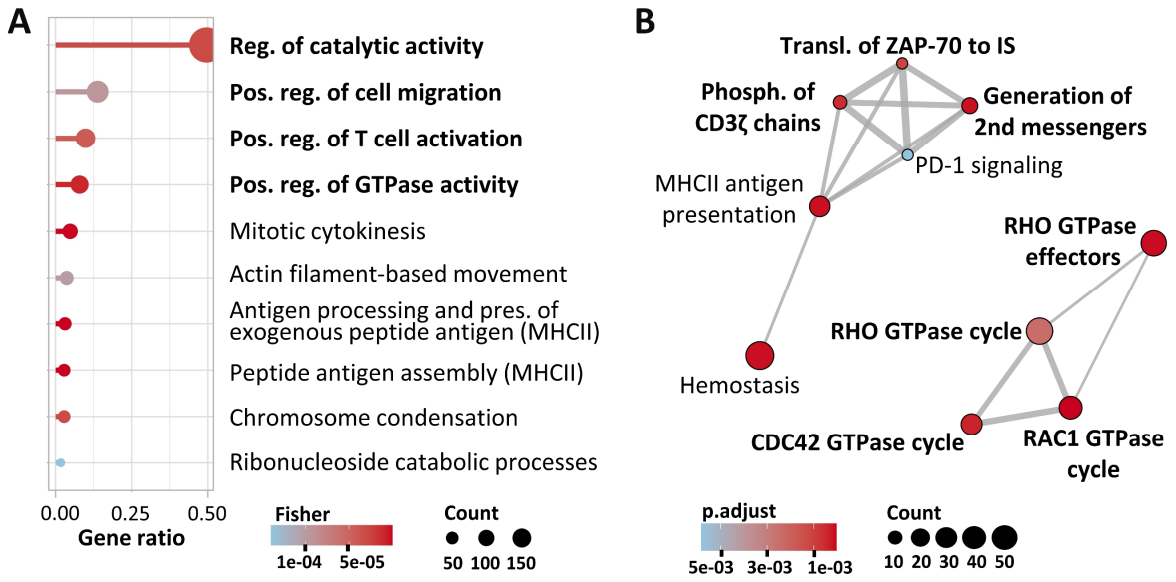

Figure 21: Gene set enrichment analysis of upregulated DEGs[173]. (A) 10 most significant TopGO gene ontology (GO) categories. (B) Reactome emapplot showing relations among 10 most significant pathways for upregulated DEGs (864) in CAR'TCR-T cells.

Likewise, gene set enrichment analysis was performed for DEGs that were significantly downregulated in CAR'TCR-T cells compared to CAR-T and TCR-T cells. As expected, most of the downregulated DEGs were linked to negative downregulation of signal transduction (Figure 22 A). This again verified the observed increase in CAR'TCR-T cell activation and signaling. Reactome analysis primarily linked the downregulated DEGs to G protein-coupled receptor (GPCR) pathways including GPCR ligand binding and signaling via Gα(i) protein (Figure 22 B). The latter is primarily required for ligand-dependent chemotaxis[178,179] and plays an initial role in supporting TCR-MHC interaction through chemokine immobilization[180]. Importantly, it was described that IS formation is accompanied by chemokine receptors, which preferentially couple to Gα(q/11), thereby excluding Gα(i) from the synapse and shifting signaling from migration to cell adhesion[180,181]. However, the results need to be interpreted carefully, since GPCRs are involved in multiple cellular mechanisms, beyond fine-tuning of proximal TCR receptor signaling[182,183].

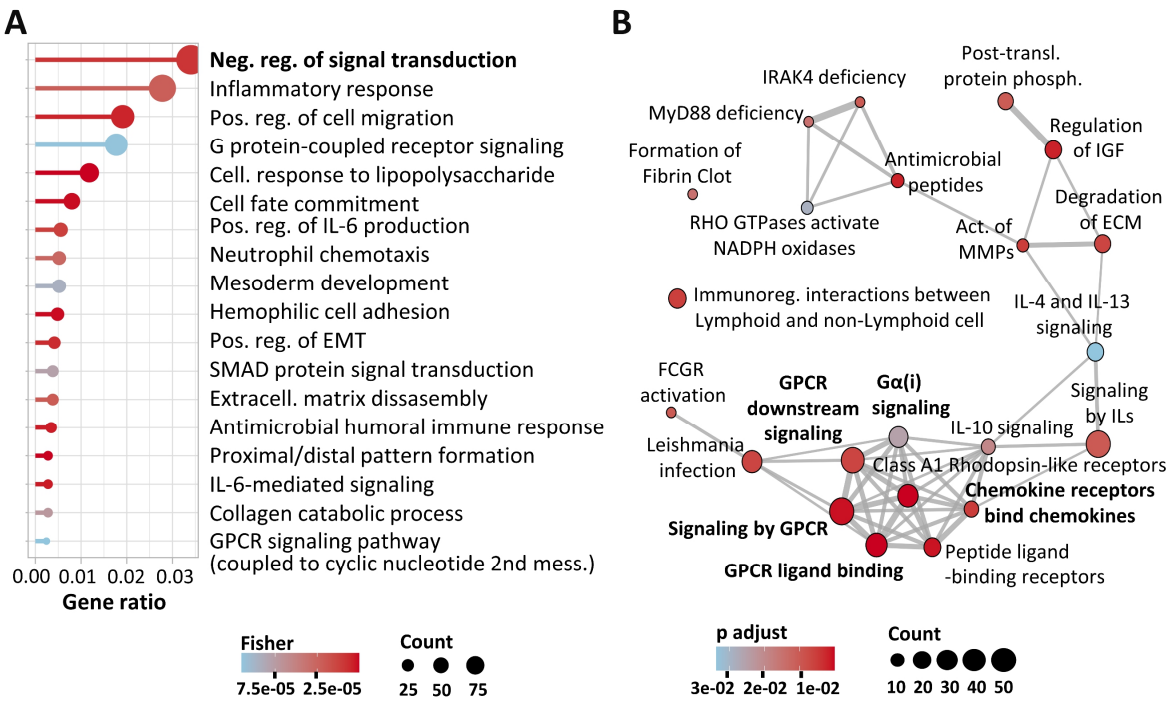

Figure 22: Gene set enrichment analysis of downregulated DEGs[173]. (A) 18 most significant TopGO gene ontology (GO) categories. (B) Reactome emapplot showing relations among 22 most significant pathways for upregulated DEGs (924) in CAR'TCR-T cells.

In general, CAR'TCR-T cells demonstrated a transcriptomic profile closer related to CAR-T than TCR-T cells, suggesting that CAR signaling was more dominant in CAR'TCR-T cells. Moreover, CAR'TCR-T cells displayed a unique transcriptomic profile, which was linked to

enhanced T cell activation, IS formation and proximal signaling. Overall, this verified the boosted cytotoxicity of CAR'TCR-T cells demonstrated in prior *in vitro* experiments.

4.3.4 Efficacy of CAR'TCR-T cells *in vivo*

Previous results have shown that $CD8^+$ CAR'TCR-T cells, co-expressing CD33-CAR and dNPM1-TCR, demonstrated increased cytotoxicity compared to CAR-T or TCR-T cells. This effect was particularly pronounced upon dual stimulation in cis. Additionally, CAR'TCR-T cells demonstrated stronger tumor elimination in case of trans stimulation, suggesting a minimized risk for antigen escape or dominance in case of a heterogeneous tumor cell population. In order to verify those findings *in vivo*, a previously established AML mouse model was used to verify the potentiated anti-tumor efficacy *in vivo*.

All effector cell conditions were manufactured using the CliniMACS Prodigy™. Since all *in vitro* experiments were performed with sorted CAR'TCR-T cells, this condition was also implemented as control and was consequently based on an 8-day instead of 12-day manufacturing process (Table 14). As illustrated in Figure 23, on day 8 of manufacturing, CAR'TCR-T cells were harvested, sorted and to increase expansion, re-activated using TransAct™. Before injection into mice, those enriched CAR'TCR-T cells were cultivated and expanded for 7 more days. For all the other conditions a 12-day manufacturing process was applied, without subsequent sorting or re-activation of the effector cells. As in previous experiments, Double-T was composed of a 1:1 mixture of CAR-T and TCR-T cells. Triple-T was manufactured through co-transduction with two LVs either encoding CD33-CAR or dNPM1-TCR, which naturally resulted in a mixture of double-positive, CAR- and TCR-only T cells.

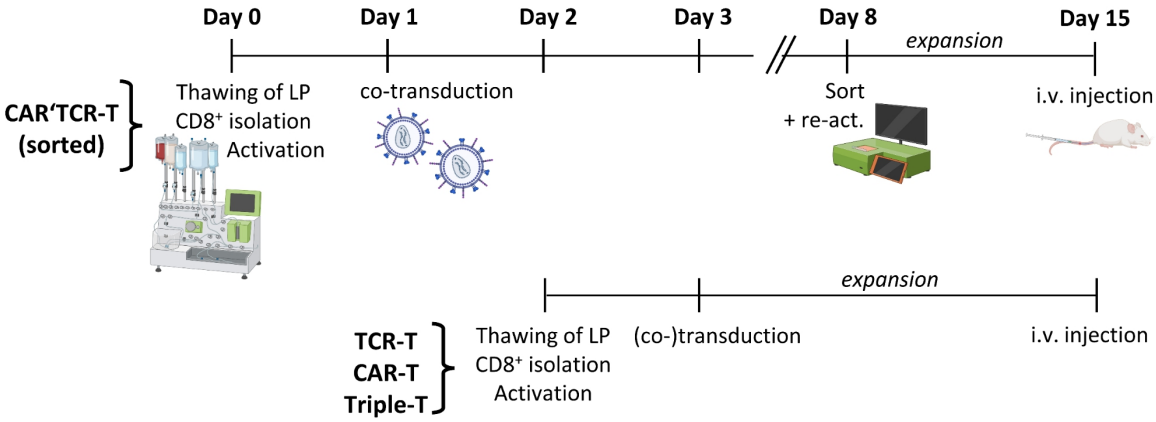

Figure 23: Manufacturing of various effector cell conditions for *in vivo* testing. All conditions were manufactured using the CliniMACS Prodigy™ with isolation of CD8+ T cells only and activation through TransAct™. (Co-) transduction was performed on day 1. A different manufacturing protocol was used for "CAR'TCR-T (sorted)" cells: on day 8, the cells were harvested, sorted for CAR+/TCR+ T cells, re-activated with TransAct™ and expanded for 7 more days. All other groups (TCR-T, CAR-T and Triple-T) were manufactured using the 12-day-process without sorting of the cells.

NSG mice were intravenously injected with 1×10^6 Oci-AML3 cells and randomized after three days of tumor engraftment (Figure 24 A and B). The following day, 5×10^6 engineered T cells were injected i.v. The frequency of engineered T cells was normalized through addition of UTD-T cells to approximately 60% for all conditions. As displayed in Figure 24 C, the sorted CAR'TCR-T cells mainly consisted of double-positive T cells, while Triple-T demonstrated an evenly distributed mixture of all cell types: 18% CAR+, 17% TCR+ and 26% CAR+/TCR+ T cells. Starting with effector cell injection, bioluminescent imaging was performed twice per week to determine tumor growth kinetics.

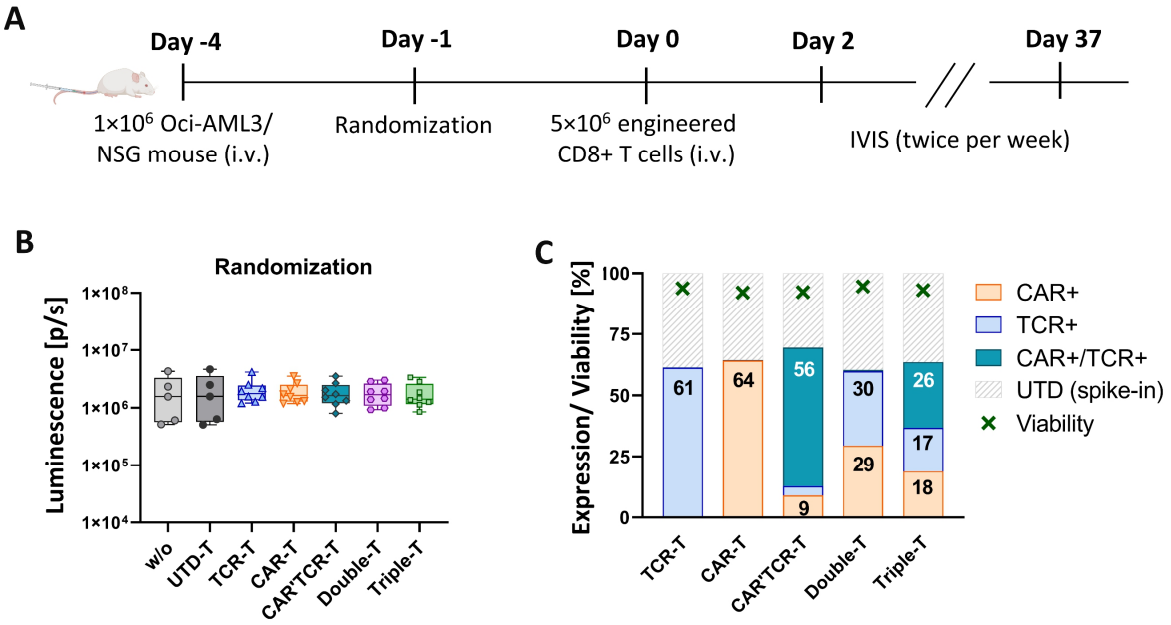

Figure 24: *In vivo* efficacy study of CAR'TCR-T cells[173]. (A) NSG mice were injected intravenously with 1×10^6 FFluc$^+$ Oci-AML3 cells four days prior to injection of 5×10^6 engineered effector cells. (B) Luminescence (p/s) of tumor load in various groups after randomization, one day prior to effector cell injection. The group that only received tumor and no effector cells is indicated by "w/o". Box and whiskers plot shows individual and median values (C) The level of CAR$^+$ and/or TCR$^+$ T cells in various effector cell conditions prior to injection: TCR-T, CAR-T, CAR'TCR-T (sorted for CAR+/TCR+ cells), Double-T (1:1 mixture of CAR-T and TCR-T), Triple-T (co-transduced, non-sorted cells expressing CAR, TCR or both). Normalization was performed through spike-in of UTD-T cells. Viability of final cell product is displayed in percent (green x).

In parallel to i.v. injection *in vivo*, the various effector cell conditions were tested in an *in vitro* co-culture assay with the target cell line Oci-AML3 m.10 (Figure 25). Overall, sorted CAR'TCR-T cells led to strongest cytotoxicity at all time-points measured (18, 26 and 42 hours). Although Triple-T and Double-T cells showed clearly delayed anti-tumor response, the level of target cell lysis was comparable to sorted CAR'TCR-T cells at latest time-point of 42 hours (> 80%). Interestingly, CAR-T and TCR-T cells demonstrated relatively weak efficacy with a maximum target cell lysis of 50% after 42 hours.

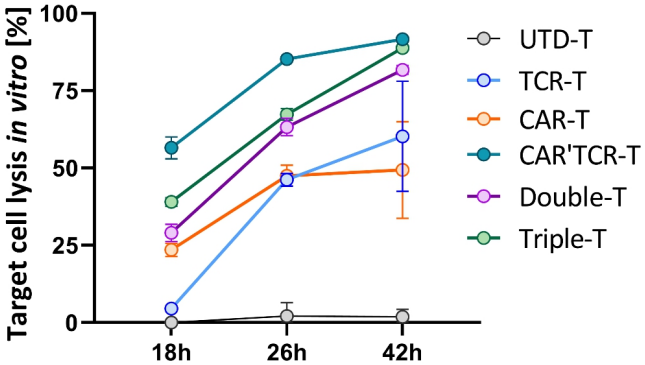

Figure 25: *In vitro* target cell lysis by engineered T cells used for *in vivo* study. In parallel to injection in NSG mice, effector cells were co-cultured with Oci-AML3 m.10 target cells *in vitro* at an E:T ratio of 1:1. Target cell lysis was analyzed after 18, 16 and 42 hours. Values show technical duplicates ±SD.

According to the *in vitro* performance displayed in Figure 25, CAR'TCR-T cells showed the strongest initial growth suppression *in vivo* (Figure 26). However, all of the treatments led to tumor outgrowth during the first 23 days. Groups treated with TCR-T or CAR-T cells reached study endpoint criteria by day 30 and day 34, respectively, and needed to be removed from the experiment. Interestingly, BLI measurements demonstrated that Double-T cells did not outperform TCR-T or CAR-T cell treatment and also led to continuous outgrowth of Oci-AML3 tumor cells. Strikingly, only mice treated with Triple-T cells demonstrated elimination of tumor cells starting with day 28. While sorted CAR'TCR-T cells showed visibly stronger anti-tumor response than TCR-T, CAR-T or Double-T cells, only one of eight mice showed tumor elimination. In the Triple-T group, three mice had to be sacrificed due to reaching of study endpoint criteria, however 5 of 8 mice showed remarkable tumor elimination. Overall, the median luminescence value in the Triple-T-treated group deceased from 3.5×10^9 p/s on day 23 to 3.4×10^7 p/s during the course of 2 weeks.

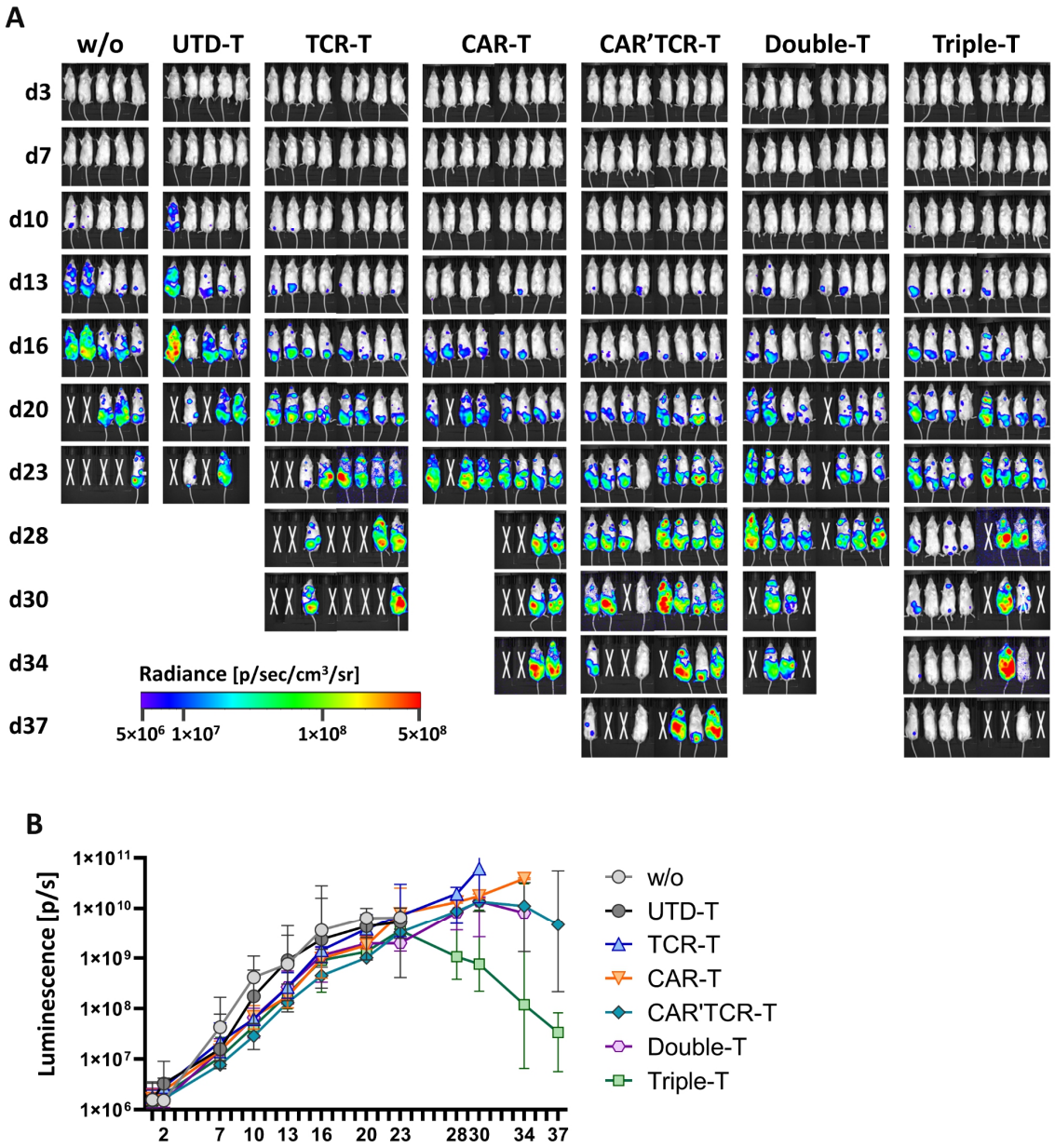

Figure 26: Efficacy of CD8⁺ CAR'TCR-T cells *in vivo*[173]. (A) Bioluminescence images of mice bearing Oci-AML3 tumors over the course of 37 days. (B) Progression of luminescence displayed as median with interquartile range starting with groups of n=8 mice, except without (w/o) effector cells and UTD-T with n=5.

Next, the bone marrow was isolated and analyzed *ex vivo* for presence of particularly CD33⁺ Oci-AML3 target cell. Antigen escape was reported to be the cause for ineffective CAR-T cell therapy in several clinical trials[184-188]. Likewise, heterogeneous tumor cell populations and outgrowth of target antigen-negative cells represent additional challenges for CAR-T cell therapy. Therefore, it was hypothesized that the group treated with CD33-targeting CAR-T cells might show lower percentage of remaining CD33⁺ cells than for instance the dNPM1-targeting TCR-T cell treatment. In contrast, no significant difference in percentage

of CD33⁺ Oci-AML3 target cells was observed between CAR-T, TCR-T, CAR'TCR-T and Double-T cell treatment, all displaying very low mean values of less than 22% (Figure 27). The Triple-T group displayed a slightly higher, but not significantly different, percentage of CD33⁺ target cells (27%). Non-treated mice or the untransduced group showed significantly higher proportions of remaining CD33⁺ Oci-AML3 cells (85% and 50%, respectively).

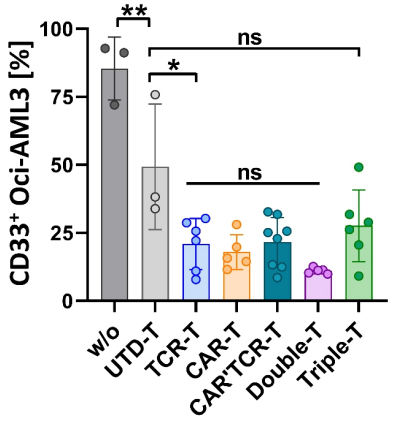

Figure 27: *Ex vivo* analysis of CD33 expression in Oci-AML3 cells. Percentage of CD33-expressing Oci-AML3 cells derived from bone marrow upon treatment with CD33-CAR and/or dNPM1-TCR⁺ T cells or without any treatment. Shown are individual and mean values ±SD. The *p*-values were calculated using ordinary one-way analysis of variance with Tukey's correction for multiple comparison (ns, not significant; *$p \leq 0.05$; **$p \leq 0.01$).

In parallel to analyzing the remaining proportion of CD33⁺ target cells, it was also crucial to assess the effector cell persistence. This is especially important in case of Double-T and Triple-T, where mixtures of different engineered T cell subtypes were injected. In order to understand why both conditions containing CAR⁺/TCR⁺ double-positive T cells (CAR'TCR-T and especially Triple-T) showed superior anti-tumor efficacy *in vivo*, it was important to analyze whether this was due to a certain proliferation benefit. Figure 28 A and B display the distribution of CAR⁺, TCR⁺ and double-positive T cells in the various treatment groups pre-injection and after termination of the experiment, respectively. Generally speaking, no pronounced differences were observed between T cells isolated from bone marrow or from spleen. In contrast to the assumption that the double-positive T cells show increased persistence, CAR-T cells accounted for the largest proportion in all of the conditions. The strongest effect was observed upon treatment with sorted CAR'TCR-T cells: while the fraction of CAR-T cells increased from 9% pre-injection to 41% in bone marrow and 57% in spleen, the double-positive fraction decreased from 56% pre-injection to 29% in bone marrow and 18% in spleen. Similar effects were observed in the group treated with Triple-T, which consisted of 18% CAR⁺ cells at time-point of injection, but increased to 57% and 63% in bone marrow and spleen, respectively. The double-positive fraction in Triple-T only decreased slightly from 26% pre-injection to 21% and 18% in bone marrow and spleen, respectively.

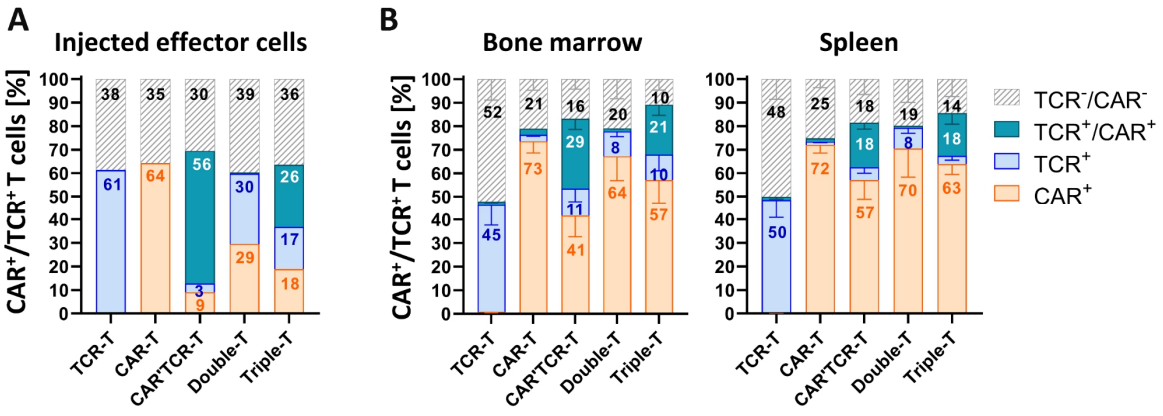

Figure 28: *Ex vivo* analysis of T cell persistence[173]. Percentage of untransduced, TCR$^+$, CAR$^+$ and double-positive T cells in each of the conditions (A) prior to injection and (B) in *ex vivo* analyzed T cells derived from bone marrow and spleen. Displayed are mean values ± SEM for n=6 mice (n=8 sorted CAR'TCR-T).

In order to understand the previous finding that the CAR$^+$ cells demonstrated highest proliferative capability in all of the conditions, the isolated T cells were analyzed for expression of exhaustion (Figure 29) and differentiation (Figure 30) markers. Prior to i.v. injection, all of the conditions showed comparable proportions of TIM-3$^+$/LAG-3$^-$ T cells (~ 35%) (Figure 29 A). Additionally, CAR$^+$/TCR$^+$ T cells showed exhaustion marker expression similar to CAR$^+$ T cells (independent of the treatment group), with approximately 40% of TIM-3$^+$/LAG-3$^+$ T cells. TCR$^+$ T cells showed a different distribution than CAR$^+$ or CAR$^+$/TCR$^+$ T cells with 4-fold lower percentages of TIM-3$^+$/LAG-3$^+$ T cells and instead a higher proportion of TIM-3$^-$/LAG-3$^+$ T cells.

Surprisingly, only marginal levels of TIM-3$^+$/LAG-3$^-$ T cells were detected during *ex vivo* analysis of T cells in bone marrow and spleen (Figure 29 B). All of the conditions showed comparable percentages of TIM-3$^-$/LAG-3$^+$ of around 30% - 40%. Moreover, T cells isolated from bone marrow and spleen displayed similar trends with a slightly more exhausted phenotype in bone marrow. CAR$^+$/TCR$^+$ T cells isolated from mice treated with sorted CAR'TCR-T showed slightly higher exhaustion marker expression than CAR$^+$/TCR$^+$ T cells isolated from Triple-T. Spleen-derived TCR$^+$ cells in Triple-T displayed only 20% of exhaustion marker expression, which was 2-fold lower than the frequencies in TCR-T, CAR'TCR-T or Double-T. Overall, the exhaustion profile of CAR$^+$/TCR$^+$ T cells was more advanced than in CAR$^+$ cells, especially showing higher TIM-3$^+$/LAG-3$^+$ frequencies (e.g. ~16% in CAR$^+$/TCR$^+$ Triple-T versus ~9% in CAR$^+$ Triple-T or ~6% in CAR$^+$ CAR-T.

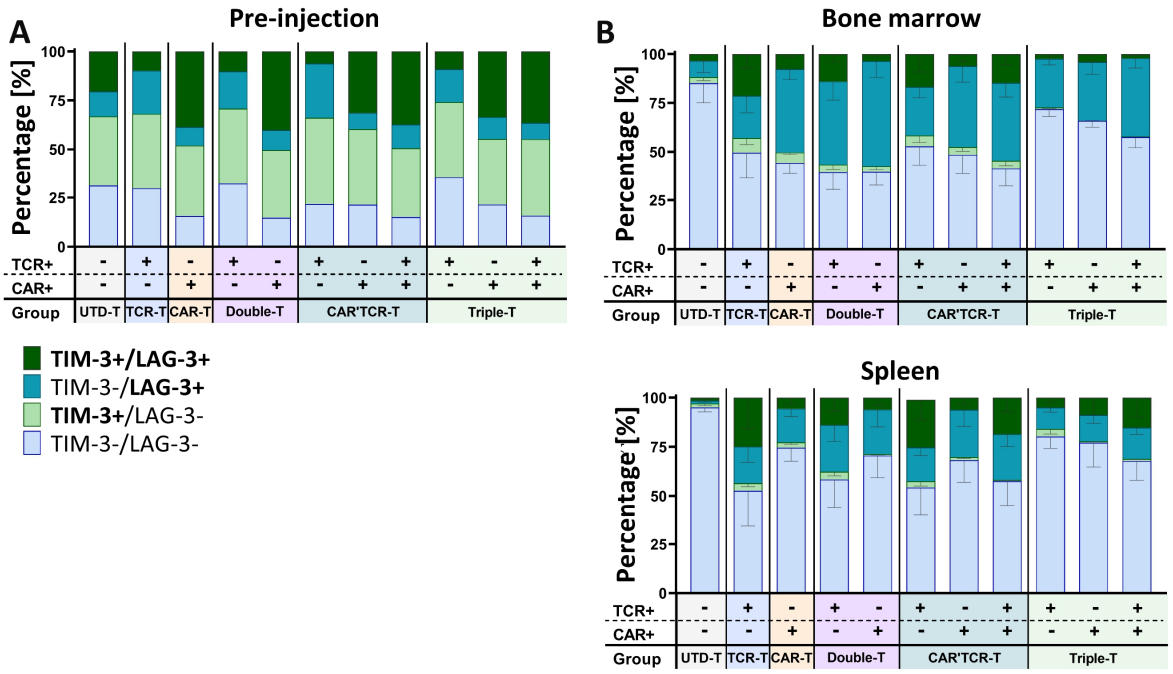

Figure 29: *Ex vivo* analysis of T cell exhaustion. LAG-3 and/or TIM-3 expression (A) prior to effector cell injection and (B) in *ex vivo* analyzed T cells derived from bone marrow and spleen. Displayed are mean values ± SEM for n=6 mice (n=8 sorted CAR'TCR-T).

Next, the aim was to assess whether there are differences in the differentiation status of the various T cell subtypes. Figure 30 A clearly showed that the sorted CAR'TCR-T group contained the greatest proportion of central memory (CM) (up to 67%) and also slightly higher level of effector memory (EM) cells prior to injection. This observation was consistent for all of the subpopulation in the sorted CAR'TCR-T condition, meaning TCR^+, CAR^+, and CAR^+/TCR^+ T cells. Similar to the differences in exhaustion marker expression (Figure 29 A), TCR^+ T cells in TCR-T, Double-T and Triple-T displayed a less differentiated phenotype than the CAR^+ T cells. TCR^+ T cells mainly consisted of memory stem cells (SCM) (~ 44%) and CM cells (~ 50%), while CAR^+ T cells demonstrated 67% - 72% of CM cells.

Ex vivo analysis of T cells isolated from bone marrow or spleen and comparison to time-point of injection, exhibited a strong shift from early to late differentiation phenotype for all of conditions and cell types (Figure 30 A and B). Again, comparable results were obtained for T cells isolated from bone marrow and spleen, with slightly increased differentiation in spleen. In contrast to the strong differences in exhaustion marker expression observed in Figure 29 B, CAR^+/TCR^+ T cells showed no differences in differentiation phenotype comparing CAR'TCR-T and in Triple-T. Although differentiation was less pronounced prior

to injection, TCR$^+$ cells displayed clearly higher proportions of terminally differentiated effector memory cells re-expressing CD45RA (EMRA) cells compared to CAR$^+$ T cells upon *ex vivo* analysis. TCR$^+$ and CAR$^+$ T cells in the group of sorted CAR'TCR-T and Triple-T consisted of EM cell populations almost twice as high as TCR$^+$ T cells in TCR-T or CAR$^+$ T cells in CAR-T. In this regard, it needs to be underlined that *ex vivo* analysis of mice treated with sorted CAR'TCR-T or Triple-T was performed approximately two weeks later than CAR-T or TCR-T, which might also explain differences differentiation or exhaustion marker expression.

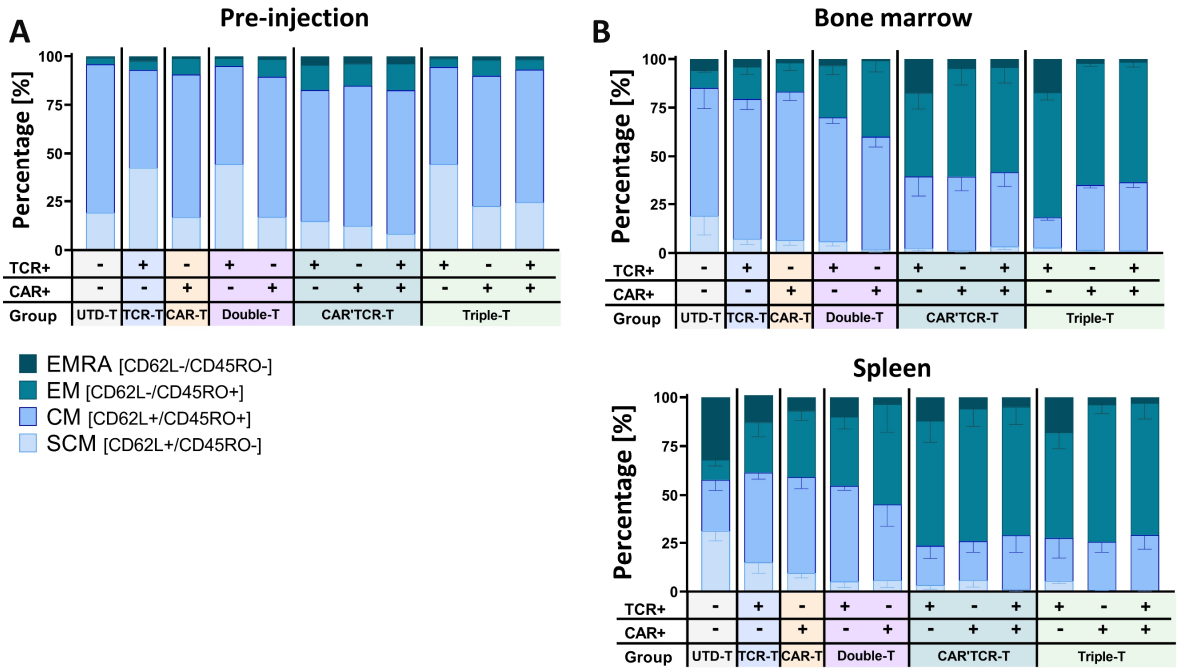

Figure 30: *Ex vivo* analysis of T cell differentiation phenotype. CD62L and/or CD45RO expression (A) prior to effector cell injection and (B) in *ex vivo* analyzed T cells derived from bone marrow and spleen. Displayed are mean values ± SEM for n=6 mice (n=8 sorted CAR'TCR-T).

In order to increase comparability and to ensure a robust and conclusive analysis of the level of exhaustion, Figure 31 only displays *ex vivo* data from mice taken out at final endpoint of the study. This side-by-side comparison revealed that CAR'TCR-T cells in Triple-T, indeed comprised a significantly higher proportion of TIM-3$^+$/LAG-3$^+$ T cells than the CAR-T or TCR-T cells (Figure 31 A). Those CAR$^+$/TCR$^+$ cells, isolated on d37 from Triple-T-treated mice, generally showed a visibly lower remaining proportion of double-negative TIM-3$^-$/LAG-3$^-$ T cells.

Figure 31 B displays *ex vivo* spleen analysis of mice also removed at study endpoint, but treated with sorted CAR'TCR-T cells. Interestingly, no significant difference was observed in LAG-3$^+$/TIM-3$^+$ frequencies between TCR$^+$, CAR$^+$ or CAR$^+$/TCR$^+$ T cells. However, despite high variability between different mice, sorted CAR'TCR-T cells generally showed higher exhaustion marker expression than Triple-T cells. This might be explained by the higher tumor burden in CAR'TCR-T- compared to Triple-T-treated mice at study endpoint (Figure 26).

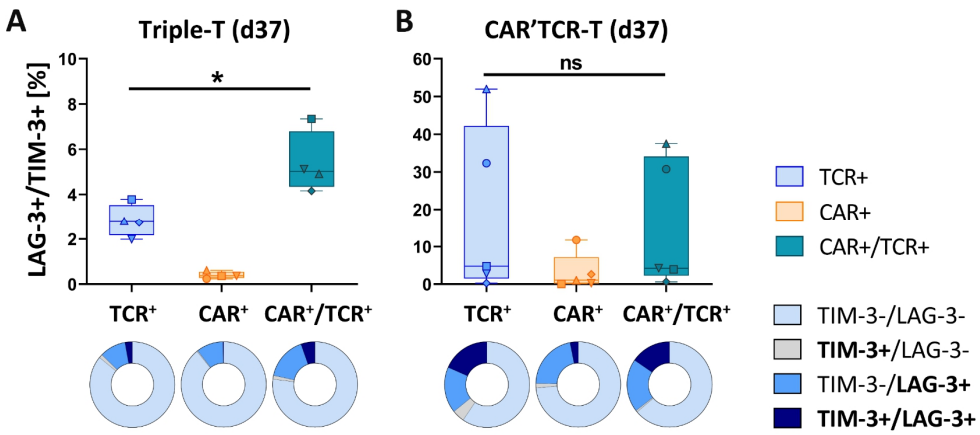

Figure 31: *Ex vivo* analysis of final end-point[173]. Frequencies of LAG-3$^+$/TIM-3$^+$ effector cell types (TCR+, CAR+ or CAR+/TCR+), isolated from spleen of mice treated with (A) Triple-T or (B) CAR'TCR-T and removed from the experiment on d37 (endpoint of study). Donut graphs below the respective T cell subtypes display the corresponding frequencies of TIM-3$^+$, LAG-3$^+$, double-negative and double-positive cells. Box and whiskers plot shows individual and median values. The *p*-values were calculated using Tukey's multiple comparison test and the mixed-effects model with Geisser-Greenhouse correction (one-way analysis of variance) (ns, not significant; *$p \leq 0.05$).

In summary, the beneficial effect of combining CAR and TCR in the same cell was proven, not only *in vitro*, but also *in vivo*. Especially the Triple-T condition, which represents the natural product of co-transduction during a potential clinical manufacture, was proven to be advantageous, even outperforming the mixture of CAR-T and TCR-T cells *in vivo*. Regarding the AML mouse model, all of the other conditions led to continuous outgrowth of tumor cells, while Triple-T represented the only treatment condition that resulted in elimination of Oci-AML3 cells from day 28 onwards.

Data presented in figures 14, 16-18, 20-22, 24, 26, 28, 31 were published in Teppert, K. *et al.* "CAR'TCR-T cells co-expressing CD33-CAR and dNPM1-TCR as superior dual-targeting approach for AML treatment". Molecular Therapy Oncology (2024)[173].

5. DISCUSSION

The main goal of this work was to assess whether it is possible, and particularly, beneficial to co-express a CAR and a transgenic TCR in the same T cell. It was hypothesized that dual-specific CAR'TCR-T cells show superiority in case of heterogeneous tumor cell populations or antigen escape. Pre-clinical[127,134] and clinical results (NCT00085930[123], NCT00840853[124,125]) have shown that additional stimulation of CAR-T cells via the endogenous TCR led to increased expansion, persistence and anti-tumor activity and even enabled functional recovery of exhausted and terminally differentiated CAR-T cells[126]. Therefore, it was hypothesized that stimulation of a transgenic TCR in CAR-T cells might have a similar beneficial outcome, while simultaneously facilitating dual-specificity.

5.1 Combination of CAR and TCR

A prerequisite for studying the combination of CAR and transgenic TCR in the same T cell was to identify the characteristics of the respective constructs itself. As expected, the HLA-A*02:01-restricted dNPM1-TCR was only functional in $CD8^+$ T cells, which might be explained by missing pMHC-TCR stabilization via the CD8 co-receptor in $CD4^+$ cells[161,171]. Surprisingly, van der Lee and colleagues observed dNPM1-TCR functionality also in $CD4^+$ T cells, although clearly reduced compared to $CD8^+$ T cells[161]. Such contradicting results could be explained by differences in the manufacturing protocol: first, retroviral instead of lentiviral transduction; second, activation via polyhydroxyalkanoate instead of TransAct™; third, mouse instead of human TCR constant regions; and finally, functionality analysis right after magnetic enrichment of TCR^+ cells versus 5 days of cultivation between sorting and the co-culture assay. Especially the latter might increase the activation status in $CD4^+$ T cells and consequently lower the threshold for dNPM1-TCR-signaling[189]. Additionally, elevated TCR expression levels might result in higher T cell avidity, thereby allowing for CD8-independent target recognition[190].

Due to the limited functionality of the dNPM1-TCR in $CD4^+$ T cells, the subsequent co-transduction experiments were performed with $CD8^+$ T cells only. For proof of concept, the dNPM1-TCR was combined with the clinically well-established second-generation Leu16-derived CD20-CAR[84,168,169] containing a 4-1BB costimulatory domain. Major aim was to assess the impact of co-transduction on the expression level and functionality of CAR and

TCR. Transducing with two lentiviral vectors simultaneously led to CAR and TCR expression in CAR'TCR-T cells equivalent to that in CAR-T or TCR-T cells, respectively. Comparable to previously reported findings on co-expression of CAR and transgenic TCR[138,139], no reciprocal inhibition between CAR and TCR was observed in CAR'TCR-T cells. More precisely, no significant difference in target cell lysis was measured between CAR'TCR-T and CAR-T or TCR-T cells upon CAR- or TCR-stimulation, respectively. This ensures that target cell lysis via CAR and TCR works independently and is consequently maintained in case of MHC downregulation or loss of target antigen. Interestingly, dual stimulation led to boosted anti-tumor activity in CAR'TCR-T compared TCR-T cells. Ugur Uslu and colleagues observed similar effects with $CD8^+$ T cells transfected with RNA encoding gp100-TCR and MCSP-CAR[139]. Three years later the work was continued, and surprisingly, dual-specific T cells expressing the same receptors led to the opposite outcome[138]: co-expression resulted in reduced lytic activity upon dual stimulation, which could either be explained by the change from electroporation to lentiviral transduction of TCR, thereby possibly impacting surface TCR density, or more likely, by the co-culture with different target cell lines.

To verify the boosted cytotoxicity in CAR'TCR-T cells with another combination, the *in vitro* experiments were repeated with $CD8^+$ T cells co-expressing dNPM1-TCR and CD33-CAR. This represents a clinically relevant combination, since CD33 is found in more than 85% of adult and pediatric AML[191]. Again, dual stimulation in trans resulted in significantly boosted TCR-dependent killing with CAR'TCR-T compared to TCR-T cells. Since CAR-T cells already caused almost 100% target cell lysis, it was impossible to detect further increase of killing with CAR'TCR-T cells. However, cis stimulation with Oci-AML3 cells expressing both CD33 and dNPM1, revealed increased lytic activity with CAR'TCR-T cells compared to not only TCR-T but also CAR-T cells. This finding can be explained by the very low CD33 levels in Oci-AML3 cells, suggesting that dual-targeting in cis was able to increase the CAR-dependent anti-tumor response and might especially be beneficial in case of dim antigen expression.

Regarding low target antigen expression, it needs to be pointed out that increased efficacy in dual-specific T cells might not necessarily be linked to co-signaling of the two receptors, but rather to enhanced binding avidity. Especially when there is competition between signaling molecules, it might be the case that either CAR or TCR is dominant and that there is no concomitant signaling. However, the results obtained upon trans stimulation indicate

otherwise, since both CAR- and TCR-dependent functionality was detected. Furthermore, latest findings from Markus Barden and colleagues suggest that despite simultaneous antigen engagement, 28ζCAR and endogenous TCR form separated immunological synapses and lead to paralleled, non-overlapping downstream signaling[192]. To assess whether this finding is restricted to a certain CAR design, it would be required to verify this effect for the combination with for instance a BBζCAR. Finally, the question of whether the observed boosting effect is based on increased avidity, could be addressed through combination of a transgenic TCR with a CAR lacking the intracellular domains. It needs to be pointed out, however, that this truncated CAR would be non-functional by itself and theoretically non-functional in absence of the TCR target.

Whole transcriptome analysis of CAR'TCR-T cells revealed their closer relationship to CAR-T than to TCR-T cells, suggesting that CAR signaling is dominant in CAR'TCR-T cells upon dual stimulation in cis. Strikingly, gene set enrichment analysis linked the differentially upregulated genes in CAR'TCR-T cells to cellular pathways such as positive regulation of T cell activation and GTPase activity, which further supported the boosted cytotoxicity observed *in vitro*. Especially the significantly upregulated GTPase activity strongly indicated for enhanced activation-dependent IS formation, which might also support receptor clustering and overall T cell signaling[116,177]. This observation did not only substantiate the boosted anti-tumor cytotoxicity of CAR'TCR-T cells, but also suggested synergistic effects through co-signaling via CAR and TCR. In-depth analysis of the DEGs would enable to identify pathways and upregulated genes that are unique to CAR'TCR-T cells. Subsequently, this could be further verified through proteomics analysis. Finally, high-resolution microscopy would be required to address whether the observed transcriptomic effects are based on physical interaction between CAR and TCR or whether there is paralleled, non-overlapping downstream signaling as described by Barden *et al.*[192].

5.2 Long-term efficacy and exhaustion of CAR'TCR-T cells

Hyperactivation and repetitive signaling via TCR or CAR was linked to T cell exhaustion, dysfunction and treatment failure[193-195]. Moreover, studies with syngeneic mouse models have shown that simultaneous engagement of CAR and endogenous TCR triggered pro-apoptotic and inhibitory pathways, eventually causing exhaustion and decreased cytotoxic

activity[131]. Therefore, it was hypothesized that CAR'TCR-T cells, which receive dual stimulation via CAR and transgenic TCR, might show faster exhaustion and consequently impaired anti-tumor activity and persistence. Interestingly, long-term co-culture experiments with repetitive target cell addition showed prolonged anti-tumor response upon dual stimulation in trans and in cis. The trans setting contained a mixture of CAR- and TCR-target cells, which is mimicking a heterogeneous tumor cell population. As expected, only CAR'TCR-T cells managed to control tumor growth, while *in vitro* co-culture with CAR-T and TCR-T led to significantly reduced target cell clearance. Moreover, CAR'TCR-T cells also demonstrated superiority upon repeated stimulation in cis, especially for the clinically relevant combination of dNPM1-TCR and CD33-CAR. Importantly, after long-term repetitive stimulation in cis, CAR'TCR-T cells exhibited higher exhaustion marker expression than CAR-T and TCR-T cells. However, a dysfunctional state was not reached, and opposed to this, CAR'TCR-T cells still displayed superior anti-tumor activity. Therefore, an even more challenging and longer experimental set-up might be required to eventually reach a state of exhaustion in those CAR'TCR-T cells.

Double-T cells demonstrated visibly lower expression of TIM-3 and LAG-3 than CAR'TCR-T cells, while cytolytic activity was comparably high up to the last round of stimulation. Additionally, IFN-γ cytokine release was observed to be higher in Double-T cells compared to CAR'TCR-T or Triple-T cells, which was the case for the first and third round of target cell addition. In this regard, it is important to highlight that Double-T contained twice the amount of gene-engineered T cells (1×10^4 CAR-T and 1×10^4 TCR-T) than the CAR'TCR-T condition (1×10^4 CAR'TCR-T and 1×10^4 UTD-T). While this experimental set-up ensured equivalent numbers of CAR- and TCR-targeting effector cells, it might also explain why Double-T cells showed higher IFN-γ concentrations and lower exhaustion marker expression. The fact that CAR'TCR-T contained only half the amount of modified, effective T cells than the Double-T condition – while simultaneously demonstrating comparable anti-tumor cytotoxicity – might suggest that the co-expression and co-signaling of CAR and TCR indeed boosts the lytic activity. This is in line with the findings of Marco Ruella and colleagues, who showed that dual-specific CD19-/CD123-targeting CAR T cells outperformed the mixture of CD19-CAR-T and CD123-CAR-T cells *in vivo*[196].

5.3 Different costimulatory domains in CAR'TCR-T cells

In this work, the dNPM1-TCR was initially combined with a 4-1BB-costimulated CAR, which is generally linked to more durable and long-term anti-tumor response in hematological malignancies[128-130]. In contrast, most of the CAR-T cell studies reporting an advantage in stimulating the native TCR were based on CD28-costimulation[124,126,127]. In addition, endogenous TCR stimulation resulted in boosted expansion and cytotoxicity of CD28ζCAR-T cells *in vitro*, which was not observed for the 4-1BB-costimulated counterpart[127]. Also previous work on combination with a transgenic TCR was based on CD28 costimulation in the CAR context[138,139].

In contrast to the work by Omer and colleagues[127], the side-by-side comparison of CAR'TCR-T cells co-expressing dNPM1-TCR and either 4-1BB- or CD28-costimulated CD20-CAR did not reveal any differences in exhaustion marker expression or the cytotoxic potential, not even after long-term repetitive co-culture. This discrepancy might be explained by variations in experimental design such as the different tumor setting and the shorter duration of *in vitro* co-culture. Therefore, *in vivo* comparison of BBζCAR'TCR-T and 28ζCAR'TCR-T would be required to further address this question. Moreover, it needs to be emphasized that the most suitable combination might be dependent on respective scFv affinity[197], target antigen density[198] and tumor type[199]. Especially for treatment of solid tumors it was demonstrated that CARs containing CD28 costimulatory domain are superior due to eliciting stronger and more rapid anti-tumor response[199].

Subsequent experiments were continued with 4-1BB-costimulated CAR constructs: firstly, to counteract the expected faster exhaustion in dual-stimulated CAR'TCR-T cells; secondly, to minimize the risk of cytokine release syndrome, which is more strongly observed in clinical trials with CARs using CD28 costimulation[129].

5.4 Combination of CAR and TCR in $CD4^+$ T cells

As described in the beginning of chapter 5.1, all of the experiments combining CAR and transgenic TCR were performed in $CD8^+$ T cells only, since the dNPM1-TCR was shown to be non-functional in $CD4^+$ T cells. Several groups have emphasized the clinical relevance of $CD4^+$ T cells in cancer treatment with adoptive cell therapies. It was observed that not only

$CD8^+$ but also $CD4^+$ CAR-T cells are capable of mediating anti-tumor activity[200-202]. Strikingly, $CD4^+$ CAR T cells maintained anti-tumor functionality, expanded and persisted longer after encounter with target cells, representing the predominant subtype even after decade-long remission[131,172].

One of the major findings was the strongly enhanced TCR-dependent killing in CAR'TCR-T cells upon dual stimulation. It was hypothesized, that such a boost of dNPM1-TCR activity might also be achieved in $CD4^+$ T cells through co-expression of a CAR. Simultaneous engagement of TCR and CAR might increase overall T cell avidity and thereby mimic the stabilizing effect of the CD8 co-receptor[190]. Therefore, a side-by-side comparison of $CD4^+$ CAR'TCR-T and $CD8^+$ CAR'TCR-T cells, co-expressing dNPM1-TCR and CD20-CAR, was performed.

Indeed, co-culture with 4CAR'TCR-T cells resulted in almost complete target cell lysis upon dual stimulation. However, also strong bystander killing was observed, indicating that the boosting effect might be fully or partly achieved through the concomitantly stimulated CAR. This demonstrates the limitation of the experimental set-up in answering the question of whether the dNPM1-TCR becomes functional in $CD4^+$ T cells through co-engagement of CAR. As described in chapter 5.1 "Combination of CAR and TCR", co-expressing the dNPM1-TCR with a non-functional, truncated CAR (lacking the intracellular domains) might mimic the increased $CD4^+$ T cell avidity, while simultaneously preventing bystander signaling and activation events via the CAR.

However, long-term co-culture experiments revealed that 4CAR'TCR-T cells showed significantly stronger target cell lysis after repeated stimulation in trans compared to 4CAR-T cells. This suggests that signaling and killing via the dNPM1-TCR is indeed involved and that the previously described boosting is not solely facilitated through CAR-dependent bystander effects.

Although these findings suggest that co-transduction with dNPM1-TCR does not have negative impact on the $CD4^+$ CAR-T cell functionality, it needs to be underlined that sharing of TCR-LV between $CD4^+$ and $CD8^+$ T cells might decrease the overall transduction efficiency. Accordingly increasing the MOI would lead to higher vector copy numbers, which is limited to 5 copies per genome by the Food and Drug Administration[203]. Another

possible solution might be the co-expression of CD8α or CD8αβ in $CD4^+$ T cells, which was reported to significantly enhance transgenic TCR functionality in pre-clinical studies[204,205] with encouraging responses in a first clinical trial[206] (NCT04044859). This might facilitate functionality of the dNPM1-TCR in not only $CD8^+$ but also $CD4^+$ T cells. Moreover, selection of high-affinity transgenic TCRs, which are naturally independent of the CD8 co-receptor[207], might represent another alternative for combination with CAR.

To sum this up, further in-depth analysis is required to understand whether co-expression of a CAR facilitates functional recovery of an MHC class I-restricted TCR in $CD4^+$ T cells. Nonetheless, no reduction in cytotoxicity was observed in 4CAR'TCR-T cells compared to 4CAR-T cells, and on the contrary, CAR-T cells co-expressing dNPM1-TCR even displayed reduced exhaustion marker expression after repetitive stimulation in all conditions.

5.5 CAR'TCR-T cells *in vivo*

The *in vivo* study primarily aimed at assessing the efficacy of CAR'TCR-T cells, co-expressing the previously published transgenic dNPM1-TCR[161] and CD33-CAR (My96-scFv)[155,208,209], in an AML mouse model with Oci-AML3 cells.

While all the treatment conditions led to continuous tumor outgrowth, only Triple-T-treated mice showed tumor elimination starting from day 23. This cellular composition of CAR-T, TCR-T and CAR'TCR-T represented the natural product of co-transduction and was manufactured using the CliniMACS Prodigy®, which underlines the clinical applicability of this approach. The fact that tumor elimination was not even achieved upon treatment with Double-T cells, a mixture of CAR-T and TCR-T, further proves the power of CAR'TCR-T cells.

One group was treated with sorted CAR'TCR-T cells, which served as experimental control according to the *in vitro* experiments and cannot be directly compared to the other groups, due to the different manufacturing protocols. Transduction with a polycistronic construct encoding for both CAR and TCR would be a more suited control, preventing the development of CAR- or TCR-only T cells as it occurs during co-transduction with separate viral vectors. However, due to a transfer vector size of almost 10 kbp only low viral titers and transduction efficiencies would be expected[210]. A possible solution might be the use of

high-capacity adenoviral vectors[211,212], which would allow to determine, whether the cellular composition in Triple-T is indeed superior compared to CAR'TCR-T cells only.

Interestingly, *ex vivo* analyzed spleen-derived T cells mainly consisted of CAR^+ T cells. This implies that the *in vitro* observed boosted anti-tumor response with CAR'TCR-T cells also occurred during *in vivo* treatment with Triple-T. The fact that CAR-T cells persisted longest, indicates that CAR'TCR-T cells were either exhausted and/or simply showed reduced proliferative capacity than CAR-T cells. This was supported by the finding that CAR^+/TCR^+ T cells in Triple-T-treated mice demonstrated significantly higher exhaustion than the CAR^+ or TCR^+ T cells in Triple-T. Omer and colleagues observed enhanced proliferation and persistence in transgenic TCR-T cells co-expressing a third-generation CD28-/OX40-costimulated CD19-CAR without CD3ζ signaling domain, compared to combination with a full second-generation CD19-CAR[213]. The hypothesis that simultaneous CAR- and TCR-engagement results in excessive CD3ζ-signaling, eventually leading to activation-induced cell death, might also be applicable to the dual-specific CAR'TCR-T cells in Triple-T. Similar findings were also published in the context of multi-targeting with two different CAR constructs, showing that split CD3ζ signaling is beneficial for long-term persistence[141]. Combining the dNPM1-TCR with a CD3ζ-lacking CD33-CAR might, however, carry the risk for failed anti-tumor response in case of MHC downregulation and thus requires careful evaluation.

Prolonged targeting of CD33 was linked to increased risk for off-tumor toxicity against non-malignant cells such as myeloid progenitors or hepatic Kupffer cells, consequently leading to severe myelosuppression or potentially deadly sinusoidal obstruction syndrome, respectively[157-159]. Therefore, it was proposed to even reduce CAR-T cell persistence for AML treatment[150], for example through implementation of safety switches[214,215], inducible systems[216] or adapter technologies[217-219]. The observed lower persistence of CAR'TCR-T cells compared to CAR-T cells might consequently even be beneficial. This again underlines the importance of evaluating whether a cell product solely containing CAR'TCR-T cells, and no CAR-T or TCR-T cells, would eventually allow for equally high *in vivo* anti-tumor response as treatment with Triple-T cells.

To prove the advantage of CAR'TCR-T cells, not only regarding boosted efficacy but also with respect to tumor heterogeneity, it would additionally be necessary to perform an *in*

vivo experiment with a mixture of different target cells. A patient-derived AML xenograft model, which perfectly recapitulates the genetic diversity and intratumor heterogeneity[220], would not only help to further verify the previous findings but might also be valuable regarding the complex immunosuppressive characteristics of AML[165,221].

5.6 Conclusion and outlook

The primary objective of the work was to evaluate in which way CAR and transgenic TCR can be combined for a novel therapeutic concept. *In vitro* and *in vivo* experiments demonstrated superiority of dual-specific CAR'TCR-T cells. Strikingly, *in vivo* no elimination of target cells was achieved with Double-T cells, a mixture of CAR-T and TCR-T cells, underlining the power and increased anti-tumor activity with CAR'TCR-T cells.

A remaining question, which still needs to be answered is whether the combination of CD33-CAR and dNPM1-TCR is superior compared to co-expression of a CD33-CAR and a second dNPM1-HLA-A*02:01-targeting CAR (dual-CAR-T). Here, several factors must be taken into account: First, prerequisite for the latter approach is the successful development of an antibody targeting dNPM1-HLA-A*02:01. Such TCR-like antibodies generally only bind to a few residues and not to the full target peptide, resulting in lowered specificity and increased risk for off-target interactions[222]. Besides, inadequate sensitivity and signal transduction were described to be other limitations of pMHC-directed CARs, thus not achieving the required therapeutic activity as respective TCRs[106,107,222,223]. Second, in-depth characterization of CARs and TCRs displayed large differences regarding architecture, IS and signaling[106,111,134]. This explains why interaction, competition, or even reciprocal inhibition between the two receptors is not expected[192], whereas overstimulation and increased risk for cytokine release syndrome were reported in the context of dual-CAR-T cells[141,224]. On top of that, even increased cytotoxicity and proliferation was observed upon co-signaling of the endogenous TCR and CAR[124,126,127,134]. Due to the exact same structure, similar effects are expected for co-engagement of a transgenic TCR. Finally, several groups are currently focusing on learning from the naturally evolved TCR, in order to design novel constructs with more physiological signaling machinery (e.g. STAR[80], TRuC[79], HIT[81], or TAC[225] receptor) displaying increased sensitivity and enhanced anti-tumor activity. This further supports the

approach of combining CAR and transgenic TCR instead of co-expressing two different CARs.

This work is based on combination of a CAR and a transgenic TCR for treatment of AML. Although similar effects were observed with two different CARs (CD33-CAR or CD20-CAR), it would next be crucial to validate the applicability for other, particularly solid tumor settings. Therapeutic success of CAR-T cells for treatment of solid tumors was shown to be limited[48]. A significant level of expectation is currently placed in transgenic TCRs, which cover a larger target repertoire by also including intracellular cancer antigens, demonstrate more sensitive tumor detection[106,107,222,223] and are expected to show better tumor penetration[143,226,227]. In addition, transgenic TCR-T cells were reported to enhance T cell persistence and overall more balanced activation due to the physiological signaling machinery[48,80]. Co-expression of a TCR in CAR-T cells might therefore also be beneficial for treatment of solid tumors. Similar to the CAR'TCR-T approach, various studies are based on dual-targeting in order to overcome the heterogeneity in solid tumors and to decrease the risk for tumor escape and recurrence[141,142,196]. Another major challenge in treatment of solid tumors is the lack of specific antigens and the resulting off-target toxicity[228]. An ideal solution is the targeting of highly tumor-specific neoantigens (such as the driver mutation in dNPM1) via transgenic TCRs. However, the process of developing such personalized treatments is more time- and cost-consuming[229], and in the end, restricted to a certain HLA-type and availability of the particular mutation. Finally, the immunosuppressive TME in solid tumors hinders T cells from infiltrating, resulting in exhaustion and insufficient anti-tumor activity[228]. CAR'TCR-T cells co-expressing a tumor-specific TCR and a CAR directed to the TME might tackle this challenge, especially as boosted functionality was also observed in trans. Already introduced approaches are for example CAR-T cells targeting the tumor vasculature[230-233], cancer-associated fibroblasts[234-238], tumor-associated macrophages[239,240] or myeloid-derived suppressor cells[230,241].

Although the use of a neoantigen-restricted TCRs has the great advantage of high tumor cell specificity, prerequisites such as the HLA-haplotype limit the number of patients, who are eligible for such personalized treatment. The dNPM1-TCR is, on the one hand, restricted to HLA-A*02:01, which is most prevalent and yet only expressed in approximately 50% of the Caucasian population[242]. On the other hand, another dNPM1-targeting TCR specific for

HLA-A*11:01 has already been identified[243] and further broadening the selection of transgenic TCRs would allow for personalized adjustments of the therapy according to HLA typing.

Another challenge, which needs to be considered in context of transgenic TCRs, is the risk for mispairing. This might influence TCR expression[244] as well as therapeutic safety due to potential development of autoreactive specificities[245,246]. Possible solutions are either knock-out of the endogenous TCR[247] or one step further, knock-in of a transgene in the TCR locus[248-250]. This would not only enable physiologically regulated TCR expression[249,251], but might also minimize the risk for GvHD with allogeneic donor-derived T cells[252,253].

In conclusion, this work demonstrates the superiority of combining CAR and TCR technologies through co-expression in the same T cell, facilitating boosted anti-tumor cytotoxicity upon stimulation in cis and in trans, while maintaining functionality and specificity in case of CAR- or TCR-only stimulation. Clinical applicability of this approach is provided by the fact that Triple-T is the natural product of co-transduction with two LVs encoding for either CAR or TCR, automatically leading to a final cellular composition of CAR'TCR-T, CAR-T and TCR-T. Most importantly, *in vivo* target cell lysis was only observed in mice treated with Triple-T cells, while all other conditions, including the mixture of CAR-T and TCR-T cells, led to continuous tumor outgrowth. This emphasizes the advantage of incorporating T cells co-expressing CAR and transgenic TCR. Furthermore, the data underlines the relevance of this combinatorial approach as valuable therapeutic alternative for treatment of AML. Current standard treatment consists of chemotherapy with optional allo-HSCT as subsequent post-remission therapy[150]. AML incidence and mortality rates are globally increasing and five-year survival rates are low[150,254]. The overall poor treatment responses have led to implementation of targeted immunotherapies[221]. Challenges that are still limiting CAR- or TCR-T cell efficacy in treatment of AML are the clonal heterogeneity, the immunosuppressive TME, on-target off-tumor toxicities and the risk for immune escape and relapse[165]. This work provides compelling evidence that CAR'TCR-T cells, co-expressing a CD33-CAR and dNPM1-TCR, might represent a powerful alternative treatment option for AML: First, targeting of neoantigens such as dNPM1 is expected to decrease the risk for adverse events due to on-target effects against healthy tissue[160]. Second, CAR'TCR-T cells exhibit dual-specificity, which might enable more comprehensive tumor cell elimination

and mitigate the chance for residual leukemic blasts[164]. Finally, only the treatment containing CAR'TCR-T cells induced a sufficient anti-tumor response *in vivo*. This substantiates the boost in anti-tumor cytotoxicity as well as the clinical potential, particularly for treatment of aggressive, chemotherapy-resistant AMLs[255].

In the recent years, adoptive T cell therapy has also emerged as promising treatment modality in autoimmune disorders[256]. CD19- and/or BCMA-targeting CAR T cells have for instance been successfully applied in several cases of systemic lupus erythematosus[257-259]. Various clinical CAR T cell trials are currently also on going for other autoimmune diseases such as myasthenia gravis, sjögren's syndrome, scleroderma or immune nephritis[256]. Due to their natural role in preventing excessive immune responses and autoimmunity, regulatory T cells are widely used for adoptive T cell treatment of autoimmune diseases[256]. Regulatory T cells expressing a CAR or a TCR were engineered for treatment of multiple sclerosis[260,261] or type I diabetes[256,262]. Considering the discoveries of this work, the combination of CAR and TCR could potentially also increase the therapeutic efficacy of adoptive cell therapies in the context of autoimmune diseases. For example, a possible approach for treatment of multiple sclerosis could involve regulatory T cells expressing a TCR against myelin basic protein[260] and a CAR targeting myelin oligodendrocyte glycoprotein[256].

In summary, further work is required to verify the findings for other combinations of CAR and TCR, allowing for application of CAR'TCR-T cells in various clinically relevant settings. The efficacy of adoptive cell therapy in solid tumors remains a major challenge[48], but the observed characteristics of CAR'TCR-T cells, including enhanced anti-tumor efficacy and dual-specificity, offer promise for their potential application and impact on solid tumors.

REFERENCES

1 Miller, Jacques F. A. P. & Sadelain, M. The Journey from Discoveries in Fundamental Immunology to Cancer Immunotherapy. *Cancer cell* **27**, 439-449, doi:10.1016/j.ccell.2015.03.007 (2015).

2 Hanahan, D. & Weinberg, Robert A. Hallmarks of Cancer: The Next Generation. *Cell* **144**, 646-674, doi:10.1016/j.cell.2011.02.013 (2011).

3 Hanahan, D. & Weinberg, R. A. The Hallmarks of Cancer. *Cell* **100**, 57-70, doi:10.1016/S0092-8674(00)81683-9 (2000).

4 Hanahan, D. Hallmarks of Cancer: New Dimensions. *Cancer discovery* **12**, 31-46, doi:10.1158/2159-8290.cd-21-1059 (2022).

5 Marshall, J. S., Warrington, R., Watson, W. & Kim, H. L. An introduction to immunology and immunopathology. *Allergy, Asthma & Clinical Immunology* **14**, 49, doi:10.1186/s13223-018-0278-1 (2018).

6 Mellman, I., Chen, D. S., Powles, T. & Turley, S. J. The cancer-immunity cycle: Indication, genotype, and immunotype. *Immunity* **56**, 2188-2205, doi:doi:10.1016/j.immuni.2023.09.011 (2023).

7 Kim, S. K. & Cho, S. W. The Evasion Mechanisms of Cancer Immunity and Drug Intervention in the Tumor Microenvironment. *Frontiers in pharmacology* **13**, 868695, doi:10.3389/fphar.2022.868695 (2022).

8 Inaba, K., Metlay, J. P., Crowley, M. T. & Steinman, R. M. Dendritic cells pulsed with protein antigens in vitro can prime antigen-specific, MHC-restricted T cells in situ. *Journal of Experimental Medicine* **172**, 631-640, doi:10.1084/jem.172.2.631 (1990).

9 Gyure, L. A., Barfoot, R., Denham, S. & Hall, J. G. Immunity to a syngeneic sarcoma induced in rats by dendritic lymph cells exposed to the tumour either in vivo or in vitro. *British journal of cancer* **55**, 17-20, doi:10.1038/bjc.1987.4 (1987).

10 Demaria, O. *et al.* Harnessing innate immunity in cancer therapy. *Nature* **574**, 45-56, doi:10.1038/s41586-019-1593-5 (2019).

11 Ho, S. S. *et al.* The DNA Structure-Specific Endonuclease MUS81 Mediates DNA Sensor STING-Dependent Host Rejection of Prostate Cancer Cells. *Immunity* **44**, 1177-1189, doi:10.1016/j.immuni.2016.04.010 (2016).

12 Iurescia, S., Fioretti, D. & Rinaldi, M. Targeting Cytosolic Nucleic Acid-Sensing Pathways for Cancer Immunotherapies. *Frontiers in immunology* **9**, 711, doi:10.3389/fimmu.2018.00711 (2018).

13 Gowen, B. G. *et al.* A forward genetic screen reveals novel independent regulators of ULBP1, an activating ligand for natural killer cells. *eLife* **4**, e08474, doi:10.7554/eLife.08474 (2015).

14 Gasser, S., Orsulic, S., Brown, E. J. & Raulet, D. H. The DNA damage pathway regulates innate immune system ligands of the NKG2D receptor. *Nature* **436**, 1186-1190, doi:10.1038/nature03884 (2005).

15 Jung, H., Hsiung, B., Pestal, K., Procyk, E. & Raulet, D. H. RAE-1 ligands for the NKG2D receptor are regulated by E2F transcription factors, which control cell cycle entry. *Journal of Experimental Medicine* **209**, 2409-2422, doi:10.1084/jem.20120565 (2012).

16 Wolf, N. K., Kissiov, D. U. & Raulet, D. H. Roles of natural killer cells in immunity to cancer, and applications to immunotherapy. *Nature Reviews Immunology* **23**, 90-105, doi:10.1038/s41577-022-00732-1 (2023).

17 Blum, J. S., Wearsch, P. A. & Cresswell, P. Pathways of antigen processing. *Annu Rev Immunol* **31**, 443-473, doi:10.1146/annurev-immunol-032712-095910 (2013).

18 Rammensee, H. G., Falk, K. & Rotzschke, O. MHC molecules as peptide receptors. *Curr Opin Immunol* **5**, 35-44, doi:10.1016/0952-7915(93)90078-7 (1993).

19 Zinkernagel, R. M. & Doherty, P. C. Restriction of in vitro T cell-mediated cytotoxicity in lymphocytic choriomeningitis within a syngeneic or semiallogeneic system. *Nature* **248**, 701-702, doi:10.1038/248701a0 (1974).

20 Delamarre, L., Holcombe, H. & Mellman, I. Presentation of exogenous antigens on major histocompatibility complex (MHC) class I and MHC class II molecules is differentially regulated during dendritic cell maturation. *The Journal of experimental medicine* **198**, 111-122, doi:10.1084/jem.20021542 (2003).

21 Zagorulya, M. & Spranger, S. Once upon a prime: DCs shape cancer immunity. *Trends in cancer* **9**, 172-184, doi:10.1016/j.trecan.2022.10.006 (2023).

22 Mikucki, M. E. *et al.* Non-redundant requirement for CXCR3 signalling during tumoricidal T-cell trafficking across tumour vascular checkpoints. *Nature communications* **6**, 7458, doi:10.1038/ncomms8458 (2015).

23 Spranger, S., Dai, D., Horton, B. & Gajewski, T. F. Tumor-Residing Batf3 Dendritic Cells Are Required for Effector T Cell Trafficking and Adoptive T Cell Therapy. *Cancer cell* **31**, 711-723.e714, doi:10.1016/j.ccell.2017.04.003 (2017).

24 Burnet, F. M. The concept of immunological surveillance. *Progress in experimental tumor research* **13**, 1-27, doi:10.1159/000386035 (1970).

25 Burnet, M. Cancer: a biological approach. III. Viruses associated with neoplastic conditions. IV. Practical applications. *British medical journal* **1**, 841-847, doi:10.1136/bmj.1.5023.841 (1957).

26 Birkeland, S. A. *et al.* Cancer risk after renal transplantation in the Nordic countries, 1964-1986. *Int J Cancer* **60**, 183-189, doi:10.1002/ijc.2910600209 (1995).

27 Penn, I. & Starzl, T. E. Proceedings: The effect of immunosuppression on cancer. *Proceedings. National Cancer Conference* **7**, 425-436 (1972).

28 Smith, J. L., Jr. & Stehlin, J. S., Jr. Spontaneous regression of primary malignant melanomas with regional metastases. *Cancer* **18**, 1399-1415, doi:10.1002/1097-0142(196511)18:11<1399::aid-cncr2820181104>3.0.co;2-r (1965).

29 Dunn, G. P., Old, L. J. & Schreiber, R. D. The Three Es of Cancer Immunoediting. *Annual Review of Immunology* **22**, 329-360, doi:10.1146/annurev.immunol.22.012703.104803 (2004).

30 Chen, B.-J., Zhao, J.-W., Zhang, D.-H., Zheng, A.-H. & Wu, G.-Q. Immunotherapy of Cancer by Targeting Regulatory T cells. *Int Immunopharmacol* **104**, 108469, doi:doi:10.1016/j.intimp.2021.108469 (2022).

31 Mittal, D., Gubin, M. M., Schreiber, R. D. & Smyth, M. J. New insights into cancer immunoediting and its three component phases--elimination, equilibrium and escape. *Curr Opin Immunol* **27**, 16-25, doi:10.1016/j.coi.2014.01.004 (2014).

32 Stanley, J. O. & Mohamed, S. A. Cancer immunotherapy: a brief review of the history, possibilities, and challenges ahead. *Cancer immunotherapy: a brief review of the history, possibilities, and challenges ahead* **3**, 250-261, doi:10.20517/2394-4722.2017.41 (2017).

33 Coley, W. B. The Treatment of Sarcoma with the Mixed Toxins of Erysipelas and Bacillus Prodigiosus. *The Boston Medical and Surgical Journal* **158**, 175-182, doi:10.1056/nejm190802061580601 (1908).

34 Waldman, A. D., Fritz, J. M. & Lenardo, M. J. A guide to cancer immunotherapy: from T cell basic science to clinical practice. **20**, 651-668, doi:10.1038/s41577-020-0306-5 (2020).

35 Barber, D. L. *et al.* Restoring function in exhausted CD8 T cells during chronic viral infection. *Nature* **439**, 682-687, doi:10.1038/nature04444 (2006).

36 Shiravand, Y., Khodadadi, F. & Kashani, S. M. A. Immune Checkpoint Inhibitors in Cancer Therapy. **29**, 3044-3060, doi:10.3390/curroncol29050247 (2022).

37 Bjoern, J. *et al.* Influence of ipilimumab on expanded tumour derived T cells from patients with metastatic melanoma. *Oncotarget* **8**, 27062-27074, doi:10.18632/oncotarget.16003 (2017).

38 Topp, M. S. *et al.* Long-term follow-up of hematologic relapse-free survival in a phase 2 study of blinatumomab in patients with MRD in B-lineage ALL. *Blood* **120**, 5185-5187, doi:10.1182/blood-2012-07-441030 (2012).

39 Syed, Y. Y. Amivantamab: First Approval. *Drugs* **81**, 1349-1353, doi:10.1007/s40265-021-01561-7 (2021).

40 Ordóñez-Reyes, C. & Garcia-Robledo, J. E. Bispecific Antibodies in Cancer Immunotherapy: A Novel Response to an Old Question. **14**, doi:10.3390/pharmaceutics14061243 (2022).

41 Gross, G., Waks, T. & Eshhar, Z. Expression of immunoglobulin-T-cell receptor chimeric molecules as functional receptors with antibody-type specificity. *Proc Natl Acad Sci U S A* **86**, 10024-10028, doi:10.1073/pnas.86.24.10024 (1989).

42 FDA. *U.S. Food and Drug Administration. Approved Cellular and Gene Therapy Products*, <https: //www. fda. gov/ vaccines-blood-biologics/ cellular-gene-therapy-products/ approved-cellular-and-gene-therapy-products> (accessed June 15, 2023).

43 Wang, V., Gauthier, M., Decot, V. & Reppel, L. Systematic Review on CAR-T Cell Clinical Trials Up to 2022: Academic Center Input. **15**, doi:10.3390/cancers15041003 (2023).

44 Rosenberg, S. Lymphokine-activated killer cells: a new approach to immunotherapy of cancer. *Journal of the National Cancer Institute* **75**, 595-603, doi:10.1093/jnci/75.4.595 (1985).

45 Rosenberg, S. A. *et al.* Use of tumor-infiltrating lymphocytes and interleukin-2 in the immunotherapy of patients with metastatic melanoma. A preliminary report. *The New England journal of medicine* **319**, 1676-1680, doi:10.1056/nejm198812223192527 (1988).

46 Zhao, Y. *et al.* Tumor Infiltrating Lymphocyte (TIL) Therapy for Solid Tumor Treatment: Progressions and Challenges. *Cancers (Basel)* **14**, doi:10.3390/cancers14174160 (2022).

47 Heemskerk, B. *et al.* Adoptive cell therapy for patients with melanoma, using tumor-infiltrating lymphocytes genetically engineered to secrete interleukin-2. *Human gene therapy* **19**, 496-510, doi:10.1089/hum.2007.0171 (2008).

48 Baulu, E. & Gardet, C. TCR-engineered T cell therapy in solid tumors: State of the art and perspectives. *Sci Adv.* **9**, doi:10.1126/sciadv.adf3700 (2023).

49 Johnson, L. A. *et al.* Gene therapy with human and mouse T-cell receptors mediates cancer regression and targets normal tissues expressing cognate antigen. *Blood* **114**, 535-546, doi:10.1182/blood-2009-03-211714 (2009).

50 Parkhurst, M. R. *et al.* T cells targeting carcinoembryonic antigen can mediate regression of metastatic colorectal cancer but induce severe transient colitis. *Mol Ther* **19**, 620-626, doi:10.1038/mt.2010.272 (2011).

51 Morgan, R. A. *et al.* Cancer regression and neurological toxicity following anti-MAGE-A3 TCR gene therapy. *Journal of immunotherapy* **36**, 133-151, doi:10.1097/CJI.0b013e3182829903 (2013).

52 Linette, G. P. *et al.* Cardiovascular toxicity and titin cross-reactivity of affinity-enhanced T cells in myeloma and melanoma. *Blood* **122**, 863-871, doi:10.1182/blood-2013-03-490565 (2013).

53 Wei, F., Cheng, X. X., Xue, J. Z. & Xue, S. A. Emerging Strategies in TCR-Engineered T Cells. *Frontiers in immunology* **13**, 850358, doi:10.3389/fimmu.2022.850358 (2022).

54 Davis, M. M. & Bjorkman, P. J. T-cell antigen receptor genes and T-cell recognition. *Nature* **334**, 395-402, doi:10.1038/334395a0 (1988).

55 Iwasaki, M. *et al.* Expression and function of PD-1 in human gammadelta T cells that recognize phosphoantigens. *European journal of immunology* **41**, 345-355, doi:10.1002/eji.201040959 (2011).

56 Park, J. H. & Lee, H. K. Function of γδ T cells in tumor immunology and their application to cancer therapy. *Exp Mol Med* **53**, 318-327, doi:10.1038/s12276-021-00576-0 (2021).

57 Girardi, M. *et al.* Regulation of cutaneous malignancy by gammadelta T cells. *Science (New York, N.Y.)* **294**, 605-609, doi:10.1126/science.1063916 (2001).

58 Street, S. E. *et al.* Innate immune surveillance of spontaneous B cell lymphomas by natural killer cells and gammadelta T cells. *The Journal of experimental medicine* **199**, 879-884, doi:10.1084/jem.20031981 (2004).

59 Liu, Z. *et al.* Protective immunosurveillance and therapeutic antitumor activity of gammadelta T cells demonstrated in a mouse model of prostate cancer. *Journal of immunology (Baltimore, Md. : 1950)* **180**, 6044-6053, doi:10.4049/jimmunol.180.9.6044 (2008).

60 Makkouk, A. *et al.* Off-the-shelf Vδ1 gamma delta T cells engineered with glypican-3 (GPC-3)-specific chimeric antigen receptor (CAR) and soluble IL-15 display robust antitumor efficacy against hepatocellular carcinoma. *Journal for ImmunoTherapy of Cancer* **9**, e003441, doi:10.1136/jitc-2021-003441 (2021).

61 Capsomidis, A. *et al.* Chimeric Antigen Receptor-Engineered Human Gamma Delta T Cells: Enhanced Cytotoxicity with Retention of Cross Presentation. *Mol Ther* **26**, 354-365, doi:10.1016/j.ymthe.2017.12.001 (2018).

62 Rozenbaum, M. *et al.* Gamma-Delta CAR-T Cells Show CAR-Directed and Independent Activity Against Leukemia. *Frontiers in immunology* **11**, 1347, doi:10.3389/fimmu.2020.01347 (2020).

63 Rudolph, M. G., Stanfield, R. L. & Wilson, I. A. How TCRs bind MHCs, peptides, and coreceptors. *Annu Rev Immunol* **24**, 419-466, doi:10.1146/annurev.immunol.23.021704.115658 (2006).

64 Crux, N. B. & Elahi, S. Human Leukocyte Antigen (HLA) and Immune Regulation: How Do Classical and Non-Classical HLA Alleles Modulate Immune Response to Human Immunodeficiency Virus and Hepatitis C Virus Infections? *Frontiers in immunology* **8**, 832, doi:10.3389/fimmu.2017.00832 (2017).

65 Choo, S. Y. The HLA system: genetics, immunology, clinical testing, and clinical implications. *Yonsei medical journal* **48**, 11-23, doi:10.3349/ymj.2007.48.1.11 (2007).

66 Marsh, S. G. E. *et al.* Nomenclature for factors of the HLA system, 2004. *Tissue antigens* **65**, 301-369, doi:10.1111/j.1399-0039.2005.00379.x (2005).

67 Wong, W. K., Leem, J. & Deane, C. M. Comparative Analysis of the CDR Loops of Antigen Receptors. *Frontiers in immunology* **10**, 2454, doi:10.3389/fimmu.2019.02454 (2019).

68 Rock, E. P., Sibbald, P. R., Davis, M. M. & Chien, Y. H. CDR3 length in antigen-specific immune receptors. *The Journal of experimental medicine* **179**, 323-328, doi:10.1084/jem.179.1.323 (1994).

69 Blevins, S. J. *et al.* How structural adaptability exists alongside HLA-A2 bias in the human alphabeta TCR repertoire. *Proc Natl Acad Sci U S A* **113**, E1276-1285, doi:10.1073/pnas.1522069113 (2016).

70 Yarmarkovich, M. *et al.* Cross-HLA targeting of intracellular oncoproteins with peptide-centric CARs. *Nature* **599**, 477-484, doi:10.1038/s41586-021-04061-6 (2021).

71 Zhang, G. *et al.* Anti-melanoma activity of T cells redirected with a TCR-like chimeric antigen receptor. *Scientific reports* **4**, 3571, doi:10.1038/srep03571 (2014).

72 Liu, H. *et al.* Targeting Alpha-Fetoprotein (AFP)-MHC Complex with CAR T-Cell Therapy for Liver Cancer. *Clin Cancer Res* **23**, 478-488, doi:10.1158/1078-0432.CCR-16-1203 (2017).

73 Rafiq, S. *et al.* Optimized T-cell receptor-mimic chimeric antigen receptor T cells directed toward the intracellular Wilms Tumor 1 antigen. *Leukemia* **31**, 1788-1797, doi:10.1038/leu.2016.373 (2017).

74 Schamel, W. W. A. The stoichiometry of the T cell antigen receptor and its implications for the signal transduction mechanism. *Signal Transduction* **7**, 311-319, doi:10.1002/sita.200600123 (2007).

75 Wucherpfennig, K. W., Gagnon, E., Call, M. J., Huseby, E. S. & Call, M. E. Structural biology of the T-cell receptor: insights into receptor assembly, ligand recognition, and initiation of signaling. *Cold Spring Harbor perspectives in biology* **2**, a005140, doi:10.1101/cshperspect.a005140 (2010).

76 Kersh, E. N., Shaw, A. S. & Allen, P. M. Fidelity of T cell activation through multistep T cell receptor zeta phosphorylation. *Science (New York, N.Y.)* **281**, 572-575, doi:10.1126/science.281.5376.572 (1998).

77 James, J. R. Tuning ITAM multiplicity on T cell receptors can control potency and selectivity to ligand density. *Sci Signal* **11**, eaan1088, doi:10.1126/scisignal.aan1088 (2018).

78 Salter, A. I. & Rajan, A. Comparative analysis of TCR and CAR signaling informs CAR designs with superior antigen sensitivity and in vivo function. **14**, doi:10.1126/scisignal.abe2606 (2021).

79 Baeuerle, P. A. *et al.* Synthetic TRuC receptors engaging the complete T cell receptor for potent anti-tumor response. *Nature communications* **10**, 2087, doi:10.1038/s41467-019-10097-0 (2019).

80 Liu, Y. *et al.* Chimeric STAR receptors using TCR machinery mediate robust responses against solid tumors. *Science Translational Medicine* **13**, eabb5191, doi:10.1126/scitranslmed.abb5191 (2021).

81 Mansilla-Soto, J. *et al.* HLA-independent T cell receptors for targeting tumors with low antigen density. *Nature medicine* **28**, 345-352, doi:10.1038/s41591-021-01621-1 (2022).

82 Gudipati, V. *et al.* Inefficient CAR-proximal signaling blunts antigen sensitivity. *Nat Immunol* **21**, 848-856, doi:10.1038/s41590-020-0719-0 (2020).

83 Burton, J. *et al.* Inefficient exploitation of accessory receptors reduces the sensitivity of chimeric antigen receptors. *Proc Natl Acad Sci U S A* **120**, e2216352120, doi:10.1073/pnas.2216352120 (2023).

84 Till, B. G. *et al.* Adoptive immunotherapy for indolent non-Hodgkin lymphoma and mantle cell lymphoma using genetically modified autologous CD20-specific T cells. *Blood* **112**, 2261-2271, doi:10.1182/blood-2007-12-128843 (2008).

85 Etxeberria, I. *et al.* Engineering bionic T cells: signal 1, signal 2, signal 3, reprogramming and the removal of inhibitory mechanisms. *Cellular & molecular immunology* **17**, 576-586, doi:10.1038/s41423-020-0464-1 (2020).

86 Guedan, S. *et al.* Enhancing CAR T cell persistence through ICOS and 4-1BB costimulation. *JCI insight* **3**, doi:10.1172/jci.insight.96976 (2018).

87 Maher, J., Brentjens, R. J., Gunset, G., Rivière, I. & Sadelain, M. Human T-lymphocyte cytotoxicity and proliferation directed by a single chimeric TCRζ /CD28 receptor. *Nature Biotechnology* **20**, 70-75, doi:10.1038/nbt0102-70 (2002).

88 Porter, D. L., Levine, B. L., Kalos, M., Bagg, A. & June, C. H. Chimeric antigen receptor-modified T cells in chronic lymphoid leukemia. *The New England journal of medicine* **365**, 725-733, doi:10.1056/NEJMoa1103849 (2011).

89 Krause, A. *et al.* Antigen-dependent CD28 signaling selectively enhances survival and proliferation in genetically modified activated human primary T lymphocytes. *The Journal of experimental medicine* **188**, 619-626, doi:10.1084/jem.188.4.619 (1998).

90 Schubert, M.-L. *et al.* Third-Generation CAR T Cells Targeting CD19 Are Associated with an Excellent Safety Profile and Might Improve Persistence of CAR T Cells in Treated Patients. *Blood* **134**, 51-51, doi:10.1182/blood-2019-125423 (2019).

91 Hombach, A. *et al.* IL12 integrated into the CAR exodomain converts CD8(+) T cells to poly-functional NK-like cells with superior killing of antigen-loss tumors. *Mol Ther* **30**, 593-605, doi:10.1016/j.ymthe.2021.10.011 (2022).

92 Kueberuwa, G., Kalaitsidou, M., Cheadle, E., Hawkins, R. E. & Gilham, D. E. CD19 CAR T Cells Expressing IL-12 Eradicate Lymphoma in Fully Lymphoreplete Mice through Induction of Host Immunity. *Molecular therapy oncolytics* **8**, 41-51, doi:10.1016/j.omto.2017.12.003 (2018).

93 Kagoya, Y., Tanaka, S. & Guo, T. A novel chimeric antigen receptor containing a JAK-STAT signaling domain mediates superior antitumor effects. **24**, 352-359, doi:10.1038/nm.4478 (2018).

94 Umut, Ö., Gottschlich, A., Endres, S. & Kobold, S. CAR T cell therapy in solid tumors: a short review. *memo - Magazine of European Medical Oncology* **14**, 143-149, doi:10.1007/s12254-021-00703-7 (2021).

95 Iwashima, M., Irving, B. A., van Oers, N. S., Chan, A. C. & Weiss, A. Sequential interactions of the TCR with two distinct cytoplasmic tyrosine kinases. *Science (New York, N.Y.)* **263**, 1136-1139, doi:10.1126/science.7509083 (1994).

96 Barber, E. K., Dasgupta, J. D., Schlossman, S. F., Trevillyan, J. M. & Rudd, C. E. The CD4 and CD8 antigens are coupled to a protein-tyrosine kinase (p56lck) that phosphorylates the CD3 complex. *Proc Natl Acad Sci U S A* **86**, 3277-3281, doi:10.1073/pnas.86.9.3277 (1989).

97 Weiss, A. T cell antigen receptor signal transduction: a tale of tails and cytoplasmic protein-tyrosine kinases. *Cell* **73**, 209-212, doi:10.1016/0092-8674(93)90221-b (1993).

98 Zhang, W., Sloan-Lancaster, J., Kitchen, J., Trible, R. P. & Samelson, L. E. LAT: the ZAP-70 tyrosine kinase substrate that links T cell receptor to cellular activation. *Cell* **92**, 83-92, doi:10.1016/s0092-8674(00)80901-0 (1998).

99 Bubeck Wardenburg, J. *et al.* Phosphorylation of SLP-76 by the ZAP-70 protein-tyrosine kinase is required for T-cell receptor function. *The Journal of biological chemistry* **271**, 19641-19644, doi:10.1074/jbc.271.33.19641 (1996).

100 Shah, K., Al-Haidari, A., Sun, J. & Kazi, J. U. T cell receptor (TCR) signaling in health and disease. **6**, 412, doi:10.1038/s41392-021-00823-w (2021).

101 Bonvini, E. *et al.* A role for guanine-nucleotide-binding proteins in mediating T-cell-receptor coupling to inositol phospholipid hydrolysis in a murine T-helper (type II) lymphocyte clone. *The Biochemical journal* **275 (Pt 3)**, 689-696, doi:10.1042/bj2750689 (1991).

102 Lewis, R. S. Calcium signaling mechanisms in T lymphocytes. *Annual Review of Immunology* **19**, 497-521, doi:10.1146/annurev.immunol.19.1.497 (2001).

103 Hogan, P. G., Chen, L., Nardone, J. & Rao, A. Transcriptional regulation by calcium, calcineurin, and NFAT. *Genes Dev* **17**, 2205-2232, doi:10.1101/gad.1102703 (2003).

104 Monaco, S. & Jahraus, B. Nuclear calcium is required for human T cell activation. *J Cell Biol.* **215**, 231-243, doi:10.1083/jcb.201602001 (2016).

105 Blanchett, S., Boal-Carvalho, I., Layzell, S. & Seddon, B. NF-κB and Extrinsic Cell Death Pathways - Entwined Do-or-Die Decisions for T cells. *Trends Immunol* **42**, 76-88, doi:10.1016/j.it.2020.10.013 (2021).

106 Harris, D. T. *et al.* Comparison of T Cell Activities Mediated by Human TCRs and CARs That Use the Same Recognition Domains. *Journal of immunology (Baltimore, Md. : 1950)* **200**, 1088-1100, doi:10.4049/jimmunol.1700236 (2018).

107 Anikeeva, N. *et al.* Efficient killing of tumor cells by CAR-T cells requires greater number of engaged CARs than TCRs. *Journal of Biological Chemistry* **297**, 101033, doi:10.1016/j.jbc.2021.101033 (2021).

108 Wang, J. *et al.* A novel adoptive synthetic TCR and antigen receptor (STAR) T-Cell therapy for B-Cell acute lymphoblastic leukemia. *American journal of hematology*, doi:10.1002/ajh.26586 (2022).

109 Watanabe, K., Kuramitsu, S., Posey, A. D., Jr. & June, C. H. Expanding the Therapeutic Window for CAR T Cell Therapy in Solid Tumors: The Knowns and Unknowns of CAR T Cell Biology. *Frontiers in immunology* **9**, 2486, doi:10.3389/fimmu.2018.02486 (2018).

110 Dong, R. *et al.* Rewired signaling network in T cells expressing the chimeric antigen receptor (CAR). *The EMBO journal* **39**, doi:10.15252/embj.2020104730 (2020).

111 Davenport, A. J. *et al.* Chimeric antigen receptor T cells form nonclassical and potent immune synapses driving rapid cytotoxicity. *Proceedings of the National Academy of Sciences* **115**, E2068-E2076, doi:10.1073/pnas.1716266115 (2018).

112 Freiberg, B. A. *et al.* Staging and resetting T cell activation in SMACs. *Nat Immunol* **3**, 911-917, doi:10.1038/ni836 (2002).

113 Graf, B., Bushnell, T. & Miller, J. LFA-1-mediated T cell costimulation through increased localization of TCR/class II complexes to the central supramolecular activation cluster and exclusion of CD45 from the immunological synapse. *Journal of immunology (Baltimore, Md. : 1950)* **179**, 1616-1624, doi:10.4049/jimmunol.179.3.1616 (2007).

114 Stinchcombe, J. C., Majorovits, E., Bossi, G., Fuller, S. & Griffiths, G. M. Centrosome polarization delivers secretory granules to the immunological synapse. *Nature* **443**, 462-465, doi:10.1038/nature05071 (2006).

115 James, J. R. & Vale, R. D. Biophysical Mechanism of T Cell Receptor Triggering in a Reconstituted System. *Nature* **487**, 64-69, doi:10.1038/nature11220 (2012).

116 Saoudi, A., Kassem, S., Dejean, A. & Gaud, G. Rho-GTPases as key regulators of T lymphocyte biology. *Small GTPases* **5**, doi:10.4161/sgtp.28208 (2014).

117 Gaud, G., Lesourne, R. & Love, P. E. Regulatory mechanisms in T cell receptor signalling. *Nature reviews. Immunology* **18**, 485-497, doi:10.1038/s41577-018-0020-8 (2018).

118 Teppert, K. *et al.* Joining Forces for Cancer Treatment: From "TCR versus CAR" to "TCR and CAR". *Int J Mol Sci* **23**, 14563, doi:10.3390/ijms232314563 (2022).

119 Meng, X., Jing, R., Qian, L., Zhou, C. & Sun, J. Engineering Cytoplasmic Signaling of CD28ζ CARs for Improved Therapeutic Functions. *Frontiers in immunology* **11**, doi:10.3389/fimmu.2020.01046 (2020).

120 Bridgeman, J. S. *et al.* The optimal antigen response of chimeric antigen receptors harboring the CD3zeta transmembrane domain is dependent upon incorporation of the receptor into the endogenous TCR/CD3 complex. *Journal of immunology (Baltimore, Md. : 1950)* **184**, 6938-6949, doi:10.4049/jimmunol.0901766 (2010).

121 Stenger, D. *et al.* Endogenous TCR promotes in vivo persistence of CD19-CAR-T cells compared to a CRISPR/Cas9-mediated TCR knockout CAR. *Blood*, doi:10.1182/blood.2020005185 (2020).

122 Pule, M. A. *et al.* Virus-specific T cells engineered to coexpress tumor-specific receptors: persistence and antitumor activity in individuals with neuroblastoma. *Nature medicine* **14**, 1264-1270, doi:10.1038/nm.1882 (2008).

123 Louis, C. U. *et al.* Antitumor activity and long-term fate of chimeric antigen receptor-positive T cells in patients with neuroblastoma. *Blood* **118**, 6050-6056, doi:10.1182/blood-2011-05-354449 (2011).

124 Lapteva, N. *et al.* T-Cell Receptor Stimulation Enhances the Expansion and Function of CD19 Chimeric Antigen Receptor–Expressing T Cells. *Clinical Cancer Research* **25**, 7340-7350, doi:10.1158/1078-0432.ccr-18-3199 (2019).

125 Cruz, C. R. *et al.* Infusion of donor-derived CD19-redirected virus-specific T cells for B-cell malignancies relapsed after allogeneic stem cell transplant: a phase 1 study. *Blood* **122**, 2965-2973, doi:10.1182/blood-2013-06-506741 (2013).

126 Tanaka, M. *et al.* Vaccination Targeting Native Receptors to Enhance the Function and Proliferation of Chimeric Antigen Receptor (CAR)-Modified T Cells. *Clin Cancer Res* **23**, 3499-3509, doi:10.1158/1078-0432.ccr-16-2138 (2017).

127 Omer, B. *et al.* Chimeric Antigen Receptor Signaling Domains Differentially Regulate Proliferation and Native T Cell Receptor Function in Virus-Specific T Cells. *Frontiers in medicine* **5**, 343, doi:10.3389/fmed.2018.00343 (2018).

128 Zhao, X. *et al.* Efficacy and Safety of CD28- or 4-1BB-Based CD19 CAR-T Cells in B Cell Acute Lymphoblastic Leukemia. *Molecular Therapy - Oncolytics* **18**, 272-281, doi:10.1016/j.omto.2020.06.016 (2020).

129 Ying, Z. *et al.* Parallel Comparison of 4-1BB or CD28 Co-stimulated CD19-Targeted CAR-T Cells for B Cell Non-Hodgkin's Lymphoma. *Molecular therapy oncolytics* **15**, 60-68, doi:10.1016/j.omto.2019.08.002 (2019).

130 van der Stegen, S. J., Hamieh, M. & Sadelain, M. The pharmacology of second-generation chimeric antigen receptors. *Nature reviews. Drug discovery* **14**, 499-509, doi:10.1038/nrd4597 (2015).

131 Yang, Y. *et al.* TCR engagement negatively affects CD8 but not CD4 CAR T cell expansion and leukemic clearance. *Science Translational Medicine* **9**, doi:10.1126/scitranslmed.aag1209 (2017).

132 Evgin, L. & Kottke, T. Oncolytic virus-mediated expansion of dual-specific CAR T cells improves efficacy against solid tumors in mice. **14**, doi:10.1126/scitranslmed.abn2231 (2022).

133 Brossart, P. The Role of Antigen Spreading in the Efficacy of Immunotherapies. *Clinical Cancer Research* **26**, 4442-4447, doi:10.1158/1078-0432.ccr-20-0305 (2020).

134 Slaney, C. Y. *et al.* Dual-specific Chimeric Antigen Receptor T Cells and an Indirect Vaccine Eradicate a Variety of Large Solid Tumors in an Immunocompetent, Self-antigen Setting. *Clinical Cancer Research* **23**, 2478-2490, doi:10.1158/1078-0432.ccr-16-1860 (2017).

135 Sallusto, F., Lenig, D., Förster, R., Lipp, M. & Lanzavecchia, A. Two subsets of memory T lymphocytes with distinct homing potentials and effector functions. *Nature* **401**, 708-712, doi:10.1038/44385 (1999).

136 Klebanoff, C. A. *et al.* Central memory self/tumor-reactive CD8+ T cells confer superior antitumor immunity compared with effector memory T cells. *Proc Natl Acad Sci U S A* **102**, 9571-9576, doi:10.1073/pnas.0503726102 (2005).

137 Kueberuwa, G. *et al.* CCR7(+) selected gene-modified T cells maintain a central memory phenotype and display enhanced persistence in peripheral blood in vivo. *J Immunother Cancer* **5**, 14, doi:10.1186/s40425-017-0216-7 (2017).

138 Simon, B., Harrer, D. C., Schuler-Thurner, B., Schuler, G. & Uslu, U. Arming T Cells with a gp100-Specific TCR and a CSPG4-Specific CAR Using Combined DNA- and RNA-Based Receptor Transfer. *Cancers* **11**, 696, doi:10.3390/cancers11050696 (2019).

139 Uslu, U., Schuler, G., Dörrie, J. & Schaft, N. Combining a chimeric antigen receptor and a conventional T-cell receptor to generate T cells expressing two additional receptors (TETARs) for a multi-hit immunotherapy of melanoma. *Experimental Dermatology* **25**, 872-879, doi:doi:10.1111/exd.13095 (2016).

140 Ruella, M. & Maus, M. V. Catch me if you can: Leukemia Escape after CD19-Directed T Cell Immunotherapies. *Comput Struct Biotechnol J* **14**, 357-362, doi:10.1016/j.csbj.2016.09.003 (2016).

141 Hirabayashi, K. *et al.* Dual Targeting CAR-T Cells with Optimal Costimulation and Metabolic Fitness enhance Antitumor Activity and Prevent Escape in Solid Tumors. *Nat Cancer* **2**, 904-918, doi:10.1038/s43018-021-00244-2 (2021).

142 Hegde, M. *et al.* Tandem CAR T cells targeting HER2 and IL13Rα2 mitigate tumor antigen escape. *The Journal of Clinical Investigation* **126**, 3036-3052, doi:10.1172/JCI83416 (2016).

143 Garber, K. Driving T-cell immunotherapy to solid tumors. *Nature Biotechnology* **36**, 215-219, doi:10.1038/nbt.4090 (2018).

144 Miyao, K. *et al.* Introduction of Genetically Modified CD3ζ Improves Proliferation and Persistence of Antigen-Specific CTLs. *Cancer Immunology Research* **6**, 733-744, doi:10.1158/2326-6066.cir-17-0538 (2018).

145 Lowenberg, B., Downing, J. R. & Burnett, A. Acute Myeloid Leukemia. *New England Journal of Medicine* **341**, 1051-1062, doi:10.1056/nejm199909303411407 (1999).

146 Pelcovits, A. & Niroula, R. Acute Myeloid Leukemia: A Review. *Rhode Island medical journal (2013)* **103**, 38-40 (2020).

147 Papaemmanuil, E. *et al.* Genomic Classification and Prognosis in Acute Myeloid Leukemia. *New England Journal of Medicine* **374**, 2209-2221, doi:10.1056/NEJMoa1516192 (2016).

148 Hollstein, M., Sidransky, D., Vogelstein, B. & Harris, C. C. p53 mutations in human cancers. *Science (New York, N.Y.)* **253**, 49-53, doi:10.1126/science.1905840 (1991).

149 Arber, D. A. *et al.* The 2016 revision to the World Health Organization classification of myeloid neoplasms and acute leukemia. *Blood* **127**, 2391-2405, doi:10.1182/blood-2016-03-643544 (2016).

150 Marvin-Peek, J., Savani, B. N., Olalekan, O. O. & Dholaria, B. Challenges and Advances in Chimeric Antigen Receptor Therapy for Acute Myeloid Leukemia. *Cancers* **14**, 497, doi:10.3390/cancers14030497 (2022).

151 Takami, A. Hematopoietic stem cell transplantation for acute myeloid leukemia. *International journal of hematology* **107**, 513-518, doi:10.1007/s12185-018-2412-8 (2018).

152 Mathé, G. *et al.* Successful Allogenic Bone Marrow Transplantation in Man: Chimerism, Induced Specific Tolerance and Possible Anti-Leukemic Effects. *Blood* **25**, 179-196, doi:10.1182/blood.V25.2.179.179 (1965).

153 Chalmers, Z. R. *et al.* Analysis of 100,000 human cancer genomes reveals the landscape of tumor mutational burden. *Genome Medicine* **9**, 34, doi:10.1186/s13073-017-0424-2 (2017).

154 Atilla, E. & Benabdellah, K. The Black Hole: CAR T Cell Therapy in AML. *Cancers (Basel)* **15**, doi:10.3390/cancers15102713 (2023).

155 Kenderian, S. S. *et al.* CD33-specific chimeric antigen receptor T cells exhibit potent preclinical activity against human acute myeloid leukemia. *Leukemia* **29**, 1637-1647, doi:10.1038/leu.2015.52 (2015).

156 Kelm, S., Schauer, R. & Crocker, P. R. The Sialoadhesins--a family of sialic acid-dependent cellular recognition molecules within the immunoglobulin superfamily. *Glycoconjugate journal* **13**, 913-926, doi:10.1007/BF01053186 (1996).

157 Pizzitola, I. *et al.* Chimeric antigen receptors against CD33/CD123 antigens efficiently target primary acute myeloid leukemia cells in vivo. *Leukemia* **28**, 1596-1605, doi:10.1038/leu.2014.62 (2014).

158 Sievers, E. L. *et al.* Efficacy and safety of gemtuzumab ozogamicin in patients with CD33-positive acute myeloid leukemia in first relapse. *Journal of clinical oncology : official journal of the American Society of Clinical Oncology* **19**, 3244-3254, doi:10.1200/jco.2001.19.13.3244 (2001).

159 Kell, W. J. *et al.* A feasibility study of simultaneous administration of gemtuzumab ozogamicin with intensive chemotherapy in induction and consolidation in younger patients with acute myeloid leukemia. *Blood* **102**, 4277-4283, doi:10.1182/blood-2003-05-1620 (2003).

160 Kang, S. *et al.* Antigen-Specific TCR-T Cells for Acute Myeloid Leukemia: State of the Art and Challenges. *Frontiers in Oncology* **12**, doi:10.3389/fonc.2022.787108 (2022).

161 Van der Lee, D. I. *et al.* Mutated nucleophosmin 1 as immunotherapy target in acute myeloid leukemia. *The Journal of Clinical Investigation* **129**, 774-785, doi:10.1172/JCI97482 (2019).

162 Morris, E. C. & Neelapu, S. S. Cytokine release syndrome and associated neurotoxicity in cancer immunotherapy. **22**, 85-96, doi:10.1038/s41577-021-00547-6 (2022).

163 Limongello, R. *et al.* Novel Immune Cell-Based Therapies to Eradicate High-Risk Acute Myeloid Leukemia. *Frontiers in immunology* **12**, doi:10.3389/fimmu.2021.695051 (2021).

164 Liu, F. *et al.* First-in-Human CLL1-CD33 Compound CAR T Cell Therapy Induces Complete Remission in Patients with Refractory Acute Myeloid Leukemia: Update on Phase 1 Clinical Trial. *Blood* **132**, 901-901, doi:10.1182/blood-2018-99-110579 (2018).

165 Tettamanti, S., Pievani, A., Biondi, A., Dotti, G. & Serafini, M. Catch me if you can: how AML and its niche escape immunotherapy. *Leukemia* **36**, 13-22, doi:10.1038/s41375-021-01350-x (2022).

166 Zhou, Q. *et al.* Depletion of endogenous tumor-associated regulatory T cells improves the efficacy of adoptive cytotoxic T-cell immunotherapy in murine acute myeloid leukemia. *Blood* **114**, 3793-3802, doi:10.1182/blood-2009-03-208181 (2009).

167 Uy, G. L. *et al.* A phase 1/2 study of chemosensitization with the CXCR4 antagonist plerixafor in relapsed or refractory acute myeloid leukemia. *Blood* **119**, 3917-3924, doi:10.1182/blood-2011-10-383406 (2012).

168 Wang, Y. *et al.* Effective response and delayed toxicities of refractory advanced diffuse large B-cell lymphoma treated by CD20-directed chimeric antigen receptor-modified T cells. *Clin Immunol* **155**, 160-175, doi:10.1016/j.clim.2014.10.002 (2014).

169 Zhang, W.-y. *et al.* Treatment of CD20-directed Chimeric Antigen Receptor-modified T cells in patients with relapsed or refractory B-cell non-Hodgkin lymphoma: an early phase IIa trial report. *Signal Transduction and Targeted Therapy* **1**, 16002, doi:10.1038/sigtrans.2016.2 (2016).

170 Ansorge, S. *et al.* Development of a scalable process for high-yield lentiviral vector production by transient transfection of HEK293 suspension cultures. *The journal of gene medicine* **11**, 868-876, doi:10.1002/jgm.1370 (2009).

171 Purbhoo, M. A. *et al.* The human CD8 coreceptor effects cytotoxic T cell activation and antigen sensitivity primarily by mediating complete phosphorylation of the T cell receptor zeta chain. *The Journal of biological chemistry* **276**, 32786-32792, doi:10.1074/jbc.M102498200 (2001).

172 Melenhorst, J. J. *et al.* Decade-long leukaemia remissions with persistence of CD4(+) CAR T cells. *Nature* **602**, 503-509, doi:10.1038/s41586-021-04390-6 (2022).

173 Teppert, K. *et al.* CAR'TCR-T cells co-expressing CD33-CAR and dNPM1-TCR as superior dual-targeting approach for AML treatment. *Molecular Therapy Oncology* **32**, doi:10.1016/j.omton.2024.200797 (2024).

174 Alexa, A., Rahnenführer, J. & Lengauer, T. Improved scoring of functional groups from gene expression data by decorrelating GO graph structure. *Bioinformatics (Oxford, England)* **22**, 1600-1607, doi:10.1093/bioinformatics/btl140 (2006).

175 Croft, D. *et al.* Reactome: a database of reactions, pathways and biological processes. *Nucleic acids research* **39**, D691-697, doi:10.1093/nar/gkq1018 (2011).

176 Yu, G. & He, Q.-Y. ReactomePA: an R/Bioconductor package for reactome pathway analysis and visualization. *Molecular bioSystems* **12**, 477-479, doi:10.1039/c5mb00663e (2016).

177 Krawczyk, C. & Penninger, J. M. Molecular motors involved in T cell receptor clusterings. *Journal of leukocyte biology* **69**, 317-330, doi:doi:10.1189/jlb.69.3.317 (2001).

178 Cinalli, R. M. *et al.* T cell homeostasis requires G protein-coupled receptor-mediated access to trophic signals that promote growth and inhibit chemotaxis. *European journal of immunology* **35**, 786-795, doi:10.1002/eji.200425729 (2005).

179 Coffield, V. M., Helms, W. S., Jiang, Q. & Su, L. Galpha13 mediates a signal that is essential for proliferation and survival of thymocyte progenitors. *The Journal of experimental medicine* **200**, 1315-1324, doi:10.1084/jem.20040944 (2004).

180 Molon, B. *et al.* T cell costimulation by chemokine receptors. *Nat Immunol* **6**, 465-471, doi:10.1038/ni1191 (2005).

181 Felce, J. H. *et al.* Single-Molecule, Super-Resolution, and Functional Analysis of G Protein-Coupled Receptor Behavior Within the T Cell Immunological Synapse. *Front Cell Dev Biol* **8**, 608484, doi:10.3389/fcell.2020.608484 (2020).

182 Wang, D. The essential role of G protein-coupled receptor (GPCR) signaling in regulating T cell immunity. *Immunopharmacology and immunotoxicology* **40**, 187-192, doi:10.1080/08923973.2018.1434792 (2018).

183 Ngai, J. *et al.* The heterotrimeric G-protein alpha-subunit Galphaq regulates TCR-mediated immune responses through an Lck-dependent pathway. *European journal of immunology* **38**, 3208-3218, doi:10.1002/eji.200838195 (2008).

184 Maude, S. L. *et al.* Chimeric Antigen Receptor T Cells for Sustained Remissions in Leukemia. *New England Journal of Medicine* **371**, 1507-1517, doi:10.1056/NEJMoa1407222 (2014).

185 Neelapu, S. S. *et al.* Axicabtagene Ciloleucel CAR T-Cell Therapy in Refractory Large B-Cell Lymphoma. *New England Journal of Medicine* **377**, 2531-2544, doi:10.1056/NEJMoa1707447 (2017).

186 Brown, C. E. *et al.* Regression of Glioblastoma after Chimeric Antigen Receptor T-Cell Therapy. *New England Journal of Medicine* **375**, 2561-2569, doi:10.1056/NEJMoa1610497 (2016).

187 O'Rourke, D. M. *et al.* A single dose of peripherally infused EGFRvIII-directed CAR T cells mediates antigen loss and induces adaptive resistance in patients with recurrent glioblastoma. *Sci Transl Med* **9**, eaaa0984, doi:10.1126/scitranslmed.aaa0984 (2017).

188 Brudno, J. N. *et al.* T Cells Expressing a Novel Fully-Human Anti-CD19 Chimeric Antigen Receptor Induce Remissions of Advanced Lymphoma in a First-in-Humans Clinical Trial. *Blood* **128**, 999-999, doi:10.1182/blood.V128.22.999.999 (2016).

189 Manz, B. N., Jackson, B. L., Petit, R. S., Dustin, M. L. & Groves, J. T-cell triggering thresholds are modulated by the number of antigen within individual T-cell receptor clusters. *Proc Natl Acad Sci U S A* **108**, 9089-9094, doi:10.1073/pnas.1018771108 (2011).

190 Roszkowski, J. J. *et al.* CD8-Independent Tumor Cell Recognition Is a Property of the T Cell Receptor and Not the T Cell 1. *The Journal of Immunology* **170**, 2582-2589, doi:10.4049/jimmunol.170.5.2582 (2003).

191 Molica, M. *et al.* CD33 Expression and Gentuzumab Ozogamicin in Acute Myeloid Leukemia: Two Sides of the Same Coin. *Cancers (Basel)* **13**, doi:10.3390/cancers13133214 (2021).

192 Barden, M. *et al.* CAR and TCR form individual signaling synapses and do not cross-activate, however, can co-operate in T cell activation. *Frontiers in immunology* **14**, 1110482, doi:10.3389/fimmu.2023.1110482 (2023).

193 Vardhana, S. A. *et al.* Impaired mitochondrial oxidative phosphorylation limits the self-renewal of T cells exposed to persistent antigen. *Nat Immunol* **21**, 1022-1033, doi:10.1038/s41590-020-0725-2 (2020).

194 Finney, O. C. *et al.* CD19 CAR T cell product and disease attributes predict leukemia remission durability. *The Journal of Clinical Investigation* **129**, 2123-2132, doi:10.1172/JCI125423 (2019).

195 Fraietta, J. A. *et al.* Determinants of response and resistance to CD19 chimeric antigen receptor (CAR) T cell therapy of chronic lymphocytic leukemia. *Nature medicine* **24**, 563-571, doi:10.1038/s41591-018-0010-1 (2018).

196 Ruella, M. *et al.* Dual CD19 and CD123 targeting prevents antigen-loss relapses after CD19-directed immunotherapies. *The Journal of clinical investigation* **126**, 3814-3826, doi:10.1172/JCI87366 (2016).

197 Drent, E. *et al.* Combined CD28 and 4-1BB Costimulation Potentiates Affinity-tuned Chimeric Antigen Receptor-engineered T Cells. *Clin Cancer Res* **25**, 4014-4025, doi:10.1158/1078-0432.CCR-18-2559 (2019).

198 Majzner, R. G. *et al.* Tuning the Antigen Density Requirement for CAR T-cell Activity. *Cancer discovery* **10**, 702-723, doi:10.1158/2159-8290.CD-19-0945 (2020).

199 Textor, A. *et al.* CD28 Co-Stimulus Achieves Superior CAR T Cell Effector Function against Solid Tumors Than 4-1BB Co-Stimulus. *Cancers (Basel)* **13**, doi:10.3390/cancers13051050 (2021).

200 Wang, D. *et al.* Glioblastoma-targeted CD4+ CAR T cells mediate superior antitumor activity. *JCI insight* **3**, doi:10.1172/jci.insight.99048 (2018).

201 Adusumilli, P. S. *et al.* Regional delivery of mesothelin-targeted CAR T cell therapy generates potent and long-lasting CD4-dependent tumor immunity. *Sci Transl Med* **6**, 261ra151, doi:10.1126/scitranslmed.3010162 (2014).

202 Sommermeyer, D. *et al.* Chimeric antigen receptor-modified T cells derived from defined CD8+ and CD4+ subsets confer superior antitumor reactivity in vivo. *Leukemia* **30**, 492-500, doi:10.1038/leu.2015.247 (2016).

203 Chen, A., Velickovic, Z. & Rasko, J. Vector copy number quality control testing for CAR T-cells: critical validation parameters. *Cytotherapy* **22**, S142, doi:10.1016/j.jcyt.2020.03.283 (2020).

204 Ghorashian, S. *et al.* CD8 T Cell Tolerance to a Tumor-Associated Self-Antigen Is Reversed by CD4 T Cells Engineered To Express the Same T Cell Receptor. *The Journal of Immunology* **194**, 1080-1089, doi:10.4049/jimmunol.1401703 (2015).

205 Anderson, V. E. *et al.* Enhancing Efficacy of TCR-engineered CD4+ T Cells Via Coexpression of CD8α. *Journal of immunotherapy* **46**, 132-144, doi:10.1097/cji.0000000000000456 (2023).

206 Hong, D. *et al.* 379 Initial safety, efficacy, and product attributes from the SURPASS trial with ADP-A2M4CD8, a SPEAR T-cell therapy incorporating an affinity optimized TCR targeting MAGE-A4 and a CD8α co-receptor. *Journal for ImmunoTherapy of Cancer* **8**, A231-A231, doi:10.1136/jitc-2020-SITC2020.0379 (2020).

207 Davari, K. *et al.* Development of a CD8 co-receptor independent T-cell receptor specific for tumor-associated antigen MAGE-A4 for next generation T-cell-based immunotherapy. *J Immunother Cancer* **9**, doi:10.1136/jitc-2020-002035 (2021).

208 Schneider, D. *et al.* A Unique Human Immunoglobulin Heavy Chain Variable Domain-Only CD33 CAR for the Treatment of Acute Myeloid Leukemia. *Front Oncol* **8**, 539, doi:10.3389/fonc.2018.00539 (2018).

209 Li, S. *et al.* CD33-Specific Chimeric Antigen Receptor T Cells with Different Co-Stimulators Showed Potent Anti-Leukemia Efficacy and Different Phenotype. *Human gene therapy* **29**, 626-639, doi:10.1089/hum.2017.241 (2018).

210 Sweeney, N. P. & Vink, C. A. The impact of lentiviral vector genome size and producer cell genomic to gag-pol mRNA ratios on packaging efficiency and titre. *Molecular Therapy - Methods & Clinical Development* **21**, 574-584, doi:10.1016/j.omtm.2021.04.007 (2021).

211 Ricobaraza, A., Gonzalez-Aparicio, M., Mora-Jimenez, L., Lumbreras, S. & Hernandez-Alcoceba, R. High-Capacity Adenoviral Vectors: Expanding the Scope of Gene Therapy. *Int J Mol Sci* **21**, doi:10.3390/ijms21103643 (2020).

212 Tasca, F. *et al.* High-capacity adenovector delivery of forced CRISPR-Cas9 heterodimers fosters precise chromosomal deletions in human cells. *Molecular Therapy - Nucleic Acids* **31**, 746-762, doi:10.1016/j.omtn.2023.02.025 (2023).

213 Omer, B. *et al.* A Costimulatory CAR Improves TCR-based Cancer Immunotherapy. *Cancer Immunol Res* **10**, 512-524, doi:10.1158/2326-6066.CIR-21-0307 (2022).

214 Tambaro, F. P. *et al.* Autologous CD33-CAR-T cells for treatment of relapsed/refractory acute myelogenous leukemia. *Leukemia* **35**, 3282-3286, doi:10.1038/s41375-021-01232-2 (2021).

215 Song, D. *et al.* Autologous T Cells Modified to Co-Express CD33-Specific Chimeric Antigen Receptor and a Kill Switch for Treatment of CD33+ Acute Myeloid Leukemia. *Blood* **130**, 1376-1376, doi:10.1182/blood.V130.Suppl_1.1376.1376 (2017).

216 Minagawa, K. *et al.* In Vitro Pre-Clinical Validation of Suicide Gene Modified Anti-CD33 Redirected Chimeric Antigen Receptor T-Cells for Acute Myeloid Leukemia. **11**, e0166891, doi:10.1371/journal.pone.0166891 (2016).

217 Cartellieri, M. *et al.* Switching CAR T cells on and off: a novel modular platform for retargeting of T cells to AML blasts. *Blood cancer journal* **6**, e458-e458, doi:10.1038/bcj.2016.61 (2016).

218 Benmebarek, M.-R. *et al.* A modular and controllable T cell therapy platform for acute myeloid leukemia. *Leukemia* **35**, 2243-2257, doi:10.1038/s41375-020-01109-w (2021).

219 Nixdorf, D. *et al.* Adapter CAR T cells to counteract T-cell exhaustion and enable flexible targeting in AML. *Leukemia* **37**, 1298-1310, doi:10.1038/s41375-023-01905-0 (2023).

220 Hassan, N., Yang, J. & Wang, J. Y. An Improved Protocol for Establishment of AML Patient-Derived Xenograft Models. *STAR protocols* **1**, 100156, doi:10.1016/j.xpro.2020.100156 (2020).

221 Aru, B. *et al.* A potential area of use for immune checkpoint inhibitors: Targeting bone marrow microenvironment in acute myeloid leukemia. *Frontiers in immunology* **14**, 1108200, doi:10.3389/fimmu.2023.1108200 (2023).

222 Chang, A. Y. *et al.* Opportunities and challenges for TCR mimic antibodies in cancer therapy. *Expert opinion on biological therapy* **16**, 979-987, doi:10.1080/14712598.2016.1176138 (2016).

223 Wachsmann, T. L. A. *et al.* Comparing CAR and TCR engineered T cell performance as a function of tumor cell exposure. *Oncoimmunology* **11**, 2033528, doi:10.1080/2162402X.2022.2033528 (2022).

224 van der Schans, J. J., van de Donk, N. W. C. J. & Mutis, T. Dual Targeting to Overcome Current Challenges in Multiple Myeloma CAR T-Cell Treatment. *Frontiers in Oncology* **10**, doi:10.3389/fonc.2020.01362 (2020).

225 Helsen, C. W., Hammill, J. A. & Lau, V. W. C. The chimeric TAC receptor co-opts the T cell receptor yielding robust anti-tumor activity without toxicity. **9**, 3049, doi:10.1038/s41467-018-05395-y (2018).

226 Tan, E., Gakhar, N. & Kirtane, K. TCR gene-engineered cell therapy for solid tumors. *Best practice & research. Clinical haematology* **34**, 101285, doi:10.1016/j.beha.2021.101285 (2021).

227 Gaissmaier, L., Elshiaty, M. & Christopoulos, P. Breaking Bottlenecks for the TCR Therapy of Cancer. *Cells* **9**, doi:10.3390/cells9092095 (2020).

228 Yan, T., Zhu, L. & Chen, J. Current advances and challenges in CAR T-Cell therapy for solid tumors: tumor-associated antigens and the tumor microenvironment. *Experimental hematology & oncology* **12**, 14, doi:10.1186/s40164-023-00373-7 (2023).

229 Xie, N. *et al.* Neoantigens: promising targets for cancer therapy. *Signal Transduction and Targeted Therapy* **8**, 9, doi:10.1038/s41392-022-01270-x (2023).

230 Chinnasamy, D. *et al.* Local Delivery of lnterleukin-12 Using T Cells Targeting VEGF Receptor-2 Eradicates Multiple Vascularized Tumors in Mice. *Clinical Cancer Research* **18**, 1672-1683, doi:10.1158/1078-0432.ccr-11-3050 (2012).

231 Chinnasamy, D. *et al.* Gene therapy using genetically modified lymphocytes targeting VEGFR-2 inhibits the growth of vascularized syngenic tumors in mice. *The Journal of Clinical Investigation* **120**, 3953-3968, doi:10.1172/JCI43490 (2010).

232 Byrd, T. T. *et al.* TEM8/ANTXR1-Specific CAR T Cells as a Targeted Therapy for Triple-Negative Breast Cancer. *Cancer Research* **78**, 489-500, doi:10.1158/0008-5472.can-16-1911 (2018).

233 Santoro, S. P. *et al.* T Cells Bearing a Chimeric Antigen Receptor against Prostate-Specific Membrane Antigen Mediate Vascular Disruption and Result in Tumor Regression. *Cancer Immunology Research* **3**, 68-84, doi:10.1158/2326-6066.cir-14-0192 (2015).

234 Werchau, N. *et al.* Combined targeting of soluble latent TGF-ss and a solid tumor-associated antigen with adapter CAR T cells. *Oncoimmunology* **11**, 2140534, doi:10.1080/2162402X.2022.2140534 (2022).

235 Wang, E. *et al.* Generation of Potent T-cell Immunotherapy for Cancer Using DAP12-Based, Multichain, Chimeric Immunoreceptors. *Cancer Immunol Res* **3**, 815-826, doi:10.1158/2326-6066.CIR-15-0054 (2015).

236 Kakarla, S. *et al.* Antitumor Effects of Chimeric Receptor Engineered Human T Cells Directed to Tumor Stroma. *Molecular Therapy* **21**, 1611-1620, doi:10.1038/mt.2013.110 (2013).

237 Gulati, P. *et al.* Aberrant Lck Signal via CD28 Costimulation Augments Antigen-Specific Functionality and Tumor Control by Redirected T Cells with PD-1 Blockade in Humanized Mice. *Clinical Cancer Research* **24**, 3981-3993, doi:10.1158/1078-0432.ccr-17-1788 (2018).

238 Lo, A. *et al.* Tumor-Promoting Desmoplasia Is Disrupted by Depleting FAP-Expressing Stromal Cells. *Cancer Res* **75**, 2800-2810, doi:10.1158/0008-5472.can-14-3041 (2015).

239 Xie, Y. J. *et al.* Improved Antitumor Efficacy of Chimeric Antigen Receptor T Cells that Secrete Single-Domain Antibody Fragments. *Cancer Immunology Research* **8**, 518-529, doi:10.1158/2326-6066.cir-19-0734 (2020).

240 Sánchez-Paulete, A. R. *et al.* Targeting Macrophages with CAR T Cells Delays Solid Tumor Progression and Enhances Antitumor Immunity. *Cancer Immunology Research* **10**, 1354-1369, doi:10.1158/2326-6066.cir-21-1075 (2022).

241 Parihar, R. *et al.* NK Cells Expressing a Chimeric Activating Receptor Eliminate MDSCs and Rescue Impaired CAR-T Cell Activity against Solid Tumors. *Cancer Immunology Research* **7**, 363-375, doi:10.1158/2326-6066.cir-18-0572 (2019).

242 Williams, F. *et al.* Development of PCR-SSOP for the identification of HLA-A*02 subtypes and determination of HLA-A*02 frequencies within different ethnic populations. *Tissue antigens* **49**, 129-133, doi:10.1111/j.1399-0039.1997.tb02726.x (1997).

243 van der Lee, D. I. *et al.* An HLA-A*11:01-Binding Neoantigen from Mutated NPM1 as Target for TCR Gene Therapy in AML. *Cancers (Basel)* **13**, doi:10.3390/cancers13215390 (2021).

244 Xue, S. A. *et al.* Enhancing the expression and function of an EBV-TCR on engineered T cells by combining Sc-TCR design with CRISPR editing to prevent mispairing. **17**, 1275-1277, doi:10.1038/s41423-020-0396-9 (2020).

245 Bendle, G. M. *et al.* Lethal graft-versus-host disease in mouse models of T cell receptor gene therapy. *Nature medicine* **16**, 565-570, 561p following 570, doi:10.1038/nm.2128 (2010).

246 van Loenen, M. M. *et al.* Mixed T cell receptor dimers harbor potentially harmful neoreactivity. *Proc Natl Acad Sci U S A* **107**, 10972-10977, doi:10.1073/pnas.1005802107 (2010).

247 Safarzadeh Kozani, P., Shokrgozar, M. A., Evazalipour, M. & Roudkenar, M. H. CRISPR/Cas9-medaited knockout of endogenous T-cell receptor in Jurkat cells and generation of NY-ESO-1-specific T cells: An in vitro study. *Int Immunopharmacol* **110**, 109055, doi:10.1016/j.intimp.2022.109055 (2022).

248 Schober, K. *et al.* Orthotopic replacement of T-cell receptor α- and β-chains with preservation of near-physiological T-cell function. *Nature Biomedical Engineering* **3**, 974-984, doi:10.1038/s41551-019-0409-0 (2019).

249 Eyquem, J. *et al.* Targeting a CAR to the TRAC locus with CRISPR/Cas9 enhances tumour rejection. *Nature* **543**, 113-117, doi:10.1038/nature21405 (2017).

250 Kath, J. *et al.* Pharmacological interventions enhance virus-free generation of TRAC-replaced CAR T cells. *Mol Ther Methods Clin Dev* **25**, 311-330, doi:10.1016/j.omtm.2022.03.018 (2022).

251 MacLeod, D. T. *et al.* Integration of a CD19 CAR into the TCR Alpha Chain Locus Streamlines Production of Allogeneic Gene-Edited CAR T Cells. *Mol Ther* **25**, 949-961, doi:10.1016/j.ymthe.2017.02.005 (2017).

252 Tipanee, J., Samara-Kuko, E., Gevaert, T., Chuah, M. K. & VandenDriessche, T. Universal allogeneic CAR T cells engineered with Sleeping Beauty transposons and CRISPR-CAS9 for cancer immunotherapy. *Mol Ther* **30**, 3155-3175, doi:10.1016/j.ymthe.2022.06.006 (2022).

253 Benjamin, R. *et al.* UCART19, a first-in-class allogeneic anti-CD19 chimeric antigen receptor T-cell therapy for adults with relapsed or refractory B-cell acute lymphoblastic leukaemia (CALM): a phase 1, dose-escalation trial. *The Lancet. Haematology* **9**, e833-e843, doi:10.1016/s2352-3026(22)00245-9 (2022).

254 Ahmed, A. *et al.* EPR22-104: A Comparison of the Burden of Leukemia Amongst Various Regions of the World, 1990-2019. *Journal of the National Comprehensive Cancer Network* **20**, EPR22-104-EPR122-104, doi:10.6004/jnccn.2021.7211 (2022).

255 Rotiroti, M. C. *et al.* Targeting CD33 in Chemoresistant AML Patient-Derived Xenografts by CAR-CIK Cells Modified with an Improved SB Transposon System. *Mol Ther* **28**, 1974-1986, doi:10.1016/j.ymthe.2020.05.021 (2020).

256 Bao, L. *et al.* Engineered T cells and their therapeutic applications in autoimmune diseases. *Zoological research* **43**, 150-165, doi:10.24272/j.issn.2095-8137.2021.363 (2022).

257 Zhang, W. *et al.* Treatment of Systemic Lupus Erythematosus using BCMA-CD19 Compound CAR. *Stem Cell Reviews and Reports* **17**, 2120-2123, doi:10.1007/s12015-021-10251-6 (2021).

258 Mougiakakos, D. *et al.* CD19-Targeted CAR T Cells in Refractory Systemic Lupus Erythematosus. *New England Journal of Medicine* **385**, 567-569, doi:10.1056/NEJMc2107725 (2021).

259 Mackensen, A. *et al.* Anti-CD19 CAR T cell therapy for refractory systemic lupus erythematosus. *Nature medicine* **28**, 2124-2132, doi:10.1038/s41591-022-02017-5 (2022).

260 Kim, Y. C. *et al.* Engineered MBP-specific human Tregs ameliorate MOG-induced EAE through IL-2-triggered inhibition of effector T cells. *Journal of autoimmunity* **92**, 77-86, doi:10.1016/j.jaut.2018.05.003 (2018).

261 De Paula Pohl, A. *et al.* Engineered regulatory T cells expressing myelin-specific chimeric antigen receptors suppress EAE progression. *Cellular Immunology* **358**, 104222, doi:doi.org/10.1016/j.cellimm.2020.104222 (2020).

262 Hull, C. M. *et al.* Generation of human islet-specific regulatory T cells by TCR gene transfer. *Journal of autoimmunity* **79**, 63-73, doi:doi.org/10.1016/j.jaut.2017.01.001 (2017).

PUBLICATIONS AND PATENTS

Publications

Teppert K, Yonezawa Ogusuku IE, Brandes C, Herbel V, Winter N, Werchau N, Khorkova S, Wöhle C, Jelveh N, Bisdorf K, Engels B, Schaser T, Anders K, Künkele A, Lock D. CAR'TCR-T cells co-expressing CD33-CAR and dNPM1-TCR as superior dual-targeting approach for AML treatment. Molecular Therapy Oncology. 2024;32(2). doi:10.1016/j.omton.2024.200797

Yonezawa Ogusuku IE, Herbel V, Lennartz S, Brandes C, Argiro E, Fabian C, Hauck C, Hoogstraten C, Veld S, Hageman L, **Teppert K**, Koutsoumpli G, Griffieon M, Mockel-Tenbrinck N, Schaser T, Groot R, Johnston ICD, Lock D. Automated manufacture of ΔNPM1 TCR-engineered T cells for AML therapy. Molecular Therapy - Methods & Clinical Development. 2024;32(2). doi:10.1016/j.omtm.2024.101224

Teppert K, Winter N, Herbel V, Brandes C, Lennartz S, Engert F, Kaiser A, Schaser T, Lock D. Combining CSPG4-CAR and CD20-CCR for treatment of metastatic melanoma. Frontiers in immunology. 2023;14. doi:10.3389/fimmu.2023.1178060

Teppert K, Wang X, Anders K, Evaristo C, Lock D, Künkele A. Joining Forces for Cancer Treatment: From "TCR versus CAR" to "TCR and CAR". Int J Mol Sci. 2022;23(23):14563. doi:10.3390/ijms232314563

Werchau N, Kotter B, Criado-Moronati E, Gosselink A, Cordes N, Lock D, Lennartz S, Kolbe C, Winter N, **Teppert K**, Engert F, Webster B, Mittelstaet J, Schaefer D, Mallmann P, Mallmann MR, Ratiu D, Assenmacher M, Schaser T, von Bergwelt-Baildon M, Abramowski P, Kaiser AD. Combined targeting of soluble latent TGF-ss and a solid tumor-associated antigen with adapter CAR T cells. Oncoimmunology. 2022;11(1):2140534. doi:10.1080/2162402X.2022.2140534.

Lock D, Monjezi R, Brandes C, Bates S, Lennartz S, **Teppert K**, Gehrke L, Karasakalidou-Seidt R, Lukic T, Schmeer M, Schleef M, Werchau N, Eyrich M, Assenmacher M, Kaiser A, Prommersberger S, Schaser T, Hudecek M. Automated, scaled, transposon-based production of CAR T cells. J Immunother Cancer. 2022;10(9). doi:10.1136/jitc-2022-005189.

Hörner S, Moustafa-Oglou M, **Teppert K**, Hagelstein I, Kauer J, Pflügler M, Neumann K, Rammensee HG, Metz T, Herrmann A, Salih HR, Jung G, Zekri L. IgG-Based Bispecific Anti-CD95 Antibodies for the Treatment of B Cell-Derived Malignancies and Autoimmune Diseases. Cancers (Basel). 2022;14(16). doi:10.3390/cancers14163941.

Patent application

Lock D, **Teppert K**, Johnston I, Brandes C, Engels B, Assenmacher M. Immune cell expressing chimeric antigen receptor and transgenic T cell receptor. MBG_134, submitted July 6, 2023.